THERMODYNAMICS OF TRANSITION METAL OXIDE-CARBIDE SOLID SOLUTIONS

A THESIS

submitted for the

DEGREE OF DOCTOR OF PHILOSOPHY

of the

UNIVERSITY OF LONDON

by

MICHAEL ANDREW WILLIAMS

Nuffield Research Group,
Department of Metallurgy,
Imperial College of Science
and Technology.

June, 1971.

A B S T R A C T

In studies of the W-C-O system, it has been shown that in the range $60{:}1 > CO/CO_2 > 12{:}1$, tungsten is the stable phase at 1200°C and 1 atmosphere total pressure. At $CO/CO_2 > 65{:}1$, tungsten monocarbide is the stable phase, with a maximum oxygen solubility of .12 ± .01 wt. %. Neglecting the small amount of oxygen solubility, the monocarbide phase was found to exist substoicheiometrically ($WC_{.91}$) at $CO/CO_2 = 65{:}1$, decreasing in nonstoicheiometry with increase in CO/CO_2 ratio. The extrapolated value for ΔG° formation of stoicheiometric WC at 1200°C was found to be - 8.6 ± .3 K.cals. In no case was W_2C formation observed.

In the Ti-C-O system, the Ti-Ti(C,O) phase boundary was studied at 1300°C using the isopiestic technique. No thermodynamic data were obtained since equilibrium was not reached after a period of 10 days at temperature. Reasons for lack of equilibrium are suggested by comparison with isopiestic studies of the U-C-O system. Only a limited number of experiments were performed due to continual alumina furnace tube failure.

Examination of one of the failed tubes, using various techniques, showed that the inner surface of the hot zone of the tube contained a large amount of connected porosity, which was not present in the cold zone. The increased porosity was shown to be associated with silica and alkaline earth loss. Further, substantial grain growth of the large inner-surface skin grains was observed in the hot zone relative to the cold zone. Mechanisms for the final failure of tubes under varying conditions of service are suggested.

TABLE OF CONTENTS

CHAPTER 1

INTRODUCTION

The carbides of groups 4, 5 and 6 of the Periodic Table, known as the hard metals, or refractory carbides, occupy an important position in today's technology. This position is due to their high melting points (melting point TiC = 3140°C) and their extreme hardness. (The Moh's hardness of diamond is 10; that of titanium carbide and tungsten carbide is 9). These properties are manifested in such applications as dispersion hardening in steels, in refractory alloys for jet engines, and also in outting tools.

In this latter application, tungsten and titanium carbides are used, bonded with cobalt, as the cutting tip. In earlier cutting tools, which used tungsten carbide on its own, bonded with cobalt as the tool tip, there was a distinct tendency towards local welding with the metal workpiece and consequent increased tool wear. Incorporation of titanium carbide prevents this local welding by producing, on oxidation, first a TiO surface layer which physically isolates the tool from the workpiece. (Note that tungsten carbide forms no protective oxide - WO_3 volatilises). Gradually further oxidation results in an outermost film of TiO_2, which provides what GOLDSCHMIDT[1] calls "a local lubricating action", at high temperatures. Thus we have the transition TiC-Ti(C,O)-TiO etc. -TiO_2 from the tip substrate to the surface, the Ti(C,O) solid solution acting as an anchor between the oxide layers produced and the carbide substrate. This has a converse aspect in that in the production of sintered carbide tool tips, if the titanium carbide used contains any oxygen or nitrogen, carbon monoxide or nitrogen will form during the sintering, thus giving rise to increased porosity and inferior

mechanical properties. Further, the intermediate oxycarbide lowers the oxidation rate of the carbide, due to the lowering of its carbon activity. This latter phenomenon may have great importance in high temperature applications, for example in rocket nosecones, where a slight lowering of the mechanical strength of the solid solution, relative to that of the pure carbide phase, may be more than compensated for by increased oxidation resistance, thus stretching the present applications of these hard metals.

At this point it is considered useful to mention a few aspects of the constitution of interstitial compounds, with particular reference to metallic oxides, nitrides, and carbides. In a simple picture, we can broadly think of an interstitial atom as one which fits into the interstices or voids between other atoms in a crystal. The two types of interstices occurring are the tetrahedral and the octahedral. The former has 4 atoms adjacent to it, and the latter 6 atoms.

Carbon, nitrogen, and oxygen, even in an unionised state, are too large to fit into tetrahedral sites in f.c.c. and h.c.p. metals, and thus go into octahedral sites on introduction into the lattice of the parent metal. In b.c.c. parent lattices, both octahedral and tetrahedral holes are very small, and thus primary solubility in these lattices is very restricted. Thus we can consider C, O, and N atoms as being inserted into the interstices to give a primary solution, the parent metal lattice retaining its original form.

However, if we consider a transition metal interstitial compound, the above simple picture does not apply, since without the non-metal atom, the structure of the compound would be entirely different, e.g. vanadium metal - b.c.c. structure; vanadium carbide (VC) - sodium chloride structure. This effect is due to interstitial atoms acting as electron donors to the metal atom. Thus in

these interstitial compounds bonding occurs between the metal and interstitial atoms, the bonding changing from mainly metallic when carbon is the interstitial, becoming more ionic when oxygen is interstitial.

Analysis of the structures of transitional metal oxides, carbides and nitrides of groups 4, 5 and 6 shows that they are close-packed regardless of the initial metal structure. Considering inter-stitial compounds of the MX type, in groups 4 and 5 they have an NaCl structure whereas in group 6 they are hexagonal.

Interstitial compounds of a particular metal and of other metals with similar atomic size, electronic and structural characteristics, tend to form complete solid solution ranges e.g. VC and VO. On the other hand both UC and UO, and TiC and TaN form only partial solid solution ranges.

It can thus be seen that when studying a ternary system, M-C-O, one should take great care to exclude other potentially interstitial substances from the closed reaction system.

In view of the present and potential uses of refractory carbides, it would be useful to have more thermodynamic information available than at present, on the systems M-C-O where M is any metal of the first, second and third long periods of groups 4, 5 and 6 of the Periodic Table. In the present equilibrium study the two systems to be investigated are the Ti-C-O and W-C-O systems. It can be shown that, assuming ideal behaviour and stoioheiometry, the partial oxygen pressure in the Ti-C-O system varies between 10^{-24} and 10^{-31} atmospheres at 1300°C, and 10^{-13} and 10^{-17} atmospheres in the W-C-O system at 1200°C. It can thus be seen that in view of the different ranges of oxygen partial pressures existing, different techniques will be required for the study of each of these systems.

CHAPTER 2

THE TUNGSTEN - CARBON - OXYGEN SYSTEM

I. REVIEW OF LITERATURE

A. TUNGSTEN - CARBON SYSTEM

(1) Constitutional Data

As seen from the constitutional diagram (Fig. 1), there are two carbides in this system, namely WC and W_2C.*

Carbon has only a very small solubility in tungsten, the maximum being 0.3 atomic per cent at 2450°C. Both WC and W_2C (at less than 2450°C) are hexagonal, the c and a parameters being as follows:-

	c	a
WC	2.837 A°	2.906 A°
W_2C	4.724 A°	2.994 A°

W_2C exhibits a small range of non-stoicheiometry but WC is, to all intents, stoicheiometric.

Tungsten itself is cubic, with a = 3.1652 A°.

(2) Thermodynamic Data

The data existing for the free energy of formation of WC and W_2C are given in Table I, page 6. Further, Kelley's comment concerning SCHENCK, WESSELCOCK & KURZEN's[8] data for W_2C, W_3C_2 and

---

* All constitutional data, unless otherwise stated, are taken from -

'Constitution of Binary Alloys' - M. HANSEN.
McGraw Hill Book Co., New York, 1958.

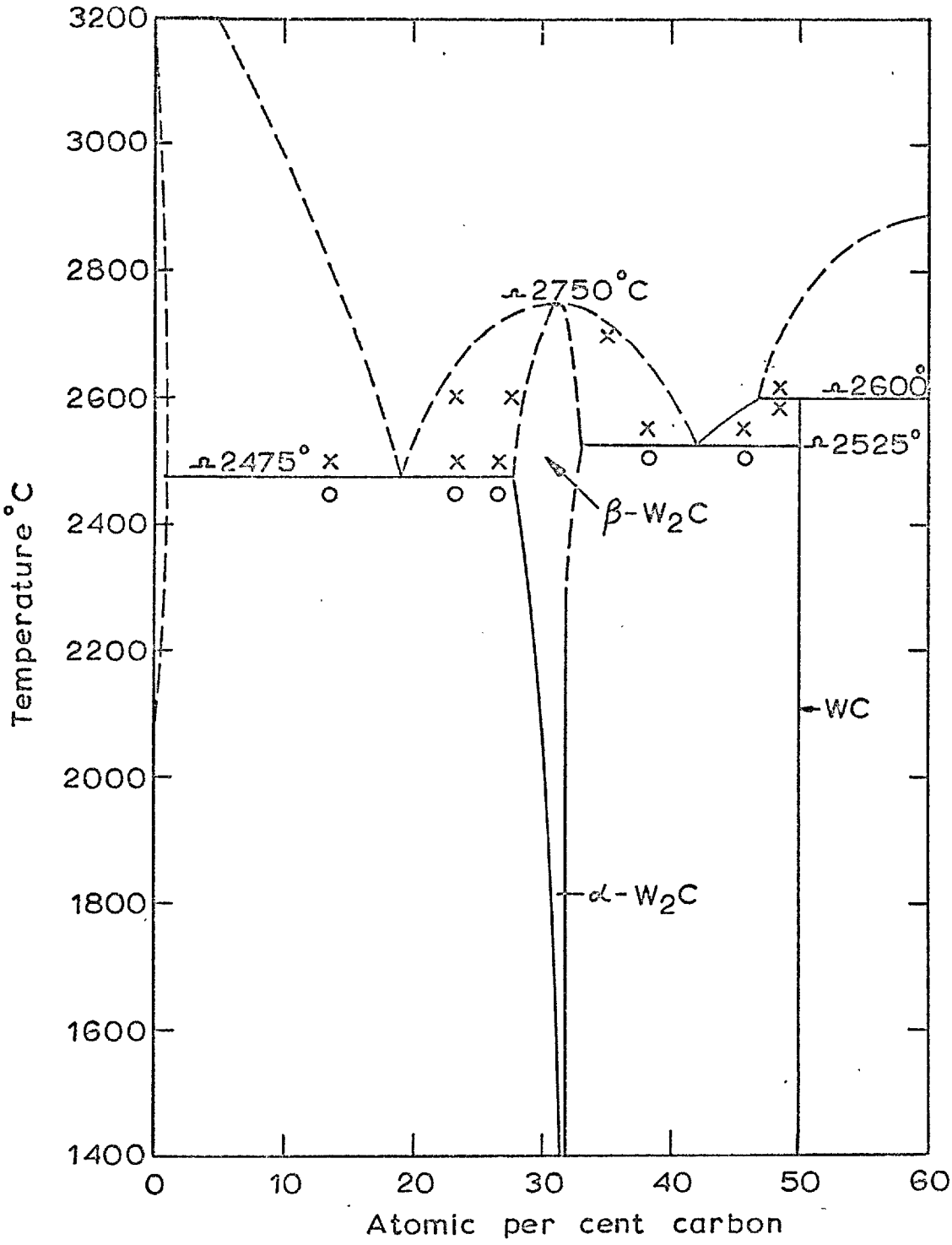

Fig.1. TUNGSTEN-CARBON EQUILIBRIUM DIAGRAM

TABLE I

Source	Comments	Data (Calories)
GLEISER AND CHIPMAN[3]	Derived from equilibration of W/WC with CO_2 between 1215°K and 1266°K, and then using KUBASCHEWSKI's[22] data for ΔG_T^o for CO and CO_2.	ΔG_T^o WC = -7690 + 0.2T
WORRELL[4]	Empirical equation using Mah's heat of formation data and GLEISER & CHIPMAN's data.	ΔG_T^o WC = -9600 + 1.0T
	Obtained from Mah's heat of formation data and an estimated entropy of formation. These two equations predict a eutectoid decomposition of W_2C at 1325°C.	ΔG_T^o W_2C = -6400 - 1.0T
ORTON[5]	Obtained from Cunningnam & McGraw's data.	ΔG_T^o WC = -8400 + 4.53T
	This suggests a eutectoid decomposition of W_2C at 1300°C.	ΔG_T^o W_2C = -2100 + 2.15T
ORTON[6]	Orton's own studies in CH_4/H_2 mixtures indicate a eutectoid decomposition of W_2C at 1215°C.	
KRIKORIAN[7]	At 298°K.	ΔG^o_{298} W_2C = -11000 ± 4000
		ΔG^o_{298} WC = -8400 ± 1000
*KUBASCHEWSKI[22]	Assessment of existing data.	ΔG_T^o WC = -9000 + 0.4T

* Note that all Thermodynamic Data, unless otherwise stated, are taken from this reference.

W_2C_2 is "the information is too meagre for calculations in which reasonable confidence may be placed."

B. TUNGSTEN - OXYGEN SYSTEM

(1) Constitutional Data

The only equilibrium diagram available for this system is a tentative one shown in Fig. 2, proposed by St. PIERRE et al[9] on the basis of thermodynamic data.

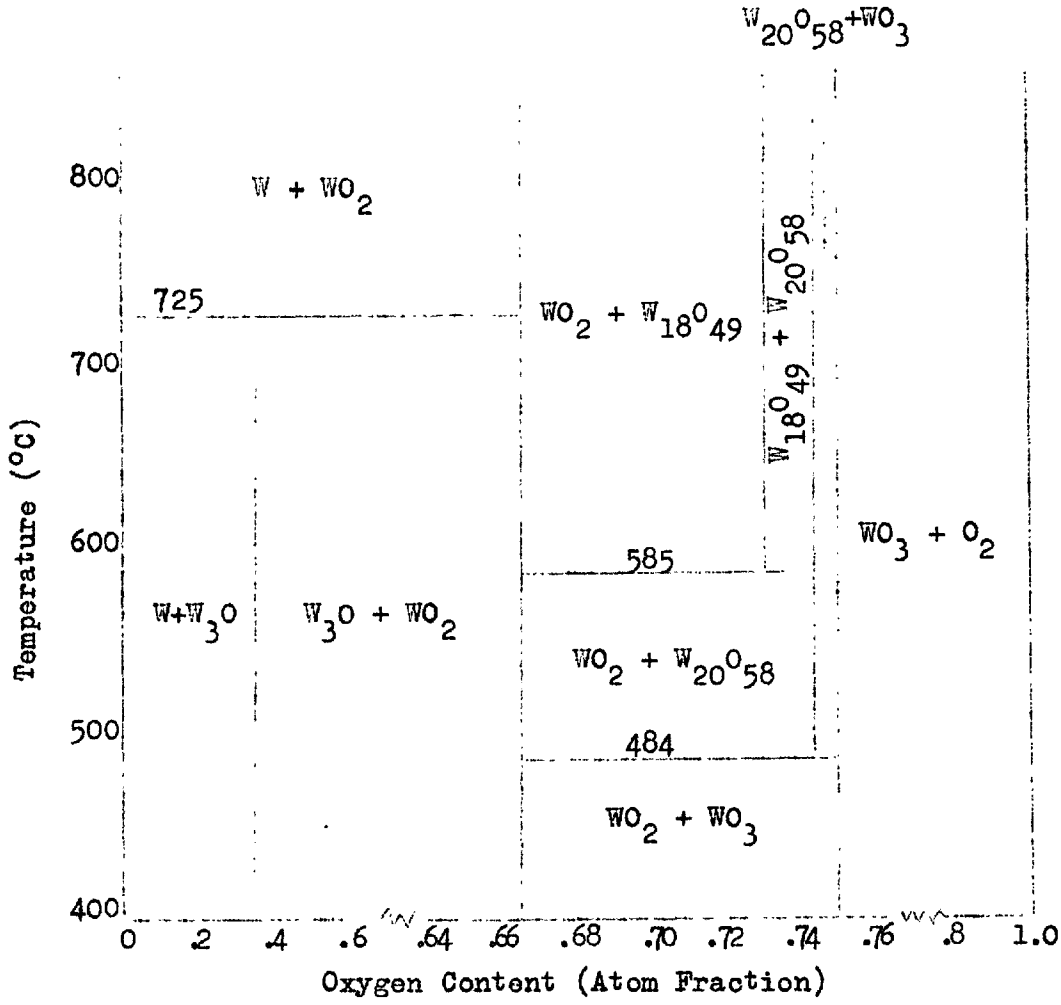

Fig. 2 - The W-O phase equilibria at 1 atm total pressure.

WORRELL[10,11] and St. PIERRE[12] et al question the existence of the W_3O phase and suggest that its observation is due to stabilisation by either impurities or certain experimental conditions of temperature and pressure, as observed for a suboxide of tantalum.

The only stable phases known to exist are as shown in Fig. 2 (less W_3O) and are as follows:-

(a) WO_2 - monoclinic structure

(b) α phase - a region from $WO_{2.65}$ to $WO_{2.76}$

(c) β phase - a region from $WO_{2.88}$ to $WO_{2.9}$

(d) WO_3 - 2 forms exist, one a low temperature form of uncertain structure, and the second a high temperature tetragonal form stable from 750°C upwards. This high temperature form is stoicheiometric.

(2) Thermodynamic Data

The free energy data for this system are reasonably well established both by e.m.f. [13,14,15,16] and gas equilibration [9,17,18] techniques. The standard free energy of formation for the reaction $W + O_2 = WO_2$ is given by

$$\Delta G_T^\circ = -138{,}500 + 36.6T \text{ cals.}$$

The limitations of this and the more recent data will be discussed in Section VI.

C. TUNGSTEN - CARBON - NITROGEN SYSTEM

No equilibrium studies have been carried out on this system. The only studies carried out have been non-equilibrium diffusion studies of GERASIMOV et al [19], which tentatively suggest possible nitrogen solution in the carbide.

D. TUNGSTEN - CARBON - OXYGEN SYSTEM

"It should be borne in mind that these carbides (i.e.tungsten carbides), like other systems, are susceptible to oxycarbide formation." STORMS [20].

WORRELL[4] has carried out a thermodynamic analysis of this system at a total pressure of 1 atmosphere, and states that no oxycarbides exist under these conditions. A ternary section and Pourbaix-Ellingham diagram constructed by Worrell are shown in Figs. 3 and 4, page 10.

LUX & IGNATOWICZ [21] showed that fast decomposition of tungsten hexacarbonyl in "high vacuum" at 350°C produced an f.c.c. structure, with lattice parameter a = 4.181 A° and composition $WC_{0.5}O_{0.46}$. When this was heated in "high vacuum" it decomposed at 900°C to hexagonal WC_x with a_o = 10.58 A° and c_o = 13.35 A°. W_2C formation was not observed.

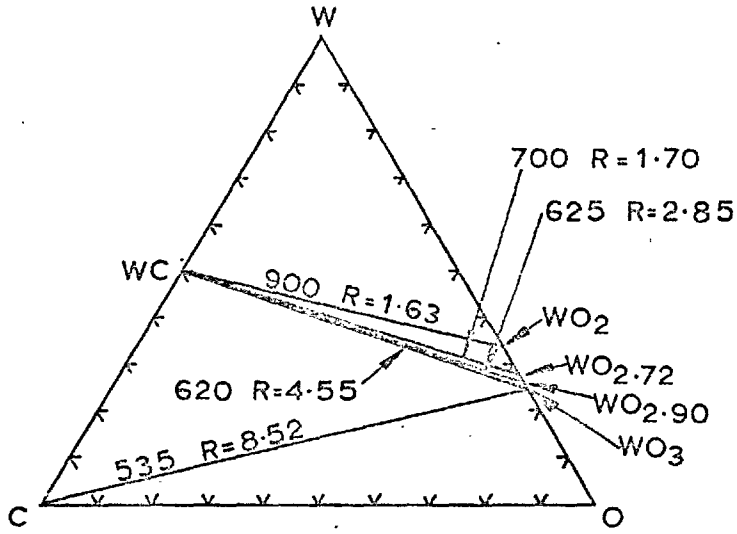

Fig.3. SOLID EQUILIBRIUM PHASES OF THE W-C-O SYSTEM AT 1atm. VAPOUR PRESSURE. (The temperature, °C and the CO_2/CO gas ratio (R) at which any two phases become unstable are indicated along the two phase line)

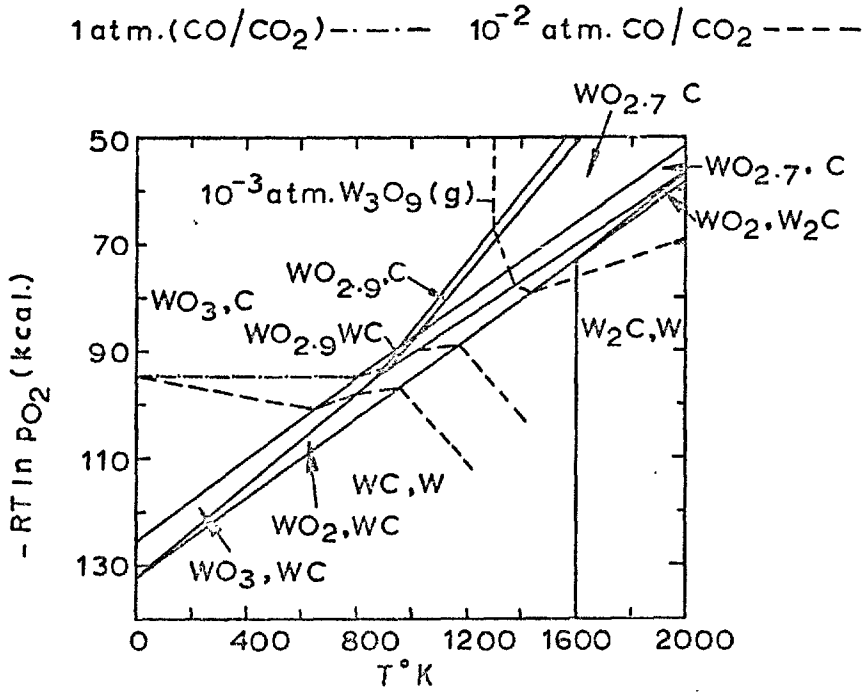

Fig.4. POURBAIX-ELLINGHAM DIAGRAM FOR THE W-C-O SYSTEM

II. THERMODYNAMIC ASSESSMENT

Let us consider that the oxycarbides formed are of general formula $WC_{1-x}O_x$, where $\frac{C+O}{W}$ does not differ significantly from Unity. (c.f. U-C-O system[23]). We can consider such compounds to be pseudobinaries of WC and WO, with ideal heats of mixing. This is, of course, only an approximation, but satisfactory for a preliminary assessment. [The oxycarbide of LUX & IGNATOWICZ[21] can be considered to be based on unstable WO, and WC; the cubic structure of WO (c.f. NbO) stabilised by WC].

Calculations were made using KUBASCHEWSKI's[22] data for the $W-WO_2$ system, these data applying up to 1500°K. Thus all data subsequently given for this system are for a temperature within this range, e.g. 1200°C.

For the reaction $W + O_2 = WO_2$, $\Delta G^\circ_T = -138{,}500 + 36.6T$. This gives $\Delta G^\circ_{1473^\circ K} = -84.6$ K.cals., and thus ΔG_{1473} per gm.atom $WO_2 = -28.2$ K.cals. No free energy data are available for WO, which is unstable with reference to pure W and WO_2, but an approximate value can be obtained from a plot of ΔG_{1473} per gm.atom v. composition for the W-O system. This indicates that ΔG/gm.atom must be less than -21 K.cals/gm.atom.

In the absence of any other information, this value for ΔG/gm.atom WO is adequate as the presence of carbon tends to stabilise WO (i.e. ΔG° formation becomes more negative).

A. W(C,O) REGION

Using the above and other thermodynamic data, we can obtain equilibrium constants at 1473°K for the following reactions:-

$$W + \tfrac{1}{2}O_2 = WO \qquad K_{WO}{}_{1473^\circ K} = 1.7 \times 10^6$$

$$CO + \tfrac{1}{2}O_2 = CO_2 \qquad K_{CO_2\ 1473^\circ K} = 3.02 \times 10^5$$

$$W + C = WC \qquad K_{WC\ 1473^\circ K} = 17.78$$

$$2CO = CO_2 + C \qquad K^1_{CO\ 1473^\circ K} = 8.71 \times 10^{-4}$$

Using the above data, and eliminating N_W, N_C, and pO_2, we obtain the expression:-

$$\frac{N_{WO}}{N_{WC}} = \frac{K_{WO}}{K_{WC}K_{CO_2}K^1_{CO}} \frac{1}{\left(\frac{p_{CO}}{p_{CO_2}}\right)^2} \frac{1}{p_{CO}}$$

which at $1473^\circ K$ gives -

$$\frac{N_{WO}}{N_{WC}} = 363.5 \frac{1}{\left(\frac{p_{CO}}{p_{CO_2}}\right)^2} \frac{1}{p_{CO}}$$

Assuming a total pressure of 1 atmosphere, we can substitute various values of CO/CO_2 and obtain corresponding values of N_{WO}/N_{WC}. A plot of N_{WO}/N_{WC} v. p_{CO}/p_{CO_2} is shown in Fig. 5, Appendix I.

Then, knowing by definition that $N_{WO} + N_{WC} = 1$, we can obtain both N_{WO} and N_{WC}, and then by substituting these known values back into the relevant equations for K, we obtain the values of $p^{\frac{1}{2}}O_2$, a_W, and a_C. These values are shown in Table 2, page 13.

TABLE 2

N_{WO}	N_{WC}	$\frac{N_{WO}}{N_{WC}}$	CO/CO_2	$p^{\frac{1}{2}}O_2$	a_W	a_C	P_{CO} (ats.)
.9987	.0013	727	1	3.31×10^{-6}	.178	4.33×10^{-4}	.5
.994	.006	174.5	5	6.62×10^{-7}	.883	3.62×10^{-4}	.83
.8	.2	4	10	3.31×10^{-7}	1.425	7.9×10^{-3}	.91
.491	.509	.954	20	1.66×10^{-7}	1.739	1.65×10^{-2}	.95
.298	.702	.424	30	1.11×10^{-7}	1.578	2.49×10^{-2}	.97
.189	.811	.233	40	8.3×10^{-8}	1.346	3.4×10^{-2}	.975
.126	.874	.144	50	6.64×10^{-8}	1.116	4.4×10^{-2}	.98
.093	.907	.103	60	5.5×10^{-8}	.997	5.1×10^{-2}	.985
.0697	.930	.075	70	4.74×10^{-8}	.87	6.03×10^{-2}	.987

From Gibb's Phase Rule, P + F = C + 2 where the symbols have their usual significance. Inside the W(C,O) region, we have a solid and gas phase in equilibrium, and thus for a 3 component system F = 3.

If we use CO/CO_2 mixtures we can control both carbon and oxygen activities and at a particular temperature, we then have an invariant system.

Alternatively, we can fix a_W together with a_C or pO_2. To fix the activity of tungsten, we require to alloy tungsten with a metal with which it forms wide solid solution ranges with little or no compound formation. This metal should also form no stable carbides. The only metals which fulfil these criteria in any way are the platinum metals, especially platinum itself which has a wide single phase region (up to 67 atomic % tungsten)[24], with no compound formation, and in which the solubility of carbon is negligible. However, no activity - composition data are available for solid solutions of any of these metals alloyed with tungsten.

B. W-W(C,O) BOUNDARY

Using $a_W = 1$, and the values for K_{WO}, K_{WC}, and $K_{CO\ 1473}$ (3.48×10^8), and assuming various values of N_{WO} and N_{WC}, we can obtain corresponding values of pO_2, a_C and p_{CO} as shown below.

TABLE 3

N_{WO}	N_{WC}	pO_2	a_C	p_{CO} (ats.)
.1	.9	3.46×10^{-15}	5.1×10^{-2}	1.04
.2	.8	1.39×10^{-14}	4.5×10^{-2}	1.85
.3	.7	3.1×10^{-14}	3.955×10^{-2}	2.42
.4	.6	5.53×10^{-14}	3.385×10^{-2}	2.77
.5	.5	1.10×10^{-13}	2.83×10^{-2}	3.28
.6	.4	1.24×10^{-13}	2.26×10^{-2}	2.77
.7	.3	1.70×10^{-13}	1.695×10^{-2}	2.43
.8	.2	2.21×10^{-13}	1.13×10^{-2}	1.85
.9	.1	2.80×10^{-13}	5.65×10^{-3}	1.04

Taking non-ideality into account, it is feasible that we can prepare $N_{WO}/N_{WC} = .1/.9$ starting from WC with excess tungsten and equilibrating with CO (or CO/purified Argon when required) at 1 atmosphere at 1200°C.

Another available technique is to equilibrate W and WC in a WO_2 crucible, these being placed in an iron crucible, which is evacuated and sealed. This assembly is then heated at 1200°C. The pO_2 is controlled by the W/WO_2 equilibrium, this giving the maximum oxygen content in the oxycarbide. At 1473°K, the pO_2 of the $W(a = 1)/WO_2$ system = 2.76×10^{-13} ats. Note that this technique can be used to fix only 1 point on the ternary diagram.

An isopiestic technique was also considered, but no metal/oxide system has a suitable vapour pressure/pO_2 combination.

C. W_2C - W(C,O) BOUNDARY

Since W_2C (if stable) is in equilibrium with WC, it should also be in equilibrium with W(C,O) over a certain composition range. Thus, if we equilibrate W_2C, WC, and WO_2 in an evacuated closed container, according to the phase rule we should again obtain an invariant system.

Note that if we consider WORRELL's[4] data for W_2C and WC formation, the respective standard free energies of formation at 1473°K are -7,900 cals. and -8,100 cals. This data suggests that both W_2C and WC can exist in equilibrium, with a given tungsten and carbon activity at this temperature.

Other Phase Boundaries of W(C,O)

The other phase boundaries of W(C,O) are the WO_2/W(C,O) boundary on the high oxygen side and the C-W(C,O) boundary on the high carbon side of the W-C-O ternary diagram.

D. C - W(C,O) BOUNDARY

A flowing gas technique for investigating this boundary is obviously unsuitable. The pO_2's are too high to use an isopiestic technique for changing the oxygen activity. Thus the only possible technique is a closed crucible one using carbon in contact with WC and WO_2. This technique obtains just 1 point. However, the equilibrium p_{CO} is prohibitively high - 810 atmospheres - and thus no investigation of this boundary will be made.

E. WO_2 - W(C,O) BOUNDARY

From the phase rule, we must control the activity of one of the components. As previously mentioned, activity/composition data for tungsten alloys are not available. Thus we must control the pO_2. Given in Table 4 are the pO_2's, a_W, a_C, p_{CO} and N_{WO}/N_{WC} in equilibrium with WO_2 at unity activity at 1473°K.

TABLE 4

pO_2 (ats.)	N_{WO}	N_{WC}	a_W	a_C	p_{CO} (ats.)
1.82×10^{-10}	3.5×10^{-2}	.9965	1.52×10^{-3}	35.84	
7.29×10^{-12}	1.74	.826	3.8×10^{-2}	1.23	
1.82×10^{-12}	.349	.651	.15	.24	114.8
4.5×10^{-13}	.695	.305	.61	2.84×10^{-2}	
2.76×10^{-13}	>1		1.0		
2.0×10^{-13}			1.39		
7.29×10^{-14}			3.79		

The above table indicates that at a pO_2 of less than 3×10^{-13} and greater than 6×10^{-12} ats., WO_2 and W(C,O) cannot exist in equilibrium. Even in the range where equilibrium is possible, p_{CO} is much greater than unity - thus this boundary will not be investigated.

III. ASSESSMENT OF TECHNIQUES

A. CO/CO_2 EQUILIBRATION

In the present state of knowledge of activities in tungsten-platinum solid solutions, this is the only technique which can be used to study the single phase $WC_{1-x}O_x$ in the range $.1 \geq x > 0$ according to the ideal model.

B. CO EQUILIBRATION

By passing CO (or CO-purified argon mixtures), this technique will be used to study the W - $WC_{1-x}O_x$ boundary in the range $.1 > x \geq 0$.

C. CLOSED CRUCIBLE EQUILIBRATION

This type of investigation will be used for the following:-

(1) investigation of the maximum oxygen content of W(C,O) at 1200°C by equilibration of W and WC, in a WO_2 crucible, these being contained inside an evacuated and sealed container;

(2) investigation of a possible W_2C/WC equilibrium at 1200°C by equilibration of WO_2, W_2C and WC as in (1).

D. OTHER TECHNIQUES

An e.m.f. technique employing the cell $W/WF_4/CaF_2(S)/W_2C/WC/WF_4$ (similar to that used by ARONSON & SADOFSKY[25] in their work on Thorium Carbide non-stoicheiometry) has also been considered for investigating the W-C system with particular regard to W_2C/WC equilibria. However, due to the high volatility of tungsten fluorides, this technique is experimentally difficult and thus will not be further considered.

IV. EXPERIMENTAL DETAILS

A. MATERIALS

The chemical materials used in the course of the experiments are as follows:-

Tungsten Carbide (WC): This was obtained as PROLITE GRADE A powder from Murex Ltd., Rainham, Essex, the purity being at least 99.7 wt.% WC, with maximum free carbon .1% and total carbon 6.1 to 6.2%.

Tungsten Powder: obtained from Murex Ltd., as PROLITE GRADE A powder, of purity greater than 99.7%W.

Tungsten Trioxide: obtained from Hopkin & Williams, Chadwell Heath, Essex, as laboratory grade material of approximately 99.5% WO_3.

B. FABRICATION TECHNIQUES

Tungsten carbide and tungsten metal were both used as pellets (except where otherwise stated), made from the "as received" powder. The material was sieved to 300 mesh size and compacted in a "vinamyl" mould of the shape given in Fig. 6, p.19, under a ram pressure of 25 T.S.I. .5 gms. of material was used for each pellet, the pellet produced being standardised to a height of 3 mm. No binder was used as it was found that the compacts were rigid enough without, if carefully handled.

C. MATERIALS ANALYSES

Analyses were performed on a central portion 3 mm. across x 2 mm. high, of the pellet produced during an experimental run. The pellet was gripped in tweezers and ground down to size on

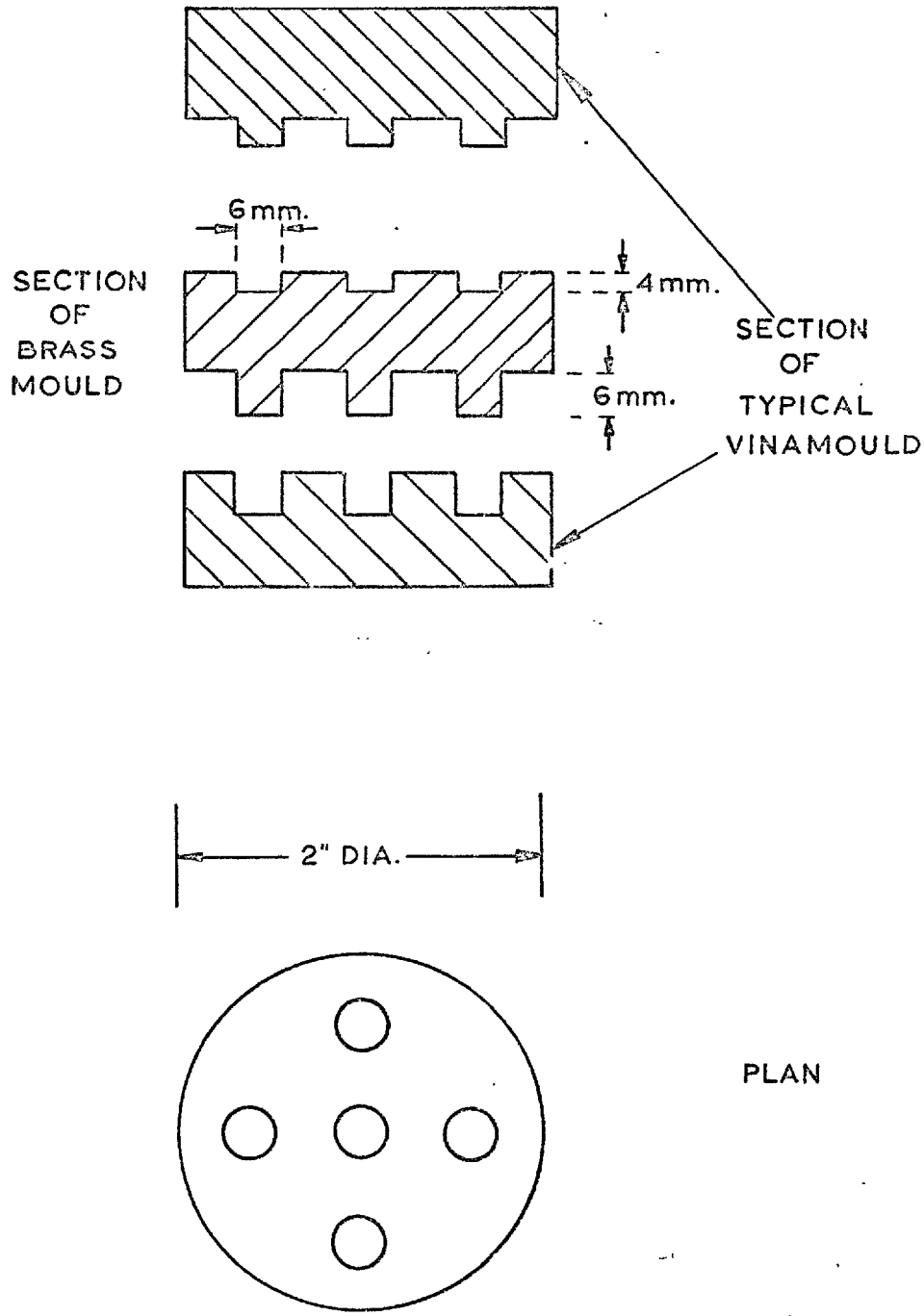

Fig.6 VINAMOULD BRASS MOULD 'PAIR'

400 mesh SiC paper under cyclohexane (to reduce any risk of surface oxidation). It was then 'cleaned' in an ultrasonic bath using cyclohexane again as the cleaning vibrating liquid medium. The following analyses were then performed:-

(1) X-ray Analysis

Both starting materials and products were subject to Debye Scherrer X-ray analysis. All materials were ground up carefully in an agate mortar in a dry box; part of the fraction passing through a 300 mesh sieve was loaded into a .3mm. dia. glass capillary* and installed in a 114.6 mm. dia. camera, except where otherwise stated. Samples were exposed to Ni filtered CuKα radiation for a period not greater than 6 hours. Initial identification of hexagonal phases was done on a Bunn Chart and lattice data was obtained using the method of successive approximations[26]. 210, 211, 300 and 301 reflections (both Kα_1 and Kα_2) were used for ascertaining the a_0 parameter. For c_0, the 102, 112, 103 (both CuKα_1 and CuKα_2) reflections, and the 113 CuKα_1 reflections were used, the 113 CuKα_2 reflection not being used because of difficulty with accurate measurement due to overlap with the 212 CuKα_1 reflection. Note that no radiation of longer wavelength to separate these two lines is suitable, as $\sin\theta$ is greater than 1 for cobalt, the next suitable target. X-ray diffractometer techniques were found to be little help in resolving the lines.

Using this method of successive approximation for c_0 and a_0, the lattice data can be taken as accurate to $\pm$ .0001 A°. All body-centred cubic patterns obtained were those of tungsten and were thus not measured.

---

* Source:- PANTAK, Vale Road, Windsor, England.

(2) Chemical Analyses

All analyses for nitrogen and oxygen were done at A.E.R.E., Harwell, as were most of the carbon analyses. The values quoted for Oxygen contained can be taken as being accurate to ± 10%; the blank observed for Oxygen analyses being about 20% of the observed Oxygen contained value.

In most cases tungsten contents were obtained by difference. Some carbon analyses were also done at the Analytical Services Laboratory, Imperial College, as were some tungsten analyses. Also, electron probe examinations for distributions of oxygen and carbon across a few samples were done at the Analytical Services Laboratory.

D. FREE-FLOWING GASEOUS EQUILIBRATIONS

The apparatus used is as shown in Fig. 7, page 22. Both flowmeters were calibrated using a soap bubble flowmeter, the orifice on the CO_2 flowmeter being adjusted to give a maximum flow-rate of 15 c.c./minute, and that of the CO flowmeter to give a maximum flow-rate of 650 c.c./minute. As can be appreciated, at the high flow-rate end of the CO range, a certain amount of scatter occurred in the calibration. At the maximum flowrate used in investigation of the W(C,O) single phase region, nominally 420 c.c./minute, this scatter was ± 10 c.c./minute. Good consistency was obtained on the CO_2 flowmeter calibration. The total error corresponded to a variation in the CO/CO_2 ratio of ±1 at the maximum CO flowrate used. At lower CO/CO_2 ratios, the error was less than this.

The Pt - 10% Rh furnace was wound so that it had a 2" long hot zone which was found to have a temperature variation of

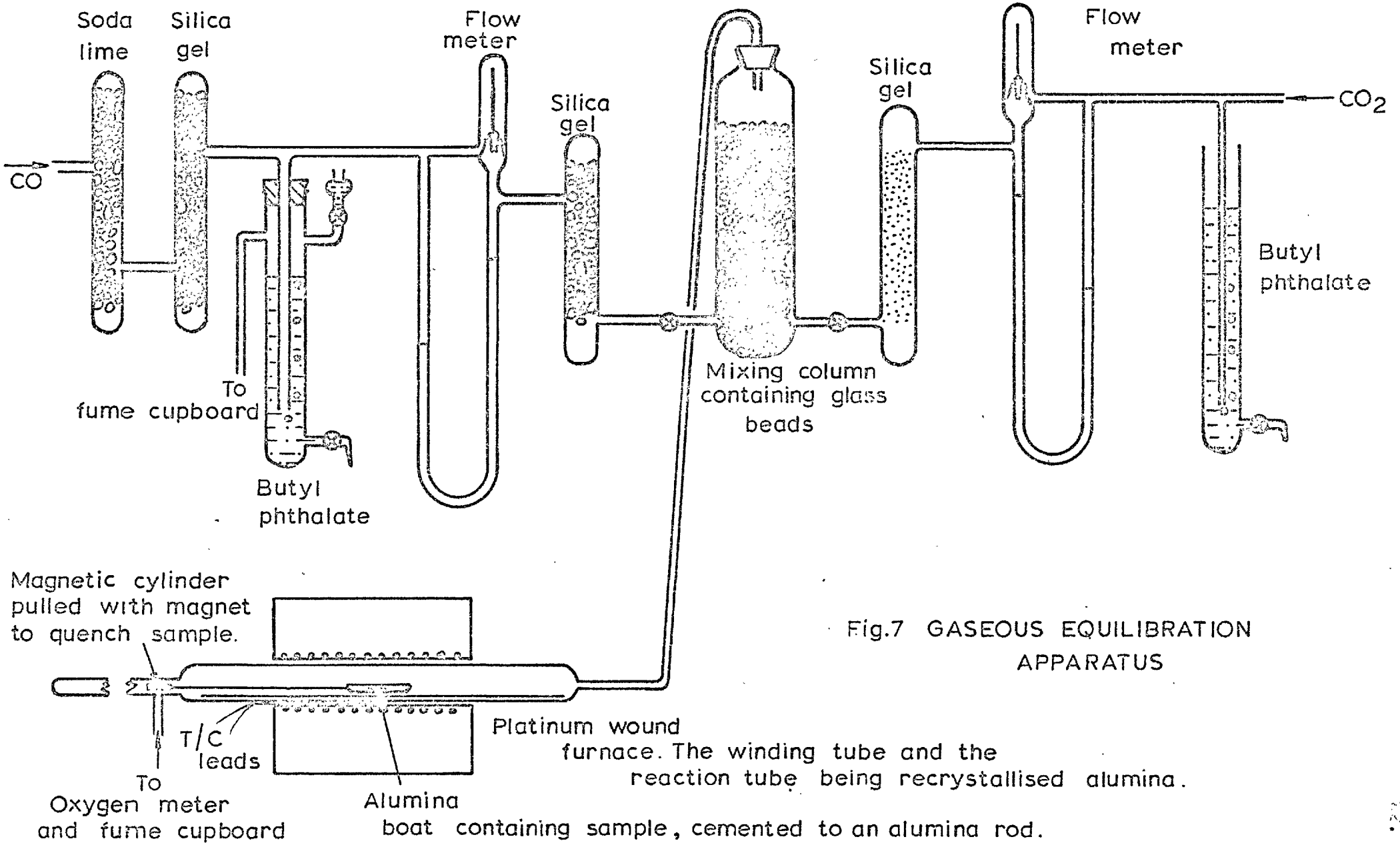

Fig.7 GASEOUS EQUILIBRATION APPARATUS

$\pm$ 1.5°C along its length. The refractory tubes were supplied by Morgans Refractories of Neston, Cheshire, the main furnace tube having dimensions 45 x 38 x 670 mm.

For introduction into the furnace, solid specimens -

/tungsten or tungsten carbide in the case of the single phase W(C,O) region, excess tungsten powder and tungsten carbide in the case of the W/W(C,O) boundary/

were placed in an alumina boat to which had been cemented, using R101 cement, an alumina rod, at the other end of which was "Araldited" a cylindrical solid piece of iron. On commencement of a run, this attachment was placed in the left-hand end of the furnace assembly.

After flushing out the apparatus with the gas mixture to be used in the run, the specimens were introduced into the hot zone of the furnace by bringing up a magnet alongside the iron piece at the end of the crucible assembly and drawing the magnet towards the furnace, taking care to avoid tipping of the crucible contents. After an appropriate time the boat assembly was magnetically withdrawn, and air quenching of the specimens took place in the cool left-hand end of the furnace assembly. The cooling of the specimens to room temperature required about 15 minutes after which time, with the gas mixture supply off, the specimens were withdrawn and placed in a desiccator prior to analysis.

Initially progress towards equilibrium was followed by using a calcia-stabilised zirconia tube (supplied by Zirconal Processes Ltd., Bromley, Kent) in connection with a vibron-electrometer (input impedance 10^{14} Ohms), to monitor the potential of the outgoing gases. However, after 2-3 days of initial stability, e.m.f. readings off the tube became erratic. After an appropriate

time, the specimens were removed, and the tube was examined and found to have extensive blackening over its end surface which had been at 800°C. Two possible causes can be put forward for the observed phenomena:-

(i) Dissolution of carbon from the gas phase at less than unit activity into the Zirconia lattice;

(ii) The Zirconia became non-stoicheiometric, due to the low oxygen partial pressure, resulting in n-type conduction and a consequent lowering of the e.m.f.

Neither of these arguments has been experimentally confirmed, but in the light of the data of STEELE[27] and in personal usage in 'carbon-free' atmospheres of much lower oxygen potentials (see Page 78, Chapter 3), it is felt that (i) is probably correct.

As a result of these troubles with the Zirconia tube, monitoring of the gas was discontinued, and the optimum time for equilibration of samples was found by exposing samples to the same conditions for successively longer periods of time until chemical and X-ray data showed equilibrium to have been achieved.

E. CLOSED CRUCIBLE EQUILIBRATION

The materials to be equilibrated were tungsten, tungsten dioxide, and tungsten carbide (WC). The WO_2 for the equilibration was prepared using the apparatus previously shown in Fig. 7, p.22. Let us consider the following reaction:-

$$WO_3 = WO_2 + \tfrac{1}{2}O_2$$

$$\Delta G^\circ_T = 63000 - 55.1T + 10.2T \log T$$

which at 1473°K yields the following data:-

$$\Delta G^{\circ}_{1473} = -29.4 \text{ K cals.}$$

equilibrium pO_2 = 2×10^{-9} ats.

equilibrium CO/CO_2 = 1:10 approx.

Thus, to prepare the WO_2, the WO_3 powder was equilibrated in the hot zone of the above furnace at 1200°C for 48 hours under a CO/CO_2 ratio of 1:1. The material produced, which did not react with the alumina boat containing it, was subjected to X-ray analysis and the powder pattern showed it to be WO_2. The initial idea was to use the WO_2 in the form of a fabricated crucible, but it was finally decided to use it in powder form mixed with tungsten powder, as this would provide a more intimate reaction mixture with the WC. It was also decided to use a 'Purox' alumina crucible as a container for the reacting species.

After carefully depositing a standard pellet of WC in the base of the alumina container, excess tungsten dioxide-tungsten powder mixture was spread over the top of it and the alumina crucible carefully transferred to the iron container*, previously de-greased in acetone, shown in Fig. 8a, p.26. Sealing and evacuation procedures are the same as those described by N.A. JAVED[23]. It was then placed, as shown, in the furnace assembly in Fig. 9, p. 27, with a getter of Ti granules on top. After evacuation of the furnace down to 55 microns with a single-stage rotary pump to show gas tightness, the furnace was flushed out with gettered argon. The exit gases were continuously monitored on a stabilised Zirconia tube at 800°C, and after the partial oxygen pressure in the exit gases was less than 10^{-12}ats.,

---

* All iron crucibles were made from Remko Pure Iron obtained from Ernst B. Westman Ltd., London.

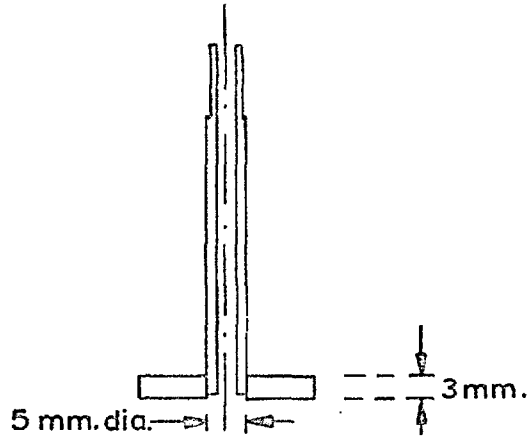

Fig. 8a.

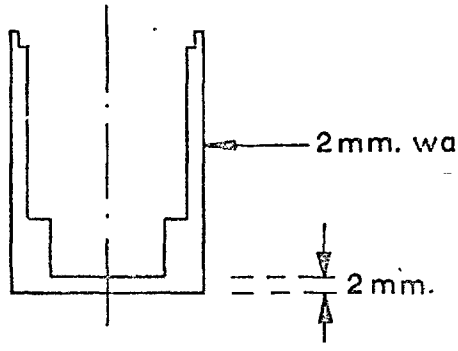

SCALE - FULL SIZE

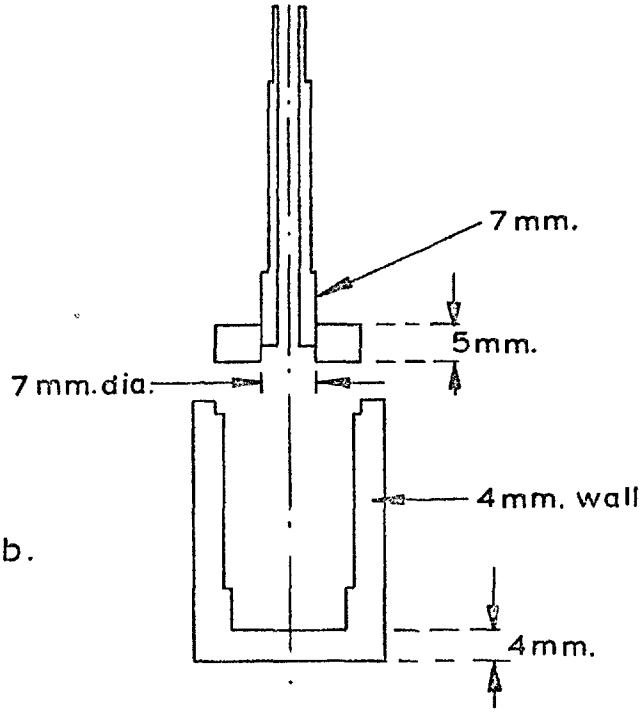

Fig. 8b.

CRUCIBLES USED IN CLOSED CRUCIBLE EQUILIBRATIONS

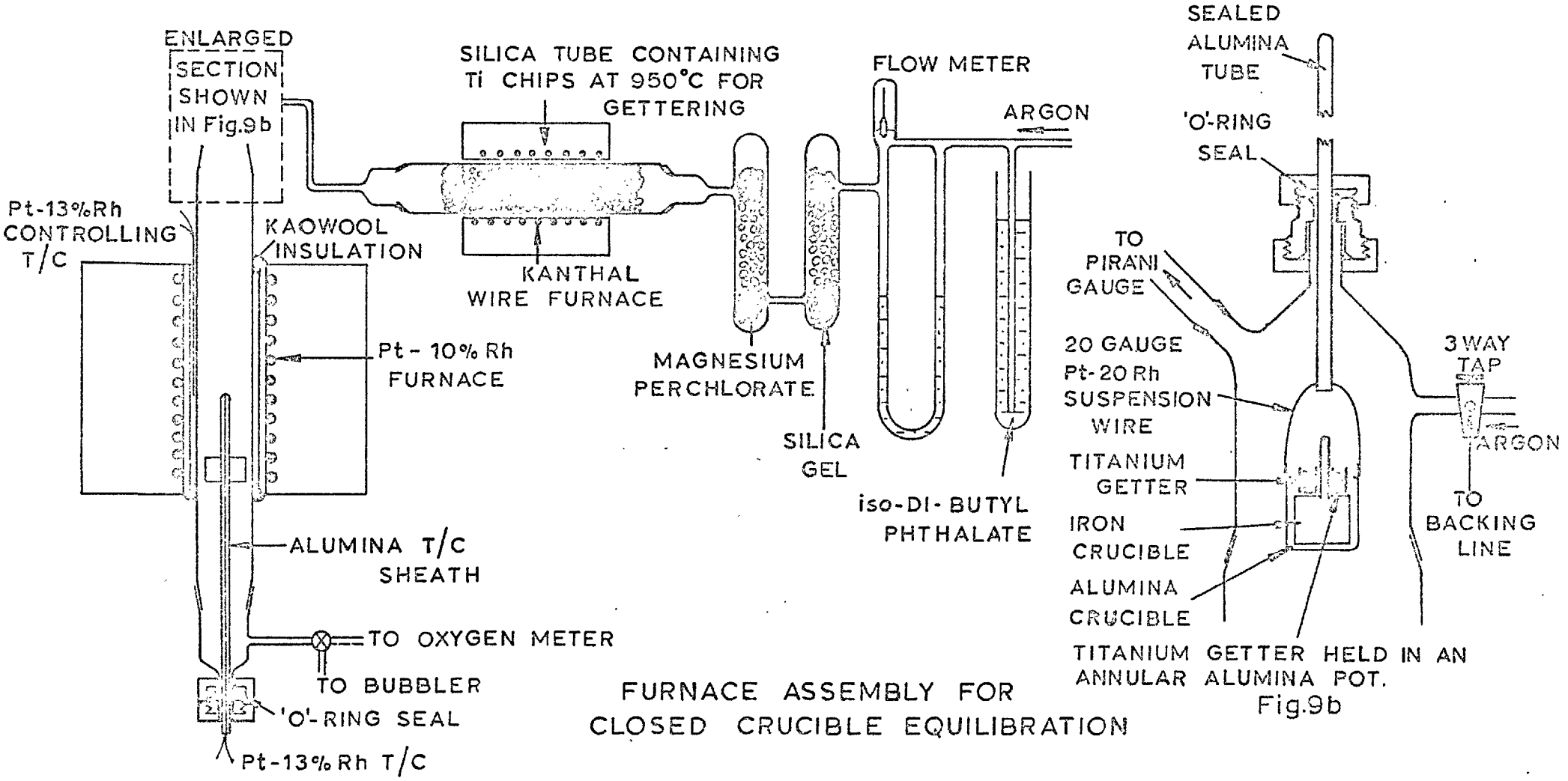

Fig.9a.

FURNACE ASSEMBLY FOR CLOSED CRUCIBLE EQUILIBRATION

Fig.9b

(the equilibrium pO_2 for Fe/FeO at 1200°C), the iron crucible assembly was inserted into the hot zone onto the top of the alumina tube containing the thermocouple. After 6 days the crucible was withdrawn from the hot zone into the cooler part of the tube to be air-quenched. When cool, the crucible was transferred to a dry box, assembled in a clamping device, and the lid removed using a "Monument" brand tube cutter. The products were then analysed by X-ray.

It was noticed that the base of the crucible had bowed out and fractured, and thus the base of the succeeding crucible was doubled in thickness. This time, the lid bowed out and the weld of the lid to the body had fractured. These failures ultimately led to the design of crucible shown in Fig. 8b, p.26, which did not fracture during experimentation. In all cases, no reaction had occurred between the alumina crucible inside the iron container, and the reacting species therein.

V. EXPERIMENTAL RESULTS

A. W(C,O) SINGLE PHASE REGION

(1) Experimental Conditions

Experiment No.	Solid Starting Materials	Equilibration time (hrs.)	CO/CO_2 gas ratio	Activity of Carbon	Partial Oxygen Pressure
1	W	100	7:1	5.3×10^{-3}	2.24×10^{-13}
2	W	140	30:1	2.5×10^{-2}	1.22×10^{-14}
3	W	120	21:1	1.7×10^{-2}	2.49×10^{-14}
4	W	120	27:1	2.26×10^{-2}	1.50×10^{-14}
5	W	120	12:1	9.6×10^{-3}	7.61×10^{-14}
6	WC	144	13:1	1.32×10^{-2}	6.48×10^{-14}
7	WC	96	65:1	5.55×10^{-2}	2.59×10^{-15}
8	WC	120	65:1	5.55×10^{-2}	2.59×10^{-15}
9	WC	142	65:1	5.55×10^{-2}	2.59×10^{-15}
10	WC	140	70:1	5.99×10^{-2}	2.24×10^{-15}
11	WC	140	45:1	3.82×10^{-2}	5.42×10^{-15}
12	WC	170	60:1	5.14×10^{-2}	3.03×10^{-15}

(2) X-ray and Chemical Analyses of Reaction Products

Experiment No.	Phase Identity	Chemical Analysis* W	C	O	Formula	Lattice Parameter Data c/a ratio
1	W(C,O)	93.68	6.1	.22¥		Hexagonal
2	W					
3	W	99.54	.04	.42		
4	W	99.69	.01	.30		
5	W	99.19	.01	.80#		
6	W	99.59	.06	.35		
7	W(C,O)	93.47	6.4	.13		.9759
8	W(C,O)	93.8	6.1	.10	$WCO_{.01}$	.9762
9	W(C,O)	94.3	5.6	.10	$WC_{.91}O_{.01}$	.9764
10	W(C,O)		5.8			.9763
11	W					
12	W					
	WC "as received"	93.49	6.4	.11		.9758

* Nitrogen analyses are not quoted since in all cases they were less than .02%.

¥ Mistakenly samples 1 and 2 were ground up together by the analyst.

\# Cooled to room temperature in gas mixture for last 10 hours of run, due to overnight power failure.

B. W-W(C,O) BOUNDARY

(1) Equilibration with CO

Experiment No.	Initial Solid Phases	p_{CO}	Final Solid Phases	Equilibration time	Lattice Parameter c/a ratio	Analysis
14	W, 'WC'	1	W(C,O)	130 hrs.	.9763	C = 6.06%

(2) Closed Crucible Equilibration

Experiment No.	Initial Solid Phases	Final Solid Phase	Equilibration time	Lattice Data
15	W, WO_2, 'WC'	W	144 hrs.*	-
16	do.	W	144 " *	-
17	do.	W	144	-

* Crucible punctured.

VI DISCUSSION

In the CO/CO_2 equilibrations, equilibrium was approached from both sides, i.e. first using tungsten and then tungsten carbide as the starting solid species. From the results on page 30 it can be seen that W is the stable phase in the range $60:1 > CO/CO_2 \gtrsim 12:1$ and W(C,O) is the stable phase at $CO/CO_2 > 65:1$. Further it can be seen that the equilibrium hexagonal phase at $CO/CO_2 = 65:1$ contains $.12 \pm .01\%$ Oxygen. This was not sufficient to compensate for the depletion of the carbon lattice. Thus, taking the general formula as WC_xO_y, x+y is less than 1 in the range studied, although depletion of the carbide lattice decreases with increasing CO/CO_2 ratio.

The above can be explained in terms of a qualitative theory of bonding.

In the transition metals bonding is considered to be of the resonating 'spd' hybrid type. Taking melting point as a criterion of bond strength, it can be seen that this increases to a maximum in group 6 of the Periodic Table, and also increases going down each group. It is considered that this maximum in group 6 arises due to the fact that if the p orbital contribution is small, an electron population/atom of approximately 6 would correspond to the maximum number of unpaired spins. Thereafter, going further across the Periodic Table, the melting point decreases. The reason for the melting point increase going down a group could be that, as one goes down a group, the hybrid orbitals are larger and thus greater orbital overlap can occur before nuclear repulsion sets in.

In the case of monocarbides of these transition metals, which are either of the NaCl type or are simple hexagonal, the maximum

melting point occurs between groups 4 and 5. Thus it has been postulated that this maximum occurs earlier than in the transition metals themselves, because C tends to act as a donor of electrons. In support of this, DEMPSEY[28] has pointed out that many of the hard metal carbides fall into approximate correspondence with the transition metals themselves as regards stability v. hybrid electron concentration per metal atom. Further, by use of a tight binding approximation, LYE & LOGOTHETIS[29] have provided experimental support for C acting as a donor of electrons. They have shown that in TiC, the Ti outer electron configuration is $3d_{\varepsilon}^{9/4}\ 3d_{\gamma}^{7/4}\ 4s^{3/4}\ 4p^{1/2}$, and the carbon configuration is $2s^2\ 2p^{3/4}$. It seems unlikely, in view of the high ionisation potential of carbon, that actual electron transfer occurs: COSTA & CONTÉ[30] suggest a semi-polar type of bond between metal and carbon atoms.

The bonding still tends to be mainly metallic, and it is suggested that metal-metal bonding is important in earlier transition metal carbides, with the C-C bonding increasing in importance in groups 6, 7 and 8.

In transition metal oxides, bonding is slightly different than in the carbides, since although oxygen still tends to act as a donor to the metal atoms, it is very much more electro-negative than carbon. Thus in the case of TiO, the bonding still tends to be mainly metallic, but there is also a greater ionic content than in TiC. TiO is the only stable group 4 monoxide, the succeeding oxides being dioxides which are mainly ionic. The trend of monoxide stability going across the table is that groups 5, 7 and 8 monoxides are stable, whereas in group 6 no monoxides exist. It is felt that not enough is known about electron distribution in oxides to give a complete picture, and a simple

picture as for the bonding in transition metals and carbides is unlikely; therefore no further description will be given here.

For oxide-carbide solid solutions, consideration of the foregoing possible description of bonding in carbides and oxides would suggest that at the temperature of experimentation

(i) for solution of carbide MC of high stability and an oxide MO of low stability, solution would tend to be very restricted at the high oxide end, but much greater at the high carbide end;

(ii) for a complete range of solid solution formation, both MO and MC should be stable, e.g. TiC and TiO;

(iii) solution of a carbide of relatively low stability and an oxide of high stability, at the high carbide end of the mixture, would tend to be very restricted due to the high oxygen electronegativity, and therefore small donating power; at the high oxide end the solution would be slightly greater.

(iv) solution of carbide and oxide of low stability will be negligible.

The Tungsten-Carbon-Oxygen system lies between classes (i) and (iv). Tungsten carbide is a carbide of medium stability, being the last stable solid monocarbide in group 6. With the non-existence of solid WO at unit activity, very restricted W(C,O) formation will occur as borne out by the results in Experiments 7, 8 and 9.

At lower temperatures the entropy contribution to the free energy of formation of WO would be less important, and thus WO would be relatively more stable. This would account for the oxycarbide observed by LUX & IGNATOWICZ[21] (see p. 9).

When CO/CO_2 mixtures are passed over W, what is the reason for different products at different CO/CO_2 ratios? The following reactions between W, CO and CO_2 are possible:-

$$1.\quad W + CO_2 = CO + WO$$
$$2.\quad W + CO = WO + C$$
$$3.\quad W + CO_2 = WC + O_2$$
$$4.\quad W + 2CO = WC + CO_2$$

Reaction 2 would be very unfavourable since a large amount of energy would be required for the oxygen states in CO to be disarranged, and this would not be compensated for by increased stability of the WO. Reaction 3 would also be unfavourable since high energy would be required to remove oxygen from the CO_2, and this would not be compensated for by the formation of WC of relatively low stability.

Thus, if we consider the equilibrium constants for equations 1 and 4, we have -

$$K_1 = \frac{p_{CO}\ a_{WO}}{a_W\ p_{CO_2}}$$

$$K_4 = \frac{p_{CO_2}\ a_{WC}}{p^2_{CO}\ a_W}$$

The trend would be that at low CO/CO_2, the production of WO would be more favourable, and at high CO/CO_2, the production of WC would be more favourable. However, WO is not stable at unit activity, and thus we obtain W as the stable phase at lower CO/CO_2, and WC with a small amount of oxygen (i.e. WO formation at very low activity) at high CO/CO_2. At even lower CO/CO_2 ratios, WO_2 formation would tend to occur.

In addition to reactions 1 to 4, further possible reactions between W and CO/CO_2 are -

$$2W + CO_2 = W_2C + O_2$$
$$2W + 2CO = W_2C + CO_2$$
$$2W + 2CO = W_2C + O_2$$

It can be seen from the CO/CO_2 equilibration results that the only range over which W_2C can exist if stable at 1473°K is in the range $65:1 > CO/CO_2 > 60:1$, corresponding to a range of carbon potentials from -8.46 to -8.69 K.cals. This range of carbon potentials could cover the equilibria W/W_2C, the single phase W_2C and the 'WC'/W_2C equilibrium. (The 'WC' will be taken as $WC_{.91}$, the species with the maximum W/C ratio observed in this investigation, the small oxygen content not being considered in this context). If W_2C is unstable, the $W/WC_{.91}$ equilibrium can be taken as occurring between CO/CO_2 = 60:1 and 65:1.

Using the carbon potential data for experiments 9, 10 and 12, in conjunction with the above possibilities, we can plot a graph of ΔG/gm.atom at 1473°K for the W - C system as shown in Fig. 10, p.37. Also superimposed on the graph are ORTON's[6] data and WORRELL's[4] data for the W-C system, and both KUBASCHEWSKI's[22] data and GLEISER & CHIPMAN's[3] extrapolated data, for WC formation.

Both GLEISER & CHIPMAN's data and KUBASCHEWSKI's data lie in the region of my results: both WORRELL's and ORTON's data are far different, and it is suggested that these be discounted. The approximate extrapolated data obtained for WC is

$$\Delta G^\circ_{1473} = -8.6 \pm .3 \text{K.cal. per mole.}$$

The position over the existence of W_2C stability is undecided, although it is felt that it is unlikely that both W_2C/W and W_2C/WC

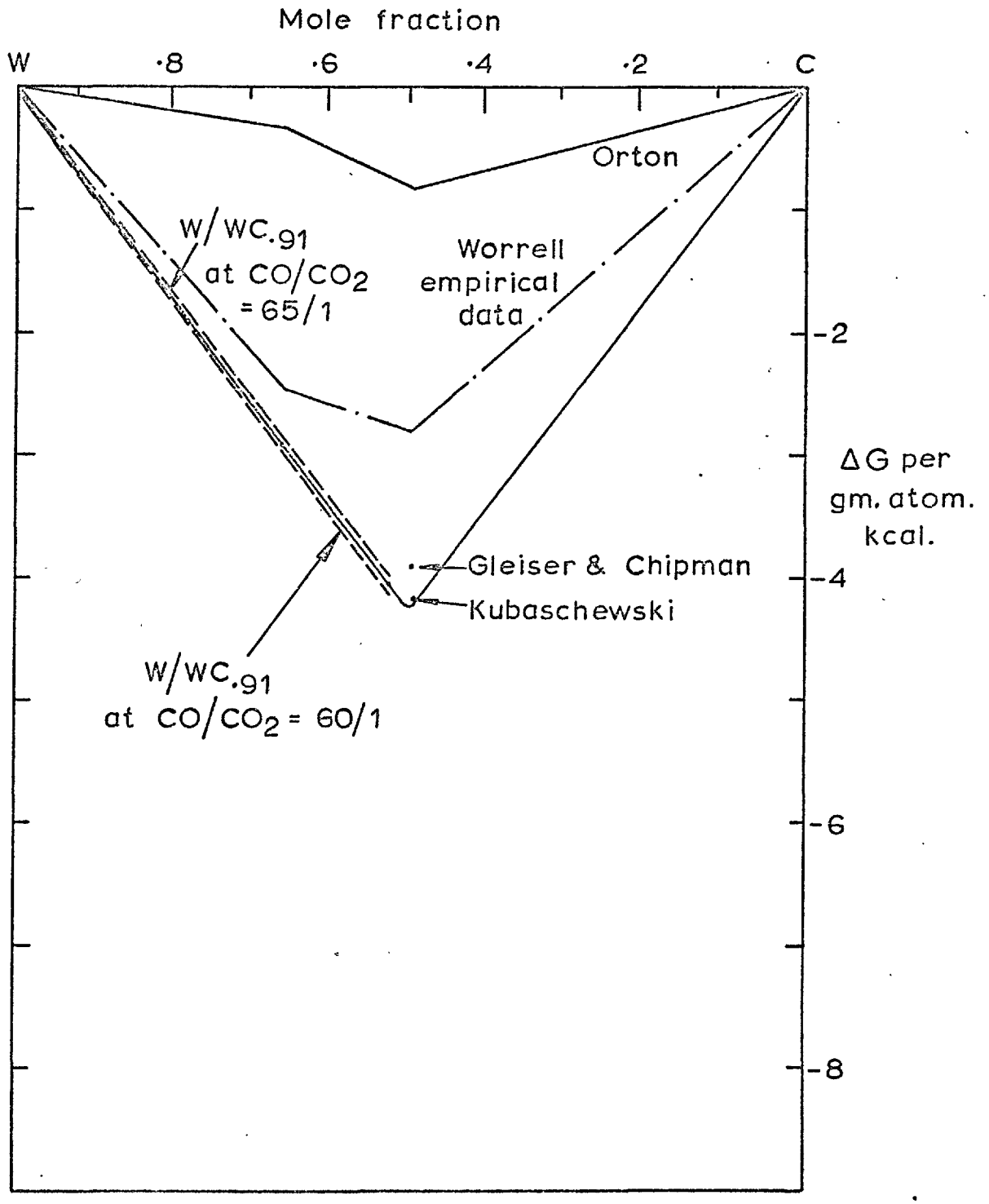

Fig.10 FREE ENERGY PER GRAM ATOM FOR W-C SYSTEM AT 1200°C

equilibria could exist over the range of carbon potentials corresponding to $65{:}1 > CO/CO_2 > 60{:}1$.

From experiment 9 it can be seen that oxygen solubility in the carbide lattice is very low. Thus essentially, these experiments show that tungsten carbide is capable of existing hypostoicheiometrically with respect to carbon, at least down to $WC_{.91}$: this contrasts with the data of COFFMAN[31] et al ($WC_{.973}$) and PARTHÉ[32] ($WC_{.986}$).

It should be noted that the WC as received was a very dilute oxycarbide and further that it had a free carbon content of .27% or greater.

Examination of the results for experiments 7 - 10 shows that the range of the c/a lattice parameter observed was .0006. In the series 7 - 9, an increase in the c/a ratio is observed. Between 7 and 8 part of this increase could be due to a lowering of oxygen content, and part due to the decrease in C content from the stoicheiometric value. Also, a further increase in c/a occurs in going from 8 to 9, the oxygen content remaining constant. This suggests a peak in the c/a value and could be explained as for TiC by NORTON[37].

As concerns the $W/WC/WO_2$ equilibrium (discounting the formation of W_2C) the following equilibria are possible:-

5. $W + WO_2 = WO$
6. $WC + WO_2 = 2W + CO_2$
7. $2WC + WO_2 = 3W + 2CO$

Considering the energy of the system, both equations 6 and 7 are possible due to the stability of the CO and CO_2 molecules, with possibly equation 7 predominating due to the greater stability of the CO. Equation 5 would tend to occur only to a small extent

since, as seen in experiment 9, even with a large amount of WC the existence of WO was very limited at 1200°C.

With the evidence in favour of KUBASCHEWSKI's data for WC being satisfactory, one can calculate the equilibrium values of the p_{CO} and p_{CO_2} for equations 6 and 7, using W, W C and WO_2 at unit activity. As mentioned in § I, B(2), the free energy for the W/WO_2 equilibrium is fairly well established, the majority falling in the range between that of KUBASCHEWSKI[22] - (ΔG° = -138,500 + 36.6T cals.) and those of FRANK, RIZZO and BIDWELL[16] (ΔG° = -137,320 + 40.62T cals.), although this latter was obtained in the temperature range 700 - 1000°C. The equilibrium p_{CO} and p_{CO_2} for equations 6 and 7, corresponding to the above values for the W/WO_2 equilibrium, and using KUBASCHEWSKI's[22] values for ΔG°_{WC}, ΔG°_{CO}, $\Delta G^\circ_{CO_2}$, are shown in Table 5, along with other useful data.

TABLE 5

Source of W/WO_2 Data	pO_2 ats.	p_{CO}(ats.)	a_C	p_{CO_2}	Total P (ats.)
KUBASCHEWSKI	2.92×10^{-13}	10.93	5.86×10^{-2}	1.8	12.73
FRANK, RIZZO AND BIDWELL	3.0×10^{-12}	36.1	5.4×10^{-2}	18.9	55

It should be noticed that the above table assumes that $W/WO_2/WC$ are all present at unit activity, where in Table 4 the derivation of values assumes WO is present combined with WC, i.e., W C is present at less than unit activity. The derivation of the values of a_{WO} given in Table 4 further involves the assumption that ΔG/gm.atom WO = ΔG/gm.atom WO_2. It can be seen from Table 4 that a_{WO} in W(C,O) in equilibrium with W/WO_2 at unit activity

is greater than 1 using the aforementioned criterion, and thus it is suggested that if there is a $W/W(C,O)/WO_2$ equilibrium, ΔG/gm.atom WO should be less negative than assumed. Partial support to ΔG/gm.atom being much less negative for WO than WO_2, is given by experiments 7 - 9, where the range of existence of W(C,O) as regards oxygen content is seen to be very restricted at this temperature, i.e. the WO activity is very low.

Further, assuming the activity of WC is approximately unity, it can be appreciated from the foregoing total pressures why ruptured crucibles occurred in Experiments 15 and 16, especially if FRANK, RIZZO & BIDWELL's data is correct. After adopting the final design of crucible, no rupture occurred during experiment 17 - this was confirmed by testing both crucible and lid for gas tightness, by "Araldite" both the sawn-off lid and the sawn-off body of the iron crucible to glass tubing and pumping out each composite. In this experiment, again tungsten was the only solid phase obtained, i.e. the equilibrium of equations 6 and 7 must have been displaced to the right, due to removal of CO and CO_2. This removal could be due to the following causes:-

(a) Permeation of CO/CO_2 through the crucible under the large physical pressure gradients obtaining - see Table 5. It is suggested that this is negligible since the CO and CO_2 are large molecules and thus diffusion of these species would be slow.

(b) Diffusion of Carbon and Oxygen through the iron. Oxygen diffusion through the crucible will be very limited, since the oxygen gradient across the crucible is very small, as is the oxygen solubility in the iron, at 1200°C. The

diffusion of carbon through the iron crucible is probably one of the main causes. The solubility of Carbon in δ iron at the CO/CO_2 ratios involved is approximately .9 wt.%[33], and by using FICK's Law with a value for D of 2×10^{-6} cm.^{2}/sec.[34], it can be shown that the loss of C is about 6.5 gms. in the 6 days of the run. The amount of carbon originally in the crucible was only about 20 mgms. (The weight of the WC pellet is approximately 300 mgm). Thus decarbonisation would be complete.

(c) Internal oxidation of the crucible.
The equilibrium pO_2 for Fe/FeO at 1200°C = 8×10^{-11} ats. If Frank, Rizzo & Bidwell's data for W/WO_2 is correct, the pO_2 corresponding to the equilibrium CO/CO_2 ratio in the $W/WC/WO_2$ mixture is 3.5×10^{-11} ats.

Obviously, to reduce the risk of internal oxidation it would be much better to use a material for the crucible which was in equilibrium with a much higher oxygen potential e.g. Nickel. However, it can be shown that over the same period (6 days), about 4.5 gms. of carbon would diffuse out. Thus even using a Nickel crucible, about 70 gms. of WC alone would be required to have excess tungsten carbide with appropriate amounts of WO_2 and tungsten. Obviously, if the carbon solubility in the iron had been more fully looked into, under the conditions obtaining within the crucible, prior to their execution, Experiments 15 - 17 would not have been attempted. Even using a nickel crucible is impractical and it is felt that study of the $W/WO_2/WC$ equilibrium by this technique is not a practical proposition.

On the W - W(C,O) phase boundary, it is noticed that all the tungsten in contact with the carbide phase has been converted to the same phase after reacting with CO nominally at 1 atmosphere pressure. Bearing these conditions in mind, a non-equilibrium situation obtains.

Regardless of the data used for the W/WO_2 equilibrium, i.e. those of KUBASCHEWSKI or FRANK et al, if p_{CO} is present at 1 atmosphere, an equilibrium should obtain between W and W(C,O), the oxygen content of the W(C,O) being dependant on which is the correct data.

At 1473°K, we can show that for equilibrium dissociation of CO to CO_2 and C, the CO/CO_2 ratio obtaining is approximately 40:1. Thus an explanation of the tungsten in original contact with WC being converted to a hexagonal phase is that partial dissociation of CO has occurred, and that under the conditions obtaining, the phase rule is satisfied. The time for this run is less than the optimum, but it is considered that equilibrium is approached - both lattice data and carbon content of the final 'tungsten species' and final carbide species are the same. It should be noted that the carbon content of the carbide produced is slightly less than that of Experiment 8 which was exposed to CO/CO_2 = 65:1 for 120 hours.

CONCLUSIONS

It has been shown that the range of oxide carbide solid solutions in the W-C-O system at 1200°C is very small, the maximum oxygen content being .13%. A qualitative bonding explanation has been suggested for this. It has further been shown that the carbide with a small amount of oxygen is capable of existing substoicheiometrically to the composition $WC_{.91}O_{.01}$, and it is

tentatively suggested that a maximum in the c/a ratio exists in the carbide lattice. It is concluded that it is not possible to study -

(i) the $W/WC/WO_2$ equilibrium due to lack of suitable crucible material,

and (ii) the W/W(C,O) phase boundary

at this temperature.

Finally, it is suggested that W_2C does not exist at 1200°C.

In view of the small range of existence of the W(C,O) phase at 1200°C, it is considered worth while that the system should be studied at a lower temperature, e.g. 900°C. Although the kinetics would be slower at this lower temperature, thermodynamic criteria would be much more favourable for a wider range of solution than that obtaining in the present investigation.

CHAPTER 3

TITANIUM - CARBON - OXYGEN SYSTEM

I. REVIEW OF LITERATURE

A. Ti-C SYSTEM

(1) Constitutional Data

The temperature-composition diagram of CADOFF & NIELSEN[25] is shown in Fig. 11. The system contains the following phases:-

α Ti - This phase is hexagonal and is generally accepted as being stable up to 881°C, and having a maximum solubility of 2 atomic % Carbon at 910 ± 30°C.

β Ti - This is a body centred cubic structure. The data in Fig. 11 suggest that this phase is stable up to 1725°C with a C solubility of 3.1 atomic % at 1750 ± 20°C. Later data of RUDY[36] et al suggest stability up to 1670°C with a maximum C content of 0.5 atomic % at 1645°C.

Samples of Titanium containing between 0.5 and 2.5 wt.% oxygen have been observed, by STONE & MARGOLIN[38], to melt at 1770°C, and thus it is suggested that the peritectic melting and the increased solubility of carbon reported by CADOFF & NIELSEN is due to oxygen contamination. The data for β Ti of RUDY are taken as being more accurate.

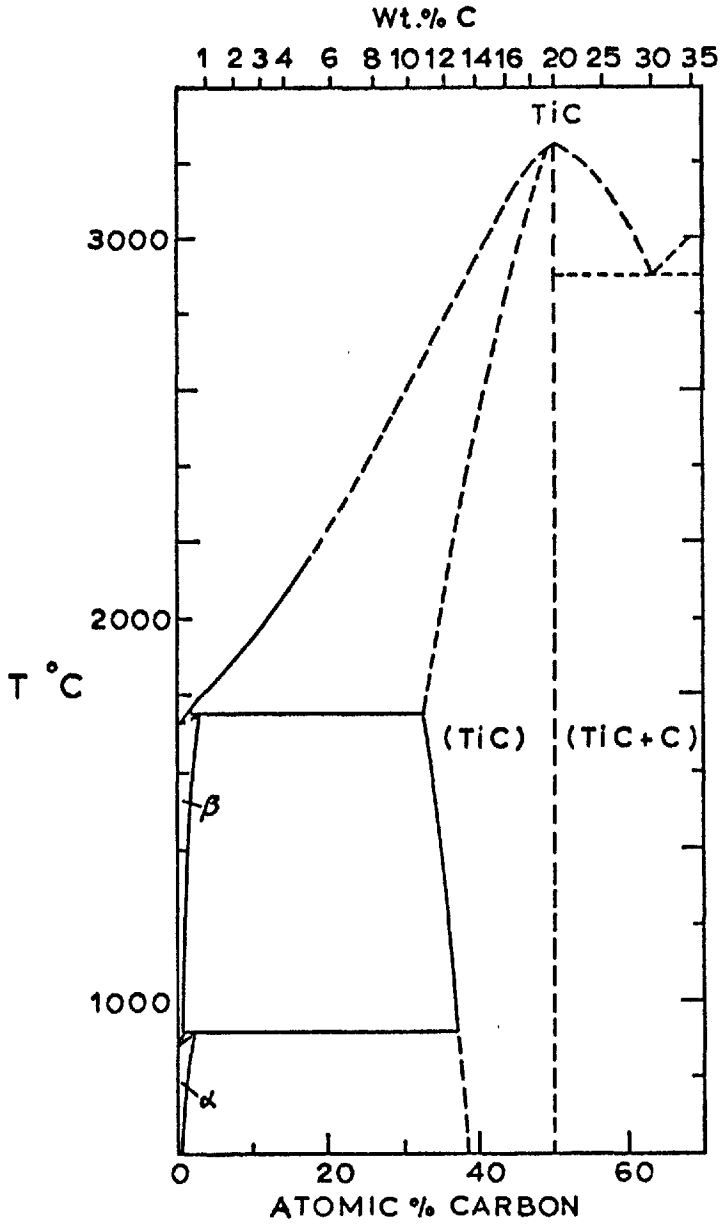

Fig.11 C-Ti CONSTITUTIONAL DIAGRAM

TiC - This is the only carbide existing in this system, and it has an NaCl structure. Fig.11 shows that its stoicheiometry varies from 50 atomic % carbon to 32 atomic % carbon at 1750 ± 20°C. RUDY's data shows that its stoicheiometry varies from 50 atomic % carbon at the C-TiC eutectic at 2776°C, to 47.5 atomic % at 2200°C on the TiC-C boundary, to a minimum of 28 atomic % at 1668°C on the TiC-Ti boundary. A good collection of all known lattice parameter data for the range of TiC existence has been compiled by STORMS[20] and is shown in Fig.12. One point of interest is the maximum "a" parameter value of 4.331A° first observed by NORTON[37], at a composition of 46 atomic % carbon.

A later investigation by GRIEVSON[39] of the Ti-C system at 1000°C showed that the range of stability of TiC was from 28.4 atomic % C on the Ti-TiC boundary, to 50.6 atomic % on the C-Tic boundary, i.e. TiC could be slightly hyperstoicheiometric as well as hypostoicheiometric. The change in C content was reflected in a change in the lattice parameter, from 4.288 A° at the Ti-TiC boundary, increasing to a maximum of 4.321 A° at 47.6 atomic % C, decreasing to 4.320 A° at the stoicheiometric composition, and then to 4.317 A° at the hyperstoicheiometric limit. Again, we notice a maximum lattice parameter at a substoicheiometric composition.

Comparison of the data of STORMS & GRIEVSON yields the following:-

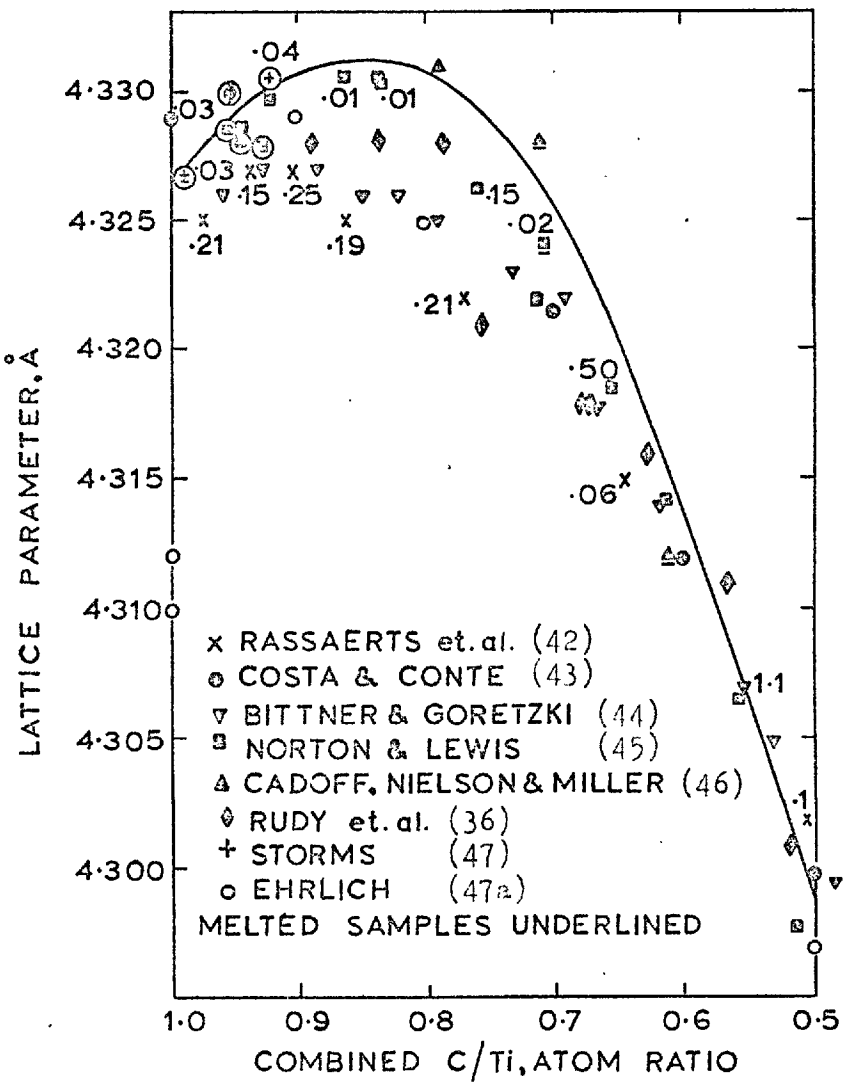

ENCIRCLED SAMPLES CONTAIN FREE C
Wt % O SHOWN.

Fig. 12. LATTICE PARAMETER OF TiC AS A FUNCTION OF COMPOSITION

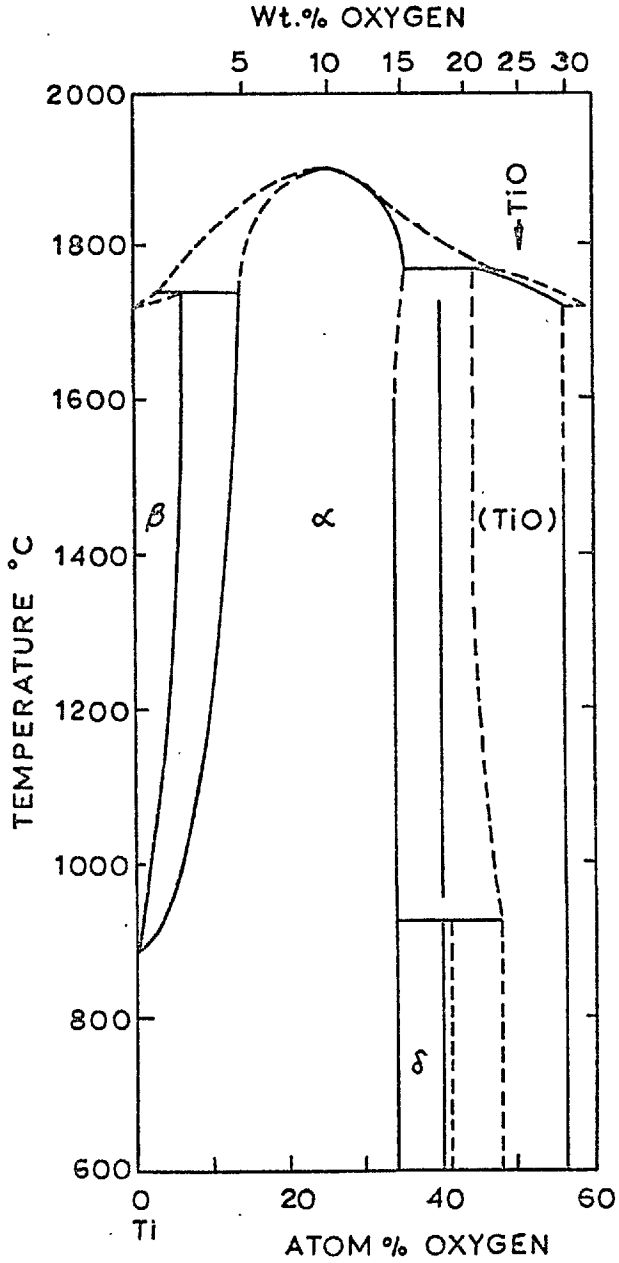

Fig. 13. OXYGEN TITANIUM PHASE DIAGRAM

	Experimenter	T.	Atomic % C	Lattice parameter of TiC at hypostoicheiometric limit
(a)	Storms	1000°C	33	4.299A°
	Grievson	"	28.4	4.288A°
				Maximum Lattice Parameter of TiC
(b)	Storms		45.9	4.331A°
	Grievson		47.6	4.321A°

Both lattice parameter, and lower stoicheiometry limits of GRIEVSON can be accounted for by assuming oxygen and nitrogen impurities in the carbide. Thus the data of STORMS should be taken as being the more reliable.

(c) The hyperstoicheiometric nature of TiC observed by GRIEVSON could possibly be due to free graphite, since carbon was at unit activity in the methane-hydrogen mixture used to produce this composition.

(d) A maximum in the plot of lattice parameter v. composition of TiC has been observed by NORTON[37], GRIEVSON[39], and STORMS[40], although not the same maximum. The decrease in lattice parameter from its maximum, as the stoicheiometric composition is approached, has been explained[37] in terms of the following effects of carbon as it is introduced into the carbide lattice:-

(i) Increase in the 'a' parameter due to distortion of the lattice - i.e. size effect.

(ii) Increased binding in the lattice and thus a tendency towards lattice contraction due to the electron donation by the carbon.

As the stoicheiometric composition is approached, (ii) becomes relatively more important than (i) with a resultant maximum in the lattice parameter. It is probable that the same mechanism is operative as regards the 'c' parameter in the case of tungsten. Suggestions that it might be due to a metal deficit on the cation sublattice have been shown to be unfounded by STORMS[40] and NORTON[37], (using precision density measurements) who found less than 0.5% of the total metal position vacant, and by GORBUNOV[41], (using neutron diffraction techniques) who found the carbon atoms statistically distributed in the octahedral voids and all the metal atom positions filled by metal atoms.

(2) Thermodynamic Data

The only free energy data available for 'Tic' of any stoicheiometry is that of KUBASCHEWSKI[22] (for $TiC_{0.996}$), obtained by using Humphrey's heat of formation data and the Cp values of Kelly, and is as follows:-

$$\Delta G^{\circ}_{T} = -44,600 + 3.16T$$

between α - β Ti transition temperature (1155°K) and 2000°K.

GRIEVSON[39] presents carbon activity - composition data for titanium carbide containing between 50.6 and 40.6 atomic % carbon at 1000°C, from which the carbon activity at the stoicheiometric composition can be shown to be .75.

B. Ti-O SYSTEM

(1) Constitutional Data

Shown in Fig. 13 (p.47) is the temperature-composition diagram for this system. Besides there being extensive solution of oxygen in Ti, the following oxides exist, each with its own range of stoicheiometry:-

(i) Ti_2O : Existence as a separate phase is dubious.

(ii) Ti_3O_2 : A hexagonal phase stable up to 925°C, having the following parameters:-

$a = 4.991\ A^\circ \quad c = 2.879\ A^\circ$

(iii) TiO : This possesses a sodium chloride structure, with $a = 4.180\ A^\circ$ at the stoicheiometric composition.

(iv) Ti_2O_3 : Rhombohedral, with 'a' = 5.45 A°.

(v)* Ti_3O_5 : Monoclinic.

(vi)* Seven other forms ranging from $TiO_{1.75}$ to $TiO_{1.9}$ - Magneli phases.

(vii)* TiO_2 : Tetragonal 'a' = 4.5937 A°
'c' = 2.958 A°
at the stoicheiometric composition.

---

* These are not shown in Fig. 13, as the portion of the diagram beyond 60 atomic % has not been sufficiently well investigated to be able to show the constitutional data with any confidence.

(2) Thermodynamic Data

TiO Various conflicting data exist for TiO. This is partially due to the wide range of stoicheiometry of TiO, in common with all compounds in this system.

The following data are presented:-

(a) KUBASCHEWSKI & DENCH[48], by equilibration of rare earth oxides with Ti metal, and plotting $\overline{\Delta G}_{O_2}$ v. oxygen content, obtained the following:-

$$\Delta G^{\circ}_{T} = -122{,}300 + 21.3T \text{ cals./mole TiO}$$

giving $\Delta G^{\circ}_{1273^{\circ}K} = -95.2$ K cals.

(b) KUBASCHEWSKI[49], using a combination of the above data with data obtained

(i) on oxygen solubility in α and β Ti, and

(ii) on TiO_{2-x}

presents a reassessment of his data which at 1000°C gives:-

$$\Delta G^{\circ}_{1273^{\circ}K} = -85 \text{ K.cal./mole TiO.}$$

(c) Using ΔH°_{298}, ΔS°_{298} and the required enthalpy and entropy increments listed by MAH[50], we obtain

$$\Delta G^{\circ}_{1273^{\circ}K} = -95.3 \text{ K.cal./mole TiO}$$

(d) WICKS & BLOCK[51] present the following:-

$$\Delta G^{\circ}_{1273^{\circ}K} = -95.5 \text{ K.cal./mole TiO.}$$

As can be seen from the above data, there is a discrepancy of about 10 K.cals. between source (b) and the other sources. Two ways of bringing (b) to conformity with (a), (c) and (d) are -

(i) to make ΔH°_{298} for TiO 10 K.cals. more negative,

or (ii) to increase S°_{298} α-TiO by 5 e.u.

ΔH°_{298} measurements made by VOLF[52] and by HUMPHREY[53] agree well with each other. If entropy contributions in TiO due to spin magnetic effects and lattice vacancy contributions are taken into account, this gives an increase of 4 e.u. in S°_{298} of α-TiO.

(e) In a mass spectrometric study, GILLES[54] obtained

ΔH°_{298} = 717 K.cals. for the reaction

$Ti_3O_5(s) = 3TiO(g) + 2[O](g)$

Taking appropriate heat capacity, entropy (S°_{298} TiO compensated as described above) and enthalpy data from Thermochemical Tables[55], we obtain -

$\Delta G^{\circ}_{1273^{\circ}K}$ = -96.2 K.cals. for $Ti(\beta) + \frac{1}{2}O_2 = TiO(\rho)$.

Thus, considering all the above data, KUBASCHEWSKI & DENCH's original data are considered to be as good as the other available data, and it is this data which will be used in subsequent calculations involving 'TiO'.

Other Titanium Oxides

KUBASCHEWSKI's[22] data for other titanium oxides are -

$Ti_2O_3 = 2TiO + \frac{1}{2}O_2$ $\quad \Delta G^{\circ} = 114{,}150 - 19.05T$

$2Ti_3O_5 = 3Ti_2O_3 + \frac{1}{2}O_2$ $\quad \Delta G^{\circ} = 88{,}500 - 19.7T$

$3TiO_2 = Ti_3O_5 + \frac{1}{2}O_2$ $\quad \Delta G^{\circ} = 73{,}000 - 23.0T$

Further data can be deduced using mass spectrometric data and thermochemical tables[55] as previously described for TiO.

C. Ti - C - O SYSTEM

TiC and TiO, having favourable atom size ratio, valence effect and crystal structure, form a continuous series of solid solutions, TiC initially dissolving oxygen by O/C substitution, but by higher oxide formation in oxygen excess.

Several investigations have been carried out on this system BRANTLEY & BECKMANN[56] obtained the following expression for the p_{CO} over TiO_2 'in equilibrium' with carbon:-

$$\log_{10} p_{CO} \text{ (ats.)} = \frac{-5024}{T} + 3.829$$

Substituting $T = 1573^{\circ}K$ (the temperature to be used in this investigation) into the above, $p_{CO} = 1.15$ ats. They assumed the relevant equation for TiO_2 reduction to be

$$TiO_2 + 3C = TiC + 2CO$$

as they detected TiO_2, C and TiC only, in the reaction mixture, by X-ray analysis. Using the relevant free-energy data, and assuming unit activity of the solid species, the equilibrium p_{CO} at $1573^{\circ}K = 0.66$ ats. Considering the time allowed for the 'equilibration' - $1\frac{1}{2}$ hours - which was obviously too short for any degree of equilibrium to be achieved, the above equation for p_{CO} can be disregarded, and likewise other papers using this data.

KUTSEV & ORMONT[57] found that in the temperature range $1600 - 2000^{\circ}C$ with an excess of carbon, both Ti_2O_3 and $TiO_{1.7}$ were reduced to TiC_xO_y at equilibrium.

KOSOLAPOVA[58] et al reacted TiO_2 and TiC in vacuum (10^{-3} mm. of Hg) at temperatures ranging from $1000^{\circ}C$ to $2000^{\circ}C$, for 1 hour, and they found that formation of solid solutions of Ti(C,O) first occurred at $1700^{\circ}C$. It is suggested that Ti(C,O)

formation would have occurred at much lower temperatures with longer holding times.

STONE & MARGOLIN[38] produced sections of the Ti-C-N, Ti-C-O and Ti-N-O systems for the composition range up to 2 wt.% C and 5 wt.% O and N respectively, i.e. the primary interstitial solution range, at temperatures ranging from 800°C to 1300°C.

D. Ti - C - N and Ti - C - N - O SYSTEMS

Although this investigation is concerned with the Ti-C-O system, it is considered worthwhile to mention ternary and quaternary formation of compounds containing nitrogen, due to the ease of mutual interchangeability of C, N and O interstitially, as mentioned in Chapter I.

A thermodynamic study has been carried out by GRIEVSON[39], who equilibrated 'TiC' of known composition with gas mixtures of known nitrogen potential. In this way he was able to investigate the whole of the Ti(C,N) phase field, and he found that across the ideal 'TiC'-'TiN' stoicheiometric solution, the behaviour was regular.

Two studies on lattice parameter-composition relationships have been carried out on this system. DUWEZ & ODELL[59] found that lattice parameters of solid solutions of stoicheiometric TiC and TiN followed Vegard's law. As well as verifying DUWEZ & ODELL's data, GRIEVSON obtained lattice parameter composition data for the non-stoicheiometric regions.

II. THERMODYNAMIC ASSESSMENT

We can consider 'Ti(C,O)' solid solutions to be pseudo-binaries of 'TiC' and 'TiO'. The pO_2 in equilibrium with Ti/TiO (stoicheiometric), both at unit activity at 1300°C is 4.4×10^{-25} ats. Thus, to avoid formation of 'TiO' as a separate phase when preparing Ti(C,O) in equilibrium with Ti, the pO_2 should be less than this.

A. Ti(C,O) REGION

Within this single phase region, we can derive an expression relating N_{TiO} and N_{TiC} to the pO_2 and C activity. Considering the equations -

$$TiC = Ti + C \qquad K_{TiC} = \frac{a_{Ti}\, a_C}{a_{TiC}}$$

$$TiO = Ti + \tfrac{1}{2}O_2 \qquad K_{TiO} = \frac{a_{Ti}\, p^{\frac{1}{2}}O_2}{a_{TiO}}$$

$$CO + \tfrac{1}{2}O_2 = CO_2 \qquad K_{CO_2} = \frac{p_{CO_2}}{p_{CO}\, p^{\frac{1}{2}}O_2}$$

$$2CO = CO_2 + C \qquad K^1_{CO} = \frac{p_{CO_2}\, a_C}{p^2_{CO}}$$

and eliminating a_C, a_{Ti} and pO_2 we obtain the expression

$$\frac{N_{TiO}}{N_{TiC}} = \frac{K_{TiC}}{K_{CO_2} K_{TiO} K^1_{CO}} \; \frac{1}{\left(\frac{p_{CO}}{p_{CO_2}}\right)^2} \; \frac{1}{p_{CO}}$$

for equilibrium with CO and CO_2 within the single phase region. At 1573°K, the above expression equals

$$\frac{N_{TiO}}{N_{TiC}} = \frac{2.635 \times 10^5}{\left(\frac{p_{CO}}{p_{CO_2}}\right)^2 p_{CO}}$$

Substituting values of CO/CO_2 in the final equation, and assuming a total pressure of 1 atmosphere, we can obtain N_{TiO} and N_{TiC}, and substituting back into the original equations, we can obtain a_{Ti}, a_C and equilibrium pO_2. These are shown in Appendix II.

A further technique that could be used for controlling the pO_2 is the isopiestic technique as used by JAVED. At 1573°K, the metal-oxide system with suitable pO_2 vapour pressure combination is Ca-CaO. The variation of log pO_2 with calcium temperature (CaO at 1573°K) is shown graphically in Fig. 14, Appendix III.

As we proceed across the Ti-rich boundary of Ti(C,O) we will have on the TiC-rich side, Ti in equilibrium with Ti(C,O), and towards the TiO-rich side, the oxide Ti_2O in equilibrium with Ti(C,O).

B. Ti - Ti(C,O) PHASE BOUNDARY

Using an a_{Ti} of unity, we can calculate the equilibrium pO_2, C activity, and p_{CO} for various values of N_{TiO} and N_{TiC} - these are shown in the following Table:-

TABLE 6

N_{TiO}	N_{TiC}	pO_2 (ats.)	a_C	a_{Ti}	p_{CO} (ats.)
.05	.95	5.2×10^{-28}	2.87×10^{-6}	1	1.29×10^{-11}
.1	.9	4.36×10^{-27}	2.81×10^{-6}		3.625×10^{-11}
.2	.8	1.75×10^{-26}	2.5×10^{-6}		6.43×10^{-11}
.4	.6	6.97×10^{-26}	1.88×10^{-6}		9.68×10^{-11}
.5	.5	1.09×10^{-25}	1.56×10^{-6}		1.04×10^{-10}
.6	.4	1.57×10^{-25}	1.25×10^{-6}		9.68×10^{-11}
.8	.2	2.8×10^{-25}	6.25×10^{-7}		6.43×10^{-11}
.9	.1	3.6×10^{-25}	3.125×10^{-7}		3.62×10^{-11}

However, at some position on the Ti-rich boundary, the Ti_2O/Ti(C,O) equilibrium will take over.

C. Ti_2O - Ti(C,O) BOUNDARY

For the reaction $Ti + \frac{1}{2}O_2 = TiO$ at 1573°K, ΔG° = -88.8K.cal. No thermodynamic data are available for Ti_2O, but we can obtain an approximate value (c.f. W-O) from a plot of Δ G/gm.atom v. composition for the Ti-O system at 1573°K. This yields a value of $\Delta G^\circ_{Ti_2O}$ = -59K. cals., and a value of $K_{Ti_2O} = 1.55 \times 10^8$ at 1573°K. Substituting for various values of pO_2, and using $a_{Ti_2O} = 1$, we obtain the data shown in the following table:-

TABLE 7

pO_2	a_{Ti}	N_{TiO}	N_{TiC}	a_C	p_{CO}
10^{-25}	316	-	-	-	-
10^{-16}	.803	10^4	-	-	-

From the above, it does not seem that a Ti_2O/Ti(C,O) boundary exists.

Other Boundaries of Ti(C,O)

Since carbon is in equilibrium with TiC, one would also expect it to be in equilibrium with Ti(C,O). Similarly, one would expect Ti_2O_3 to be in equilibrium with Ti(C,O).

D. C - Ti(C,O) BOUNDARY

If we use excess carbon to fix the carbon activity and various values for a_{TiC}, we can calculate a_{Ti}, pO_2 and p_{CO} at 1573°K as shown below:-

N_{TiC}	N_{TiO}	a_{Ti}	a_C	pO_2 (ats.)	p_{CO} (ats.)
.9	.1	2.81×10^{-6}	1	2.89×10^{-16}	3.32
.1	.9	3.125×10^{-7}	1	1.89×10^{-12}	268

To control the pO_2, the following techniques are available:-

(1) CO/CO_2 Mixtures or Pure CO

It can be shown that the CO/CO_2 ratio in equilibrium with carbon at 1573°K is very large, practically pure CO for a total pressure of 1 atmosphere. Using p_{CO} = 1 atmosphere, and unit C activity, we obtain the following data:-

a_{TiO}	a_{TiC}	$p^{\frac{1}{2}}O_2$ (ats.)
0.028	.972	5.12×10^{-9}

(2) Isopiestic Technique

Equilibrium pO_2 v. T_{ca} values are given in Fig. 14, Appendix III.

(3) Using TiO_2 as the oxygen potential controlling medium, we can calculate, for the reaction $TiO_2 + 3C = TiC + 2CO$, the p_{CO} for various activities of TiC. Data are given below for the extremes of activity:-

N_{TiC}	N_{TiO}	p_{CO} (ats.)
.1	.9	8.72
.9	.1	2.6

(4) (a) By using a Ti_3O_5/TiO_2 mixture in contact with TiC, we can control the O and Ti activities, thus giving an effective 'TiO' activity. The data obtained are as shown below:-

$$a_{Ti} = 1.585 \times 10^{-11}$$

$$p^{\frac{1}{2}}O_2 = 6.76 \times 10^{-6} \text{ (ats.)}$$

$$N_{TiO} = 2.24 \times 10^{-4}$$

(b) Similarly to (a), using a Ti_2O_3/Ti_3O_5 mixture we obtain

$$a_{Ti} = 6.17 \times 10^{-7}$$

$$p^{\frac{1}{2}}O_2 = 1.15 \times 10^{-8} \text{ (ats.)}$$

$$N_{TiO} = 1.49 \times 10^{-2}$$

E. Ti_2O_3 - Ti(C,O) BOUNDARY

Using the equilibrium $Ti_2O_3 = 2TiO + \frac{1}{2}O_2$, and assuming various activities of TiO and unit activity of Ti_2O_3, we obtain the equilibrium pO_2's shown below:-

N_{TiO}	pO_2 (ats.)
.9	6.35×10^{-24}
.8	1.015×10^{-23}
.7	1.73×10^{-23}
.6	3.2×10^{-23}
.5	6.64×10^{-23}
.4	1.63×10^{-22}
.3	5.13×10^{-22}
.2	2.6×10^{-21}
.1	5.76×10^{-20}

These pO_2's all come within the range of the isopiestic technique using Ca/CaO as the pO_2 controlling species.

III. ASSESSMENT OF TECHNIQUES

A. CO/CO_2 EQUILIBRATION

From the data shown in Appendix II it seems at first sight that we can study most of the single phase Ti(C,O) region using this technique. However, using the free energy data for the equation -

$\frac{4}{3}$ TiC + O_2 = $\frac{2}{3}$ Ti_2O_3 + $\frac{4}{3}$ C - ΔG° = -128,320 cals. at 1573°K

it can be shown that for C and O activities corresponding to CO/CO_2 ratios less than 1000, Ti_2O_3 is the stable phase. Thus with the experimental difficulties obtaining at CO/CO_2 ratios in excess of this, this technique will not be used to study the single phase Ti(C,O) region or its phase boundaries.

B. ISOPIESTIC TECHNIQUE

(1) Ti(C,O) Phase

The whole range of partial oxygen pressures likely to be encountered within this region can be covered using this technique* (See Appendix III).

To reduce the activity of Ti, we must alloy it with a metal X conforming to the following specification:-

(a) it must not form carbides;
(b) it must not react with Ca unless data on a Ti - Ca - X ternary are known.

The most feasible solvents for Ti are lead and gold. However, data are unavailable for either of these in a ternary

---

*No Ti-Ca composition diagram is available for this system. Ca-Ti interaction was shown by KOMAREK[60] et al to be negligible at 830°C, the maximum Ca temperature used by them.

with Ti-Ca, and thus, due to lack of time for determination of this data, the single phase Ti(C,O) region will not be investigated.

(2) Ti-Ti(C,O) Boundary

The whole range of this boundary can be covered using an isopiestic technique to fix the pO_2 using Ca/CaO as the metal vapour-oxide species in equilibrium with Ti and TiC. From the thermodynamic analysis it would seem that no Ti_2O/Ti(C,O) boundary exists.

(3) Ti_2O_3 - Ti(C,O) Boundary

The whole range of this boundary also can be covered using the isopiestic technique. The range of pO_2's and p_{Ca}'s are as given below:-

pO_2 1573°K	p_{Ca}
6.35×10^{-24}	.018 mm.
5.76×10^{-20}	1.76×10^{-4} mm.

The pO_2's along both of the above boundaries correspond to using calcium in the solid state. With the low partial pressures of Ca, the kinetics of the Ca/CaO equilibrium will be slow, and with this low oxygen capacity/unit time, equilibration times will be quite long. [Note that the experiments of KOMAREK[60] et al on the Ti-O system were for 100-4300 hours.]

Also, the question arises as to whether CaC_2 will be formed. In Appendix IV relevant carbon activity data for the Ti-C-O system and for the formation of CaC_2 at unit activity are given, from which it can be seen that on the boundaries to be investigated, CaC_2 formation is no problem.

C. CLOSED CRUCIBLE TECHNIQUE

From this Chapter, Section II, D, it can be seen that the available techniques allow us to investigate the C-Ti(C,O) boundary up to an $a_{TiO} = 0.03$ and thus it is felt that investigation of this boundary to this limit is not worth while.

Thus the boundaries to be investigated will be the Ti-Ti(C,O) boundary and, if time permits, the Ti_2O_3 - Ti(C,O) boundary.

IV. EXPERIMENTAL DETAILS

A. PRINCIPLES OF THE ISOPIESTIC TECHNIQUE

The application of the technique to this system essentially involves equilibration of a species with calcium oxide and calcium vapour of known activity. The samples to be equilibrated are held in close physical contact with calcium oxide and equilibrated with calcium vapour inside a closed and evacuated iron crucible placed vertically in a temperature gradient. The vapour pressure of Calcium is kept constant by placing the calcium at the lowest temperature in the system and keeping it constant. At equilibrium the oxygen potential of the calcium/calcium oxide couple is the same as that of the oxygen in the Ti(C,O). It can be calculated using the following equations:-

$$Ca(g) + \tfrac{1}{2}O_2 = CaO \qquad \Delta G_T^\circ = -RT\ln \frac{a_{CaO}}{p^{\frac{1}{2}}_{O_2} p_{Ca}}$$

$$\text{(i)} \quad \Delta G_T^\circ = RT\ln pO_2^{\frac{1}{2}} + RT\ln p_{Ca}$$

where T is the temperature of the carbide samples.

p_{Ca} is the calcium pressure in equilibrium with calcium (liquid or solid) at some lower temperature.

The relative partial molar free energy of oxygen in the sample is given by

$$\text{(ii)} \quad \overline{G}_O - G_O^\circ = \overline{\Delta G_O} = RT\ln pO_2^{\frac{1}{2}}$$

Combination of (i) and (ii) thus gives

$$\overline{\Delta G_O} = RT\ln p^{\frac{1}{2}}O_2 = \Delta G_T^\circ - RT\ln p_{Ca}$$

Thus, if we vary the calcium temperature and therefore the pressure from one experiment to the next, we can vary the oxygen potential in the equilibrated samples.

B. CHEMICAL MATERIALS REQUIRED

(1) Titanium Carbide

Initially TiC, nominally of composition

Total Carbon	19.6%
Free Carbon	.5% max.

was obtained from Murex Ltd. Subsequent analysis of the Titanium Carbide showed the composition to be

	%
W	3
Si	2
Fe	.2
Ti	75
C	19.5
O	.4
N	.9
Total other impurities	.5

and after much searching purer Titanium Carbide of typical percentage composition -

	%
Ni	.002
SiO_2	.025
CaO	.017
Fe	.012
Total Carbon	19.6
Free Carbon	.38

was obtained from The London & Scandinavian Metallurgical Company, London, S.W.19.

(a) Titanium

This was obtained from Johnson Matthey & Co. Ltd., Hatton Garden, London, as specpure grade sponge containing .1% maximum metallic impurities.

(3) Titanium Dioxide

The source of this was Hopkin & Williams, Essex, as "Purified Titanium Oxide" of not less than 98.7% TiO_2. Slightly purer supplies of TiO_2 (not less than 98.9%) were obtained as "Tiona-G Anastase Pigment" from Laporte Industries, Grimsby, Lincs.

Specpure TiO_2 was obtainable from Johnson Matthey & Co. Ltd., but at a prohibitive price.

(4) Calcium Oxide

This was used in the form of crucibles obtained from Consolidated Beryllium, Milford Haven, Pembrokeshire.

(5) Calcium Metal

Supplies of Calcium Metal were obtained from Koch Light Labs., Colnbrook, Bucks., as 99.9% pure grain, having the following impurities in p.p.m. -

Si	Al.	C.	B.	N_2	Cd	Cl	Fe	Li	Mg	Mn
<50	100	40	.2	<50	0.2	80	30	<10	<1000	15

C. PREPARATION OF MATERIALS

(1) Calcium

Although essentially of the composition previously given, all supplies of this material contained substantial amounts of oxide and nitride. Initial equilibrations were made using selected pieces of calcium which appeared shiny, but subsequent analyses of the equilibrated specimens showed these to contain greater than 2 wt.% nitrogen, a possible major source of which was the calcium. As a result of this it was subsequently decided to distil the calcium and this was done in the following manner.

The apparatus used in the distillation is shown in Fig. 15. On the whole, the procedure described by AHMAD[61] was adopted, with the following modifications. Initially the temperature of the tip of the condenser probe (3-400°C) suggested by AHMAD was used. However, it was found that the product obtained was very finely divided and thus easily oxidisable, and was difficult to remove from the condenser probe. The procedure found to give

Key to Fig. 15

1. Iron Crucible.
2. Ceramic Radiation Shield.
3. Iron Inductor.
4. Iron Probe for Calcium deposition.
5. Mullite Sheath for Thermocouple and cooling Argon.
6. Chromel-Alumel Thermocouple to take probe temperature.
7. Chromel-Alumel Thermocouple to take Calcium container temperature.
8. Pyrex glass envelope.
9. Rubber Connector.
10. Chromel-Alumel Thermocouple sealed into rubber with screw clamp, attached to T-piece.
11. Ceramic disc.
12. Rubber bung.
13. Refined Calcium.
14. Coils for Induction Heating.

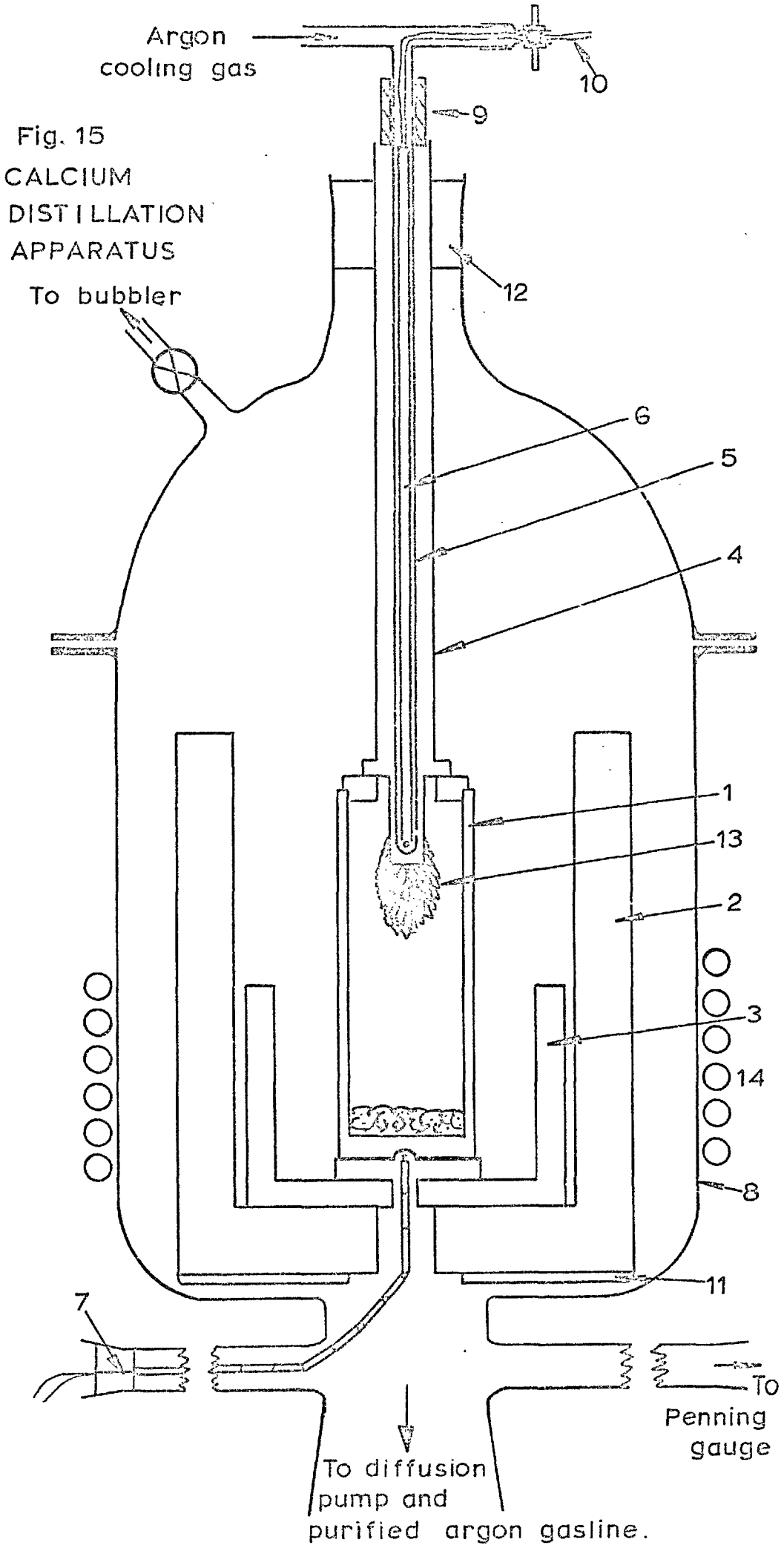

Fig. 15
CALCIUM
DISTILLATION
APPARATUS

the best results was to have the probe at about 370°C for the first hour of the final distillation, to promote nucleation, and subsequently at 450°C to promote growth. Under these conditions the calcium obtained was columnar.

The probe was then removed from the apparatus under a stream of gettered argon and transferred to a dry-box in an argon-filled envelope. The calcium grains could easily be torn from each other and from the probe with thoroughly degreased pliers. The calcium was then placed in a clean glass container in the dry box, the sealed container being removed from the dry-box, evacuated and replaced in the box. Under these conditions the calcium remained quite shiny for greater than 2 months. The total time required to prepare each batch of calcium was about 3 days.

(2) Titanium Monoxide

The titanium monoxide used was prepared by carefully mixing appropriate proportions of TiO_2 and titanium fines ($<$350 mesh) in agate mortar, and then transferring to a thoria crucible, which was installed in a vacuum furnace and gradually heated up to 1600°C. It was kept at this temperature for 4 hours, then taken up to 1700°C (1650°C being the lowest temperature on the liquidus, occurring at the equimolar ThO_2-TiO_2 composition) and then cooled to room temperature over a period of 12 hours. The thoria crucible, after the preparation, was black due to solid solution formation, but the contents of the crucible were yellowish, the colour of 'TiO'.

D. FABRICATION TECHNIQUES

Titanium carbide, and later titanium carbide-titanium oxide mixtures, were used in pellet form. The same fabrication procedures as for tungsten carbide (Chapter 2, § IV, B) were employed, and the same pellet size prepared. Where titanium oxide-titanium carbide mixtures were used as the starting material the titanium oxide was prepared "for pelletising" as follows.

In order to avoid any surface oxidation, the cylinder of TiO, previously prepared, was ground up in an agate mortar in a drybox. The material was very brittle and diffioult to grind up. After grinding up, the 'TiO' was mixed in appropriate proportion with TiC according to the region of the phase boundary under study, and then pelletised. It was found that good compaction of the TiO-TiC mixtures was not obtained till the 'TiO' was less than 350 mesh size. Although the compacts were handleable with care, they were nevertheless less rigid than the purely 'TiC' compacts.

E. MATERIALS ANALYSIS

All analyses of equilibrated pellets were performed on the central portions of the pellet - the dimensions of the central portion being the same as for tungsten (See Chapter 2, § IV, C).

The preparation of the central portion in the case of TiC-TiO-based pellets was the same as for tungsten. However, TiC-based solid solutions were too hard to prepare by this technique and had to be ground to size under cyclohexane using a 'Dremel Mototool' with a diamond-impregnated bit.

(1) Chemical Analyses

All chemical analyses of Ti, C, O, N and Ca (see later) were done at A.E.R.E., Harwell. The accuracy for oxygen analysis is the same as given in Ch. 2, § IV, C(2), the blank observed for the oxygen analysis, using TiC as the starting material, being about 20% of the observed oxygen content value, and when using TiC-TiO mixtures as the starting material, the blank can be considered negligible.

Apart from the equilibrated specimens, the following were also submitted:-

TiC as received	$<$350 mesh
TiO ground-up powder	$<$350 mesh

Electron probe micro-analyses were done at the Analytical Services Laboratory, Imperial College.

(2) X-ray Analyses

The general procedure was the same as that adopted for WC (See Ch. 2, § IV, C(2)). An additional aspect of the procedure was that two layers of Aluminium cooking foil were placed between the specimen and the film to cut out moderate darkening of the film in the back reflection region (due to fluorescence). Optimum exposure times were approximately 5 hours for the cubic phases, and 8 hours for the titanium metal.

For accurate values of the 'a' parameter in the 'TiO', TiC, and equilibrated specimens, the Nelson-Riley extrapolation was used, the most important high angle lines being the CuKα_1, and CuKα_2 reflections from the 331, 420 and 422 planes.

To obtain sharp lines on the X-ray portions of 'TiO', the final procedure adopted was to take a sample $<$250 mesh from the

partially ground material, since when a < 350 mesh sample was used extreme line broadening was obtained in the back reflection region.

X-ray analysis of the titanium after equilibration with Ti(C,O) was also done in order to characterise it. Samples < 250 mesh of the aforementioned Ti and of Ti "as received" were obtained by slight grinding with a pestle and mortar in the drybox.

F. DESIGN OF FURNACE ASSEMBLY, TEMPERATURE CONTROL, AND TEMPERATURE PROFILE

The furnace, brasshead assembly and temperature control equipment are essentially those used by JAVED[23]. The whole assembly is shown in Fig. 16 (p.71). Scructural modifications to the assembly are as follows.

It was considered essential to have a more satisfactory method for supporting the furnace tube than just with clamps at the base of the furnace. The jubilee clip assembly shown in Fig. 16C(p.73) was therefore designed and made, and fixed rigidly by means of the radiating arms, to the frame. To avoid bending of the tube it was steadied at the top by a loose clamp.

A scaffolding assembly was incorporated into the frame so that the bottom brasshead was well supported and accurately positioned when attached to the tube.

Further changes included -

(a) a modified thermocouple support assembly, shown in Fig. 16D (p.73);

(b) evacuating facilities, and an internal oxygen cell/getter assembly - the oxygen cell being used to monitor the oxygen potential of the incoming gas - shown in Fig. 16A (p.72).

Fig. 16

GRADIENT FURNACE ASSEMBLY

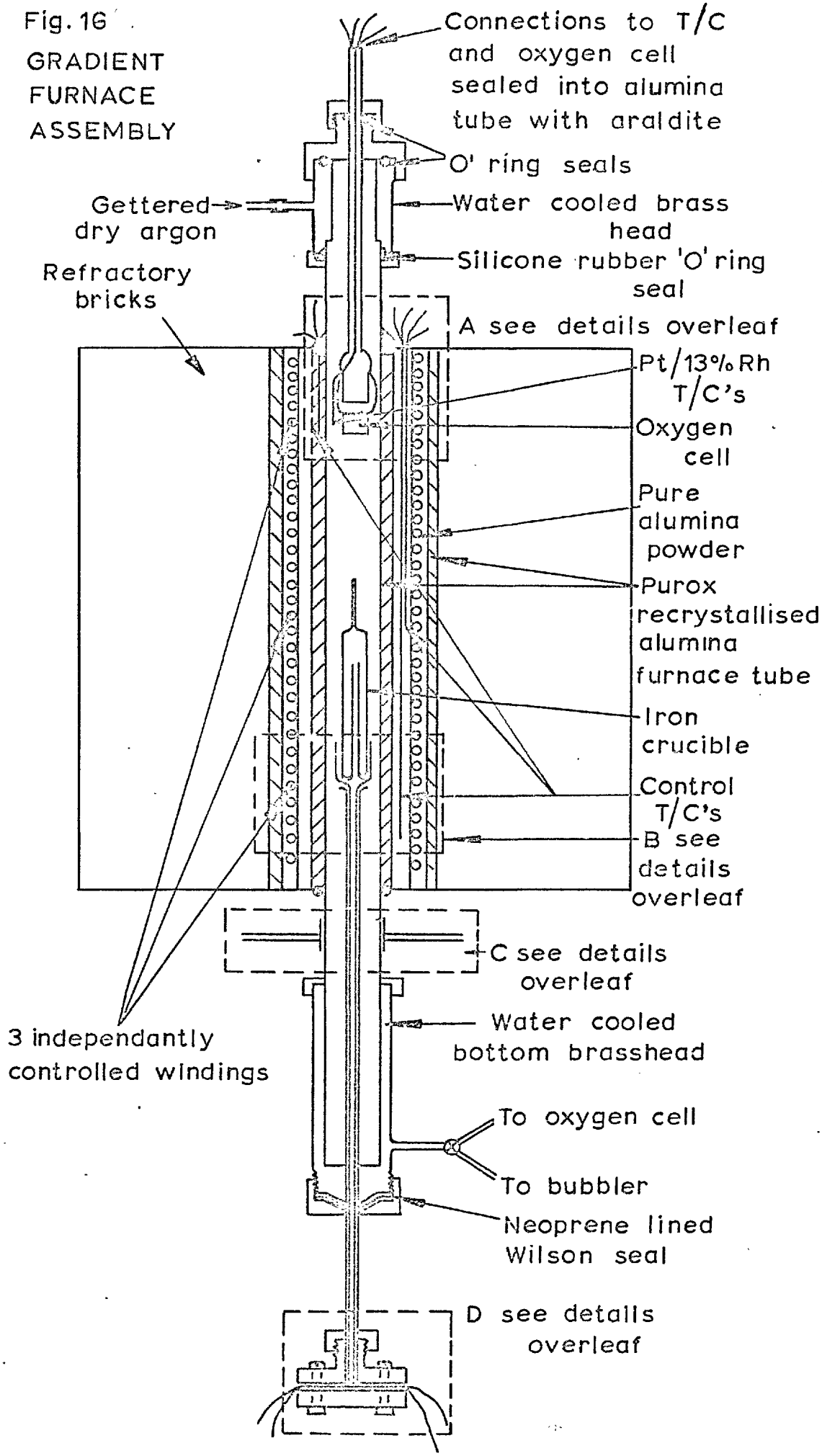

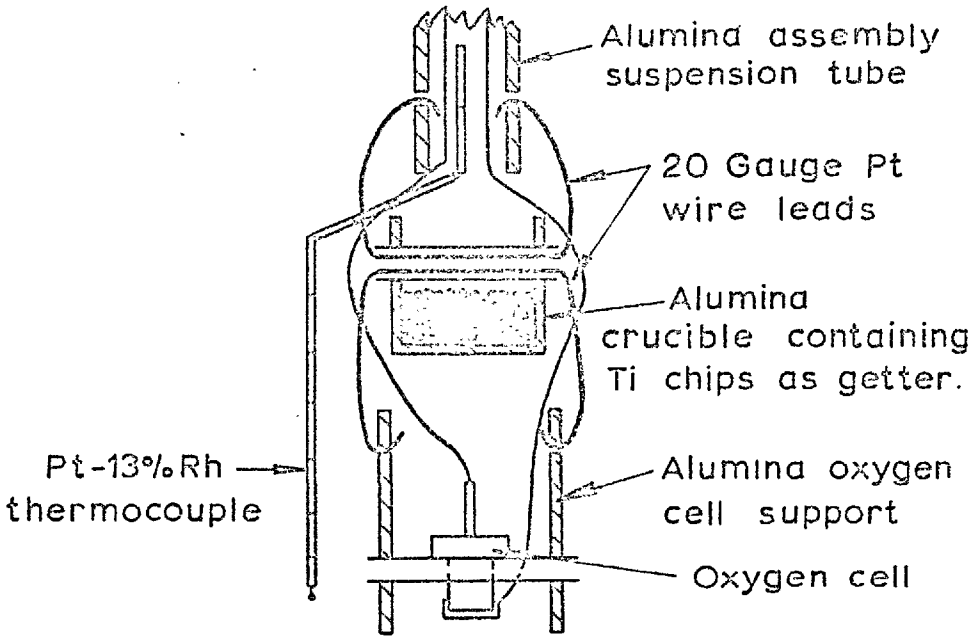

Fig.16A- OXYGEN CELL ASSEMBLY

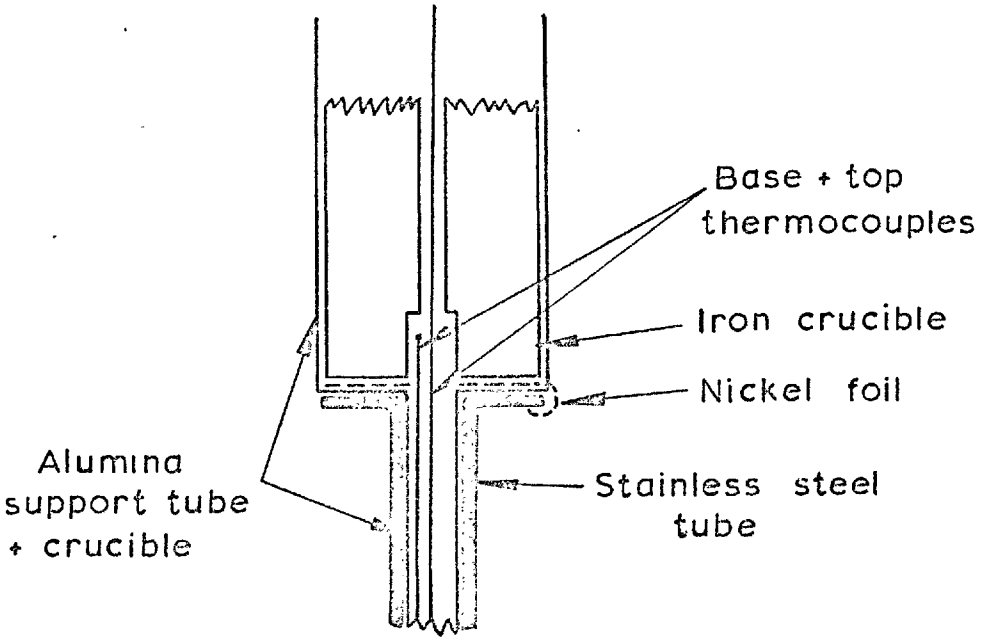

Fig.16B - SUPPORT ASSEMBLY FOR IRON CRUCIBLE

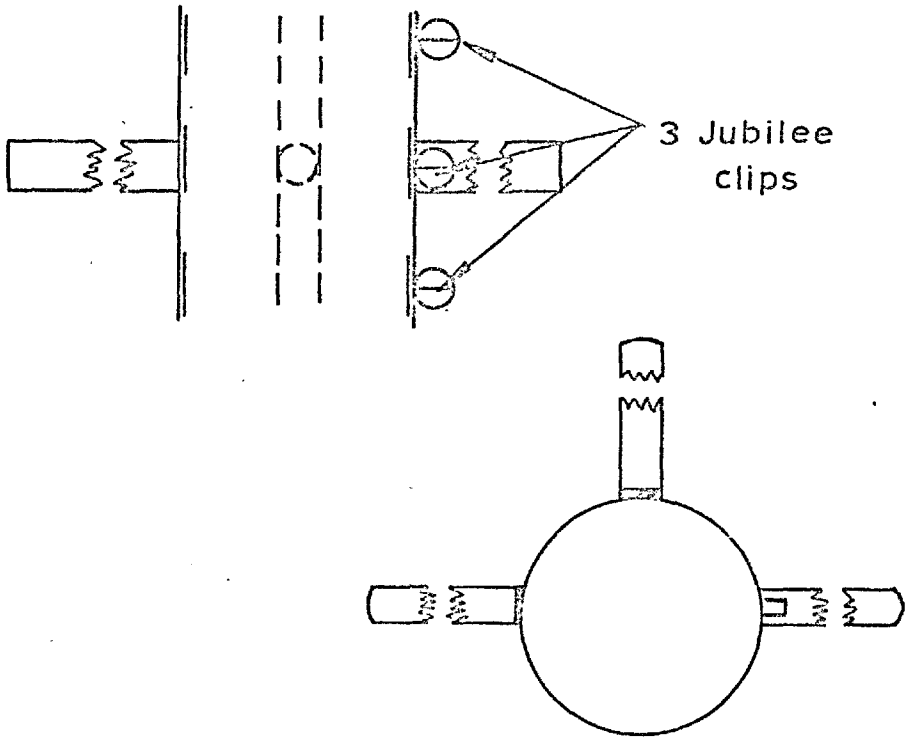

Fig.16C- JUBILEE CLIP ASSEMBLY

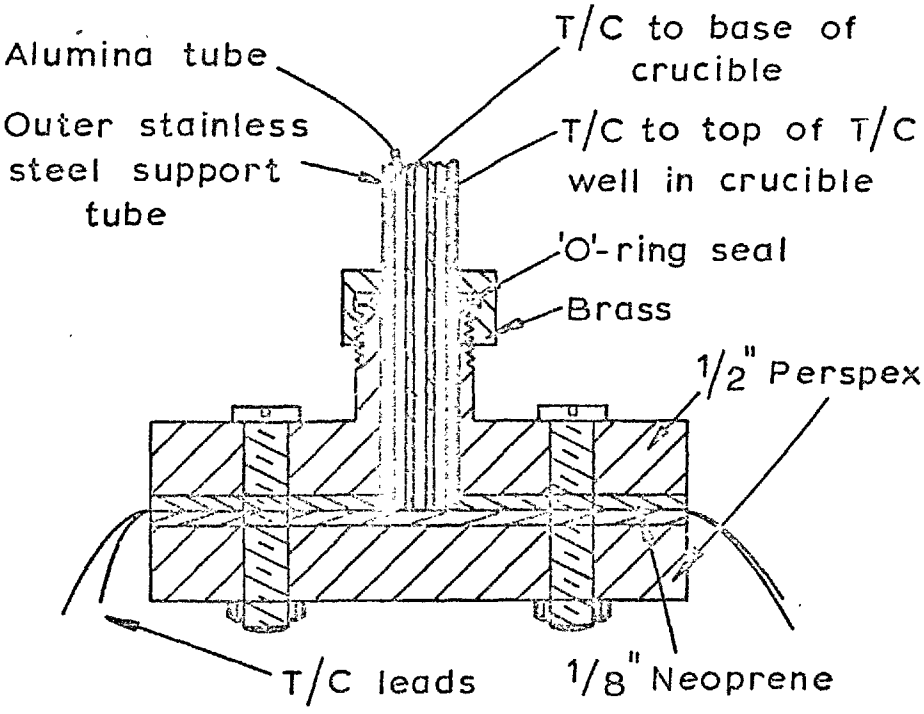

Fig.16 D- GAS TIGHT THERMOCOUPLE ENTRY ASSEMBLY

The reason for these modifications was that, after initial failures due to crucible oxidation caused by air leakage into the furnace, it was considered essential to be able to test for large-scale leaks before crucible insertion, and to monitor continuously the oxygen potential in the argon gas surrounding the iron crucible.

It was found that, due to the large thermal mass of the crucibles to be installed, it was not possible to obtain a complete and accurate temperature profile of the furnace, because by moving the crucible through the furnace the temperature distribution was completely altered.

In order to establish a suitable temperature profile and to ascertain the length of crucible required for a particular experiment, use was made of JAVED's temperature distribution. The crucible was installed in the furnace (after flushing-out procedures, to be described later) and after finding the approximate position of maximum temperature (1300°C), the magnitudes and time of operation of the on/off power to each winding and the crucible position were adjusted to obtain the required specimen temperature (1300°C) and base temperature required for a certain experiment. A short movement of the crucible up and down the furnace as appropriate showed the approximate temperature gradient, and the lengths of crucibles for other runs could then be decided accordingly.

Such a short temperature traverse with the crucible showed that the temperature gradient at the base of the crucible was approximately 40°C /cm. Shown overleaf are the calcium temperatures required on the boundaries to be investigated -

Ti-Ti(C,O) Boundary				Ti_2O_3 - Ti(C,O) Boundary			
N_{TiO}	N_{TiC}	pO_2	$T^{o}_{Ca}C$	N_{TiO}	N_{TiO}	pO_2	$T^{o}_{Ca}C$
.05	.95	5.20×10^{-28}	852	.1	.9	6.35×10^{-24}	621
.1	.9	4.36×10^{-27}	789	.2	.8	1.01×10^{-23}	609
.2	.8	1.74×10^{-26}	750	.3	.7	1.73×10^{-23}	601
.4	.6	6.97×10^{-26}	719	.4	.6	3.20×10^{-23}	587
.5	.5	1.09×10^{-25}	705	.5	.5	6.64×10^{-23}	574
.6	.4	1.57×10^{-25}	695	.6	.4	1.63×10^{-22}	560
.8	.2	2.8×10^{-25}	684	.7	.3	5.13×10^{-22}	539
.9	.1	3.6×10^{-25}	678	.8	.2	2.60×10^{-21}	521

It can be seen for example on the Ti/Ti(C,O) phase boundary that the Ca temperature difference between e.g. $N_{TiO} = 0.9$ and $N_{TiO} = 0.8$ is only $6^{o}C$. With these small temperature differences, such a steep temperature gradient as previously mentioned is undesirable, but this was the shallowest gradient obtainable with the available apparatus.

C. DESIGN OF CRUCIBLES

In view of the aforementioned steep gradient, it follows that accurate positioning of the thermocouple at the specimen was important, but more critical was the positioning of the thermocouple at the surface of the calcium. Accordingly, the crucible shown in Fig. 17 (p.76) was designed. The widened base of the thermocouple well avoided damage to the base thermocouple on introduction of the crucible into the alumina support.

Fig. 17.

CRUCIBLE DESIGN FOR STUDY OF Ti / Ti-C-O BOUNDARY

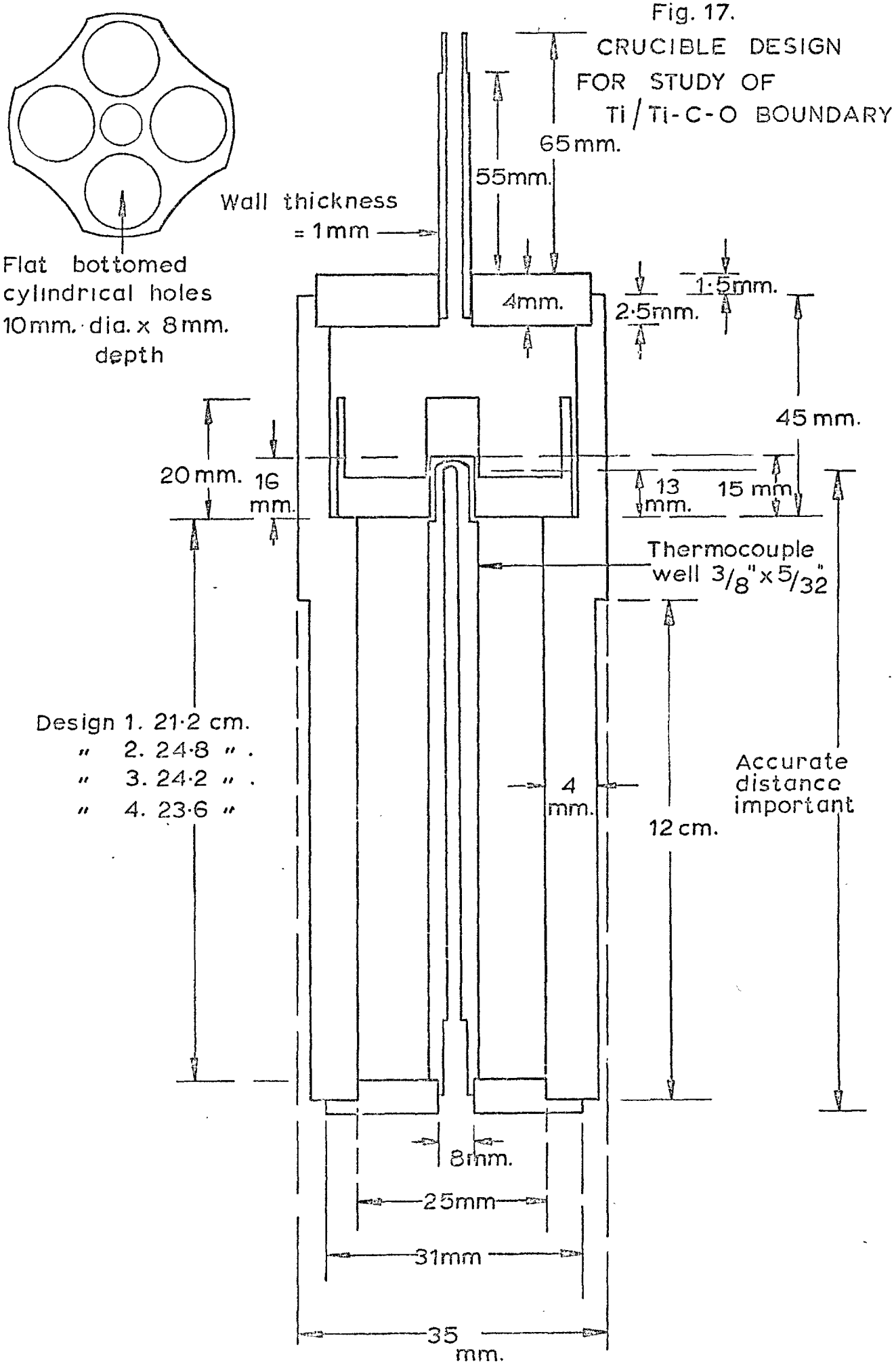

H. EXPERIMENTAL PROCEDURE

First, the thermocouple to take the calcium temperature in the crucible was adjusted so that it would be opposite the top level of the calcium. The approximate height of the calcium in the crucible was estimated by installing in the crucible the amount of calcium required, and obtaining the height of the surface of the calcium above the base of the crucible. Note that the amount of calcium required is that needed to provide the vapour for equilibration with the calcium oxide and for gettering within the crucible.

The bottom brasshead was then tested for gas tightness by inserting a sealed glass tube, which had a vacuum connection, into the O-ring seal and evacuating. Achievement of a vacuum of 40 microns was considered adequate proof of gas tightness.

The complete iron crucible to be used for a particular experiment was then taken out of the argon-filled drybox - where all crucibles were stored to avoid rusting - and all parts were thoroughly cleaned using carbon tetrachloride. Four calcia crucibles were then removed from the silica-gel desiccator in which they were kept, and each crucible was placed in the iron block. Titanium granules less than 36 mesh were then used as a lining on the base of each calcia crucible, the standard carbide or carbide-oxide mixture pellet (see § IV, D) was then placed on top of this, and titanium granules were then placed carefully in between the pellet and calcia crucible walls and were also piled up on top of the pellets to the brim of the calcia crucibles. The quantity of titanium used for each run was greatly in excess of that actually required.

The requirements of the Ti were that it should

(i) act as a getter for the air left in the crucible after evacuation, and for the oxygen coming out of the solution when oxide-carbide mixtures were used;

(ii) take up the carbon when TiC changed stoicheiometry; and

(iii) still be present at unit activity so that the titanium activity in the oxide-carbide solid solutions was fixed.

The filled block was inserted into the iron crucible and the crucible was evacuated and sealed (see Ch. 2, § IV, E). After placing a small alumina cap over the top thermocouple to avoid Pt-Fe solution, the crucible was then carefully placed over the thermocouples and into the crucible support in the lower brasshead assembly. An annular alumina holder containing Ti chips was then placed on top of the crucible and the whole assembly attached via an O-ring seal to the bottom end of the furnace tube, being supported in position by the scaffolding support previously described. Water cooling connections were then fitted onto the brasshead and the Zirconia tube oxygen cell attached to the outlet side of the brasshead.

The furnace was then flushed out with Argon gettered in an external Ti chips furnace at 750°C (but see p.80), the top oxygen cell/getter assembly being introduced over a period of 2 hours up to 800°C. When the oxygen potential on the outlet was considered low enough*, the crucible was gradually pushed up to a predetermined

---

* By experience, it was found that little or no crucible oxidation occurred when the pO_2 inside the furnace tube was less than 10^{-17} ats. When the tube was whole, this low pO_2 was easily achieved by installing the getters previously described.

height in the hot zone of the furnace by means of the stainless steel push rod.

At first it was difficult to measure the specimen and calcium temperature - measured using a Tinsley potentiometer - due to the crucible acting as an inductive load. This was subsequently rectified by setting the crucible on an annular piece of .006" thick nickel foil. This was attached to the stainless steel tube, which was earthed.

The time taken by the crucible to reach its equilibrium temperature after insertion was 2 - 3 hours. In all cases, where a crucible of the same length as for a previous experiment was being used, the temperature of the thermocouple at the base of the crucible was different by about 2 - 5° at the same position in the furnace. In such cases, it took about 24 hours of adjusting the height of the crucible in the furnace, and variac and controller settings, to obtain the required conditions. In cases where a crucible of different length to that in a previous run was being used, both specimen and calcium temperatures were different from that expected (due to a different thermal mass), adjustment as previously described being required for about the first 48 hours before "stability" was achieved.

With the temperature in the laboratory ranging by $\pm$ 3°C at least over the day, the minimum variation in the "stabilised" temperature of the calcium was $\pm$ 1.5°C and often $\pm$ 2°C was the best that could be achieved.

The pO_2 on the inlet and outlet side was continuously monitored on the oxygen cells. After the desired equilibration time, the crucible was air-quenched by withdrawing it over a period of 3 - 4 minutes (so as to reduce burning of the Neoprene

Wilson seals to a minimum) by means of the stainless steel rod, into the water-cooled bottom brasshead.

It should be noted that even with the shortest crucible used, the level of the specimens inside was just above the top of the bottom brasshead. This resulted in a minimum specimen temperature inside the brasshead of about 160°C, achieved in half-an-hour. In view of the long equilibration times employed, however, this comparatively short quenching time was considered satisfactory. After withdrawal of the top oxygen cell to lower temperatures, The Ti chips furnace and Argon were both switched off, and after detaching the water-cooling and outlet side oxygen cell, the whole bottom brasshead assembly was removed. After cooling to room temperature the crucible was removed from the brasshead assembly, entered into the drybox, through a vertical port, and opened as described in Chapter 2, § IV, E. In all cases the calcia crucibles and the specimens contained therein had stuck together and the specimens had to be prised out of the crucibles. The oxide-carbide solid solution and equilibrating solid species were then separated from each other and analysed as described in Ch. 2, § IV, E.

Essentially this was the procedure followed in all runs. Initially, however, any massive leaks (when the tube was cold, and before insertion of a run when the tube was hot) were tested for by pumping out the whole furnace assembly. If 45 microns was attainable after about 20 minutes' pumping with a single stage rotary pump, the assembly was taken as being gas tight.

This procedure was satisfactory when the tube was cold, but when pumping out when the furnace was at temperature, quite frequently no vacuum was obtained. On the few occasions when a

good vacuum was obtained, and a successful experiment performed, a vacuum was unobtainable on the next run. Thus either the tube had failed between runs with the furnace standing at temperature, or during subsequent pumping-out operations. On each occasion when tube failure occurred, all O-ring seals were checked, and replaced when considered defective. Top and bottom brassheads and the copper connecting tube between top brasshead and pump were also checked. When all the above tests proved negative as regards leaks, it was deduced that the furnace tubes must have failed: the furnace was then cooled slowly to room temperature over a period of 12 hours, top and bottom brassheads removed, and the furnace tube taken out.

In all such cases of failure, cracking had occurred in the hot zone of the furnace tube.

After 3 tube failures it was decided to pump out the furnace tube assembly only when cold, as a check for gas tightness.

Despite discontinuing the evacuation of the furnace when hot, 3 more tubes failed.

The longest period that a tube remained serviceable, i.e. without crucible oxidation occurring, was 3 months. Failure of each one, as found by the previous procedure, was due to either cracking in the hot zone, or to high-temperature porosity. Moreover, the perpetual heating and cooling of the furnace considerably strained the platinum windings, both the top and middle windings having to be replaced twice. The above failures were obviously time consuming as the furnace had to be re-calibrated each time, as described in Chapter 2, § IV, F.

Because of the failure of 6 tubes within eighteen months it was decided to discontinue experimentation.

The results obtained and a discussion of them are given in the following Sections.

V. EXPERIMENTAL RESULTS

A. DETAILS OF MATERIALS AND CONDITIONS USED ($a_{Ti} = 1$)

Experiment No.	Nominal pO_2	Starting 'Carbide Phase'	TiO Analysis			TiC used	Ca used	Comments
			Ti	O	N			
2X1-R	1.55×10^{-26}	TiC				Murex	Koch Light	
2X2	1.55×10^{-26}	TiC				Murex	Koch Light	
2X3-R	1.66×10^{-26}	'TiO'-TiC Mixture				London & Scandinavian	Redistilled Koch Light	No 'TiO' analysis available. Proportions used were 9/1 Molar, assuming stoicheiometric TiO and TiC.
2X4	1.63×10^{-26}	$TiC_{.14}O_{.83 \pm .08}$	72.1	23.4		London & Scandinavian	Koch Light	1.42% known impurities in 'TiO'. Error quoted in TiC-TiO mixture is only that inherent in vacuum fusion analysis.
2X5	1.6×10^{-26}	$TiC_{.14}O_{.83 \pm .08}$	72.1	23.4		London & Scandinavian	Distilled Koch Light	Do.
3X1	3.5×10^{-27}	$TiC_{.58}O_{.35 \pm .03}$	72.0	22.0	.04	London & Scandinavian	Distilled Koch Light	Do.

B. DETAILS OF PRODUCTS OF EXPERIMENTS

Experiment No.	Experiment time (hours)	Chemical Analysis wt.%					Phases present in Equilibrated Pellet	Corrected Ti(C,O) Formula	Lattice Parameter a_o A^o	Comments
		Ca	Ti	C	N	O				
2X1-R	178		75.7	19.5	0.4	0.17	Cubic Ti(C,O)	$TiC_{O.007}N_{.018}$	4.2304 ±.0005	All carbon less .5% was combined C.
2X2	250		76.4	18.6	0.35	0.15	Cubic Ti(C,O)	$TiC_{.97}O_{.007}N_{.015}$	4.2304 ±.0004	Some C removal
2X3-R	250	4	72.5	2.2	0.8	16.5	CaO, Ca_3N_2, Ti(C,O)	$TiC_{.12}O_{.78}$	4.230 ±.001	Ca present. Total + known impurities = 97.3%
2X4	154	3	75.1	2.7	2.3	18.4	Ca_3N_2, Ti(C,O) Possibly CaC_2 No CaO.		4.2303 ±.0004	Higher N_2 due to Koch Light C_a.
2X5	100	3	73.1	2.6	0.4	15.4	Possibly CaC_2 Ti(C,O)	$TiC_{.14}O_{.78}$	4.230 ±.002	Total analysis + known impurities = 95.8%
3X1	120	10	64.0	9.3	0.22	9.5	CaO Ti(C,O)	$TiC_{.58}O_{.60}$	4.305 ±.002	Total analysis + Impurities = 94%

VI. DISCUSSION OF RESULTS

A. SIGNIFICANCE OF X-RAY AND CHEMICAL DATA

The number of experiments carried out was restricted by the tube failures previously described. As far as the acquiring of positive thermodynamic data is concerned, the results are of limited value. The aim of this discussion is therefore to analyse why the experiments were unsuccessful despite continuous changes in technique.

(1) TiC as Starting Carbide Phase

It can be seen from Fig. 18 (p.86) that even after 250 hours of equilibration (2X2), some C removal has occurred, but the composition of the product is far from the approximate Ti/Ti(C,O) phase boundary. This would thus suggest very slow diffusion of carbon along the non-metal sublattice. In view of this it was decided to use TiO-TiC mixtures as the starting carbide phase, so that the amount of carbon to be transported through the lattice would be reduced. The proportions of TiO and TiC used in the mixture were commensurate with the ideal composition of Ti(C,O) in equilibrium with a certain pO_2 and unit activity of Ti.

At this stage, the "Murex TiC" was analysed and found to have quite a high impurity content. No indication of this impurity content was obtained on the X-ray film as, although some line broadening of the cubic lattice was observed for the "as received" sample, this disappeared in 2X1-R and 2X2, suggesting line broadening due to cold work, rather than to impurities. It should further be noted that the lattice parameters of the Murex TiC of experiments 2X1-R and 2X2, and of the purer TiC subsequently used, were the same to the 3rd place of decimals, and thus comparatively

Fig.18

PARTIAL Ti(C,O) DIAGRAM WITH AUTHOR'S RESULTS SHOWN.

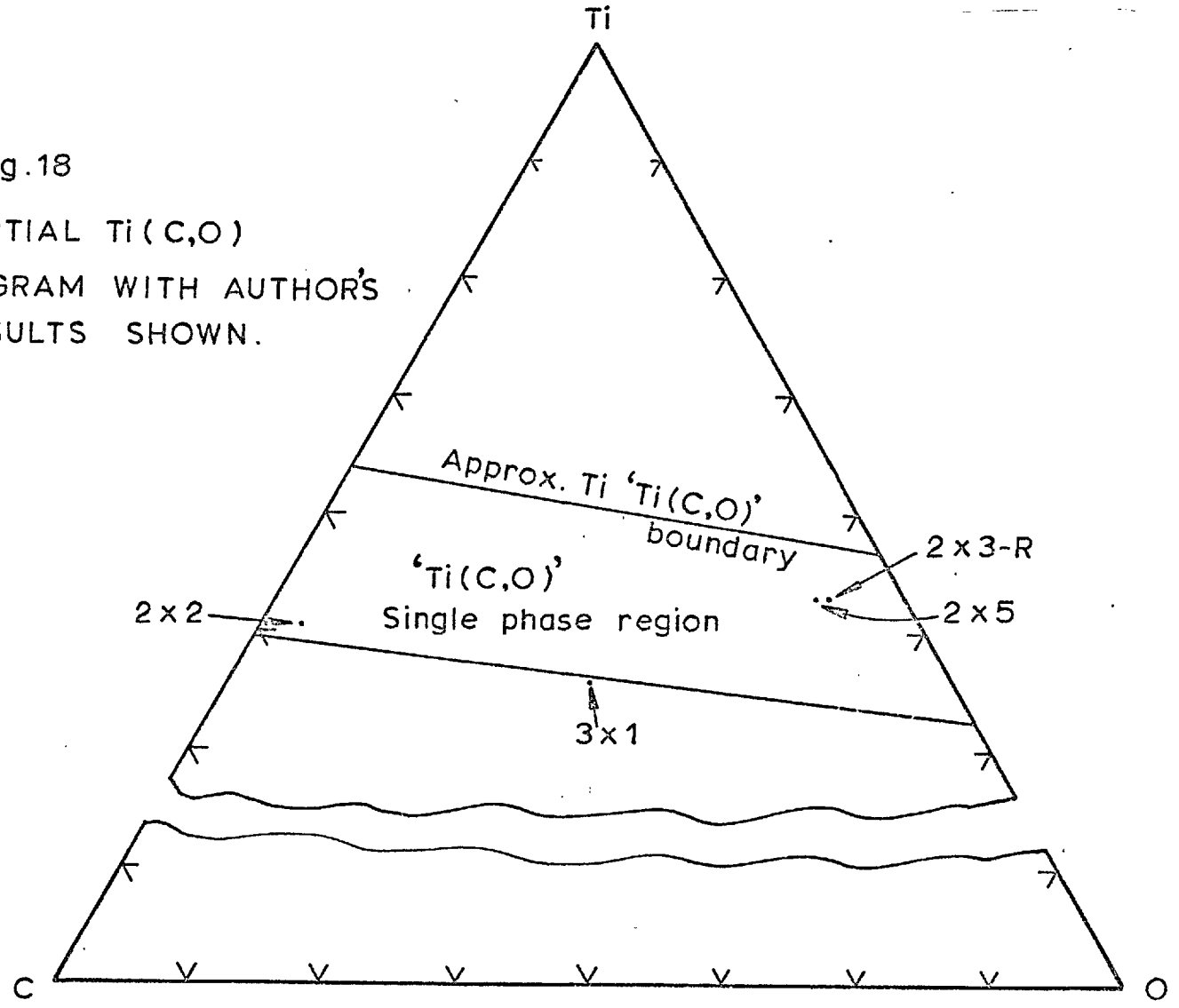

large amounts of impurities, e.g. 5%, have a negligible effect on the lattice parameter.

(2) TiC-TiO as the Starting "Carbide Phase"

(a) Chemical Data

It was observed in both cases of 'TiO' analysis that the material balance of Ti and Oxygen was much less than 100%. 1.4% of this can be taken as being due to known impurities in the Ti and TiO_2 used in the preparation. The balance could be either Ti and oxygen, as 'TiO' is capable of existing hypo- or hyper-stoicheiometrically, or Thoria from the preparation crucible, although this was not detected by X-ray nor was it analysed for. Regarding the carbide-oxide solid solutions, total analysis of 2X5 is much less than 100%, with the composition being the same as that of the starting material within experimental error. In all cases where the total analysis was less than 100%, it was considered suitable to attribute the difference firstly to known impurities, and the balance to oxygen. It should be noted that apart from the errors inherent in vacuum fusion analysis, analysis for oxygen in titanium and its oxides is particularly difficult, and liable to some inaccuracy, due to the steep slope of the $\overline{\Delta GO}_2$ v. oxygen content plot at low oxygen values.

Further, in the above sample, 2X3 and 3X1, all the nitrogen was taken as being combined with the calcium, the remainder of the calcium being present as CaO (see also p.88). X-ray fluorescence of sample 2X3 showed uniform distribution of calcium throughout the pellet, this obviously being due to the greater porosity of the mixed starting pellet compared with the carbide starting pellet.

Despite calcium penetration it was considered at this stage

that the calcium level was tolerable, in view of the beneficial effects on diffusion in a porous structure. In 2X4, no refined calcium was available In this case, the analysis was greater than 100%, with an increased nitrogen content due to the nitrogen contamination in the calcium used. Taking into account the known impurities, the total analysis is 102.6%.

With regard to 2X3, the calcium temperature and thus the oxygen partial pressure were nominally to be the same as 2X4 and 2X5. However, on checking the position of the base thermocouple subsequent to the experiment, it was noticed that it was about 4 mm. higher than the calcium surface in the crucible. The corrected temperature was 7° lower and therefore if equilibrium had been achieved, the oxygen content would have been greater than that for 2X4 and 2X5.

Experiment 3X1 was intended for 250 hours, but was terminated earlier due to excessive furnace tube leakage. The high calcium content is due to the higher p_{Ca}. Using the previously mentioned criteria (p.87) for calculating the Ti(C,O) formula, a composition outside the range of stability of any Ti(C,O) phase is obtained. Thus this method of calculation at these high calcium contents is invalid. Further, it should be noted that the starting carbide composition used in this experiment was well inside the Ti(C,O) single phase region (p.83).

(b) X-ray Data

For specimens with short "equilibration" times, e.g. 3X1 and 2X5, accurate measurement of the Ti(C,O) cubic lattice was not possible; however, the lines of 2X4 and 2X3 were much sharper and it is therefore suggested that approximately 150 hours is required for formation of a single cubic phase from the TiO-TiC mixture

at 1300°C.

With increasing length of the experiment, the calcium content in the product increases. Experiments 2X3, 2X4 and 2X5 at the lower p_{Ca} show the following trend:-

Experiment	Equilibration time	Lines present in excess of cubic phase
2X3	250 hours	1 of CaC_2*, many of γCa_3N_2.
2X4	154 "	1 of CaC_2* and 1 of γCa_3N_2, or 2 of CaC_2
2X5	100 "	" " " * " " " " " " " "

*The carbide lines are probably a result of the small amount of free carbon present in the "as received" carbide.

Consideration of the high nitrogen content of 2X4 suggests that most of the nitrogen must be present as a quaternary Ti(C, O, N). At higher p_{Ca}'s i.e. 3X1, the only impurity lines observed were those of CaO. The above distribution of lines is more or less consistent with the technique given on page 87 for determining oxygen content of the Ti(C,O) compound formed.

As stated previously, none of the oxide-carbide solid solution compositions produced lay on the Ti/Ti(C,O) boundary. One reason for this, apart from the suspected slow kinetics, could be the possible final absence of titanium at unit activity. With this in mind, X-ray examinations of Ti in contact with the final product were carried out for the 2X5 and 3X1 samples.

A cubic pattern with the 'a' parameter always much greater than that of the Ti(C,O) solution with which it was in contact was always present, although not as great as that of TiC. Among the other lines present, Ca_3N_2 and CaO were clearly identified.

The one line of Ti whose position does not alter with change in c/a ratio (which is a function of impurity content) is the 101 reflection which was seen to be present. The other Ti lines were difficult to identify absolutely due to their changing position with impurity content and superimposition on other lines present.

From the foregoing it would appear that

(i) periods of time far in excess of 10 days are required for equilibration at 1300°C.

(ii) TiC-TiO mixtures should be used as the starting 'carbide phase' to keep equilibration times to a minimum. Presintered specimens should be used to cut down calcium contamination.

(iii) Redistilled calcium is necessary to avoid quaternary Ti(C, N, O) formation.

(iv) Errors of ± 10% are inherent in oxygen analysis by vacuum fusion. In analysing oxygen-containing titanium compounds, the total error can be considerably higher.

(c) Thermodynamic Aspects

Original calculations for the $T_{Ca's}$ corresponding to the pO_2's existing on the Ti/Ti(C,O) boundary were in error. Thus when a TiC-TiO mixture was used as the starting material, the proportions used did not correspond with the pO_2 obtaining in the experiment. Thus in all experiments both oxygen and titanium would have to diffuse out to correspond with any composition on the phase boundary. The following points should be noted -

(i) Since Ti was always present in excess, none of the foregoing conclusions is invalidated, and equilibrium was approached from both sides.

(ii) The differential of $\pm$ 4 K.cals. in the data used for the free energy of formation of TiO gives a differential in the calcium temperatures used of $\pm$ 50°C.

By analogy with the Ti - C - N[39] system and the U - C - O[23] system, regular solution behaviour with negative deviations from ideality would be expected in the Ti - C - O system.

As far as improvements to the existing apparatus are concerned, it is considered essential to have a furnace with at least 5 Pt-Rh windings, with eurotherm proportional control rather than on-off Hg-switch control: this latter was subject to repeated failure. Volatilisation of impurities under the reducing conditions employed within the furnace was considered to be the main source of furnace tube problems (see Chapter 4). In order to reduce this volatilisation, it would be useful to use a furnace atmosphere of higher oxygen potential, thus necessitating the use of a crucible material having no oxidation problems

at these higher potentials, e.g. Ni. However Ni combines with Ca and thus cannot be used. In order to reduce the effect of developed high temperature porosity to a minimum, it is suggested that 2 concentric tubes could be used with flowing argon gas between the two. In conjunction with the latter, the scale of the experiments could be decreased by using narrower Fe crucibles and equilibrating only 2, instead of 4, samples at a time.

B. COMPARISON OF U-C-O AND Ti-C-O SYSTEMS WITH REFERENCE TO THE APPLICATION OF THE ISOPIESTIC TECHNIQUE

In the U-C-O system, the equilibration times at similar temperatures of study were 120 hours using sintered UC pellets. In connection with this short equilibration time relative to that in the present investigation, the following should be noted:-

(1) In polycrystalline specimens of TiC and UC, grain boundary diffusion is more important than volume diffusion at temperatures less than half the melting temperature. However, grain boundary diffusion is a function of crystal size, and thus variations in diffusion coefficient values are bound to exist. As diffusion data in single crystals is not available for UC, polycrystalline data are used for comparison of self-diffusion coefficients, and these are given below.

Average $D_{1573^{o}K}$ for Carbon ($cm^2/sec.$)	Data Source	Compound Formula
3.09×10^{-9}	Lee & Barrett[62]	UC
1.58×10^{-11}	Lee & Barrett[62]	$UC_{.966}$
4.27×10^{-13}	Sarian's[63] data extrapolated from 1450°C.	$TiC_{.97}$
6.6×10^{-14}		$TiC_{.887}$

Thus it is seen that the diffusion coefficient of carbon in TiC is approximately 2 to 3 magnitudes lower than that in UC. Therefore, all other things being equal, Ca/CaO equilibration with UC will be much faster than TiC.

(2) The kinetics on the U/U(C,O) boundary will be faster at 1573°K than on the Ti/Ti(C,O) boundary, since uranium is liquid at this temperature.

(3) The kinetics of the Ca/CaO equilibration will be very much slower in this investigation than in the U-C-O investigation. In the regions studied in the latter, calcium was always liquid giving higher p_{Ca} in contact with the carbide, than in the present investigation where Ca was always solid.

VII. CONCLUSIONS

It is considered that with the improvements suggested in § VI, C of this Chapter, investigation of this system is quite feasible using the isopiestic technique. However, because of the low diffusion rates obtaining, equilibration times are protracted.

It is therefore suggested that 2 or more experimental rigs would be required to make equilibrium thermodynamic investigations a feasible proposition.

CHAPTER 4

FAILURE OF ALUMINA TUBES IN SERVICE

I. INTRODUCTION

As mentioned in Chapter 3, § IV, H, failure of a number of 54 x 45 x 1000 mm. recrystallised alumina furnace tubes occurred in the course of experimentation. Initial failures occurred when evacuation of the hot furnace was used as a test for gas tightness before insertion of an experiment. Latterly, failures occurred in the course of experiments. No tests were carried out on the former category of failures and these were returned to the manufacturers. The latter failures were of 2 types -

(a) hot zone porosity without cracking; and

(b) hot zone porosity with cracking.

It was on tubes that failed due to cause (b) that tests were performed to try to ascertain the cause of ultimate failure.

II. REVIEW OF LITERATURE

ON

PERMEATION AND CHANNEL FLOW IN SINTERED ALUMINA CERAMICS

Loss of imperviousness in dense sintered oxides after long periods of heating was initially reported by RYSCHKEVITCH[64]. Most of the work on this topic has recently been carried out by ROBERTS[65-68] et al. Their work was done on sintered high purity alumina tubes (5-8% porosity) which were impermeable at room temperature. The experiments involved holding areas of such tubes from various manufacturers at 1500-1750°C under vacuum, and studying the permeation of oxygen, nitrogen and argon into them; the final and "as received" structures of the tubes were subjected to analysis and related to the permeation behaviour. Tests were carried out on tubes for various periods of time up to and including that required for catastrophic deterioration.

In experiments where the period of study was much less than that required for catastrophic deterioration, permeation experiments under 1 atmosphere external gas pressure showed that tubes which had large grains on the interior and/or exterior surfaces exhibited selective permeation of oxygen; these skins were in many cases greater than 0.500 mm. thick. Those without such grains were permeable in all the gaseous environments used. In the former case, the permeation was considered to be controlled by solid state diffusion of oxygen along grain boundaries in the surface skins, which did not contain connected porosity. In the latter, although connected porosity was detected throughout the tube wall, the kinetics of diffusion were not characteristic of

channel flow processes, the permeation being attributed to surface diffusion along the pore walls.

Experiments to deterioration[68] on (1) pore free sintered alumina materials and (2) sintered alumina with 5-8% porosity, under internal vacuum, gave the following results:-

(1) This material with initially no porosity and no surface skin exhibited discontinuous grain growth on its surfaces after being at 1650°C for approximately 60 hours. After about 70 hours, channelling developed along 3 grain edges; this was shown to be associated with Silica loss.

(2) This material, which had both internal and external skins, deteriorated after 30 hours at 1700°C; channels were formed in these skins at 3 grain edges. It was suggested that this channelling was again due to volatilisation of impurities.

More recently work has been done by DHAVALE[70] on loss of impermeability of Alumina tubes at 1700°C under conditions of internal tube evacuation with oxygen on the outside, internal and external evacuation, and oxygen flow on either side of the tube.

The results confirm that under these conditions, the loss of impermeability and the onset of channel flow (deterioration) is caused by impurity volatilisation from grain boundaries.

III. ANALYSIS OF DETERIORATED TUBES

The techniques used to try to ascertain the cause of tube failure were optical microscopy, scanning electron microscopy, density determinations by mercury displacement, dye impregnation, and chemical and electron probe microanalyses. Such techniques were applied to the hot zone (approximately 1½" long) and cold zone areas of the tube. The tube chosen for investigation had had its hot zone at 1320°C for approximately 2200 hours, the period of time under reducing conditions being 800 hours.

A. OPTICAL MICROSCOPIC EXAMINATION

To obtain a mounted specimen, an annulus was cut perpendicular to the tube axis, on a CAPCO cutting machine using water soluble oil as lubricant. Sections of these annuli were then mounted in metallurgical Mounting Plastic* with the cut face in the same plane as the base of the mount. A section was then taken perpendicular to the axis of the mount.

Initial tests were performed on cold zone samples to try to obtain a polishing technique that would produce a good final polish with the minimum of grains being pulled out. Among the techniques tried was that recommended by FRYER & ROBERTS[67] of polishing straight onto a lead lap impregnated with 6 μ diamond. This technique was tried for a maximum of 1 hour. Various other approaches were tried, using both lead and fibre lap surfaces,

---

*Supplied by North Hill Plastics, London, N.16.

silicon carbide papers, and various grades of diamond powder, for varying lengths of time. The method found to produce, for this material, a polished surface with the minimum of pullouts was polishing on dry 600 mesh silicon carbide papers for 5 minutes, and then for a further 5 hours on a lead lap impregnated with Kristalap 1μ diamond spray. Typical microstructures obtained by using ROBERTS' technique and that finally adopted are as shown in Figs. 19a and 19b, page 107, the black centres being due to pullouts and pores*.

Having perfected a polishing technique, sections were taken from the hot zone adjacent to the cracked section of the tube, and from the cold zone, and mounted and polished as previously described. Typical microstructures under normal reflected light of the inner edge of hot and cold zone specimens are shown in Figs. 22a and 22b, page 108. It can be seen that the hot zone sample contains occasional fissures connecting the inner surface to the tube interior. Further comparison of the polished structures reveals an approximate doubling in the number of pores at 3 grain edges (typical pores shown circled) in the inner edge of the hot zone specimen relative to the cold zone. Both of the aforementioned phenomena were also observed by DHAVALE[70].

Under dark ground illumination, the inner hot zone skin could be seen to have pores between 2 and 5μ wide. These were much more 'arterial' in nature than either the pores in the outer edge of the hot zone, or in the inner and outer edge of the cold zone,

---

* Note that all optical microscopy was done on a Vickers ZETOPAN microscope, using reflected light.

these being of similar diameter. Pores in the inner region of both hot and cold zones tended to be slightly larger than the those previously described (5 - 8 μ) and arterial, but could not be followed very far in the material. In no cases was β alumina observed.

After examination of the polished section the mount was dissolved in trichlorethylene, and the specimen thoroughly cleaned of all debris in an ultrasonic bath using the same solvent as liquid medium. It was then thermally etched in air for about 8 minutes at 1600°C in a molybdenum furnace and removed over a period of 5 minutes to room temperature.

On first examination of the etched specimens under the microscope, it was noticed that large numbers of interference fringes and blobs of another phase were present on the surface of the specimen, these tending to obscure the detail of the structure (Fig. 21, p.107) in some areas. It was thought at first that this debris might have arisen from the walls of the alumina furnace tube, or from the alumina crucible containing the specimen, during etching. However, after using a lid on top of the Alumina crucible and subsequently a thoria crucible with lid during etching, the debris still remained. It was thus decided that the debris must be a product of the etched specimen. After trying various solvents it was found that most of the small areas of debris could be removed, and the structure satisfactorily studied by treatment with 1% HF for $\frac{1}{2}$ hour. The larger areas of debris remained and could not be removed even after 2 hours. In view of its dissolution in HF, it was assumed that the debris was a glassy phase, possibly derived from the silica content of the specimen.

Shown in Figs. 23a and 23b (page 109) are typical hot and cold zone etched structures. It can be seen from Fig. 23a that a large amount of grain growth has occurred in the inner surface skin of the hot zone section along the tube axis - in this dimension the largest grains are $\geq 550\,\mu$. The maximum grain size in the cold zone was approximately 400 μ. Furthermore, this growth of hot zone grains relative to the cold zone can be seen to extend to sub surface-skin grains: using FULLMAN's[69] formula for average particle diameter, the approximate average grain size is 14.0 μ for the cold zone and 15.9 μ for the hot zone, i.e. an average 14% increase in grain size in the hot zone over the cold zone in this area. It should also be pointed out that extensive intragranular porosity exists in these skin grains.

The outer edges of both hot and cold specimens are seen to be essentially similar (figs. 24a and 24b, page 110) having grains approximately 14 μ in size. In this tube no discontinuous grain growth (c.f. DHAVALE[70] and ROBERTS[67]) similar to that on the inner tube wall, was observed for any of the specimens examined.

As concerns the structure of the tube wall interior, it is very similar in both hot and cold sections (Figs. 25a and 25b, page 110). By the method previously described, the average grain size is approximately 16 μ for both hot and cold zone interior sections. There is a tendency for slightly greater intergranular porosity in the hot than in the cold interior.

B. SCANNING ELECTRON MICROSCOPY

This technique was used to examine fractured surfaces perpendicular to the axis of the tube in the hot zone adjacent to the crack, and in the cold zone. Gold coatings were applied to the specimens to make them conducting, and they were examined at normal incidence at 25 Kv. Typical structures are shown in Fig. 26a and 26b, and 27a and 27b (page 111). Comparison of Figs. 26a and 26b shows that the inner skin grains of the hot zone sample contain larger internal pores than similar grains in the cold zone. Furthermore the definite presence of previously closed pores can be seen centre left in Fig. 26a and to the top right in Fig. 26b. Figs.27a and 27b are generally typical of interior and outer edge hot and cold zone structures. Due to the 3-dimensional picture obtained, much of the detail regarding porosity in these regions cannot be observed, and grain sizes in the conventional sense are difficult to ascertain.

C. DENSITY DETERMINATIONS

Density measurements were taken on two samples from both the hot and cold zones of the tube The technique used was mercury displacement using a densitometer as shown in Fig. 28, p.103. Tests were carried out on fractured samples weighing approximately 1 gram. Care was taken to avoid air being trapped above the sample on insertion into the bulb under the mercury surface. Seven trials were made with each specimen and 5 trials on the blank. Temperature corrections were applied to the mercury density in all cases. The results obtained were:-

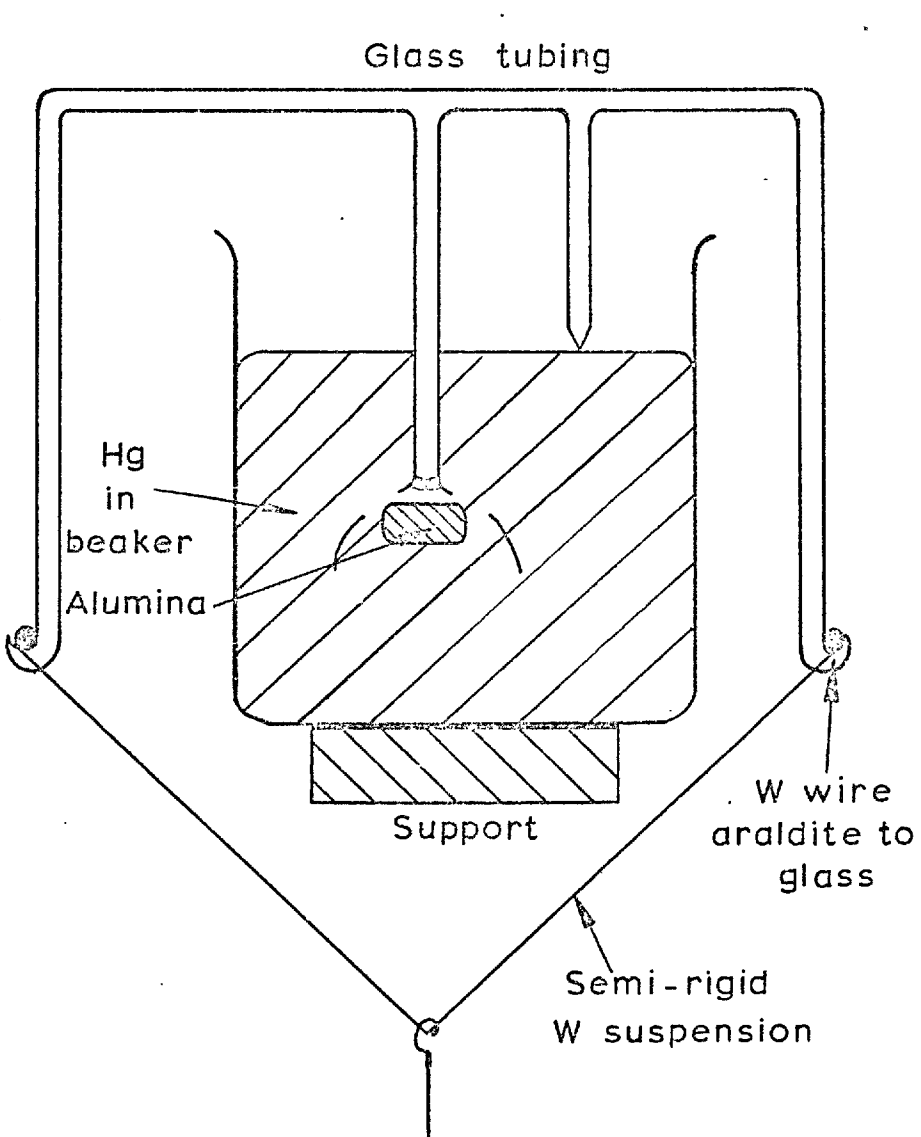

Fig. 28. MERCURY DENSITOMETER

Scale - Full size

	DENSITY (gm/cc)		DERIVED POROSITY
	Specimen 1	Specimen 2	%
Hot Zone	3.63	3.62	9.15
Cold Zone	3.67	3.68	7.89

D. DYE IMPREGNATION

Impregnation was carried out in an apparatus similar to that used by ROBERTS[67]. The specimens, each about 1½" long, were obtained from the same sections of the tube as used for previous tests. These were carefully degreased in carbon tetrachloride and dried overnight in an oven at 120°C. After cooling, they were placed in the impregnation apparatus which was closed off, evacuated for half-an-hour, and then flooded with a Fluorescein type of dye*. Impregnation times of 35 minutes were found to be adequate. The specimens were then removed from the apparatus and the excess dye carefully wiped off using absorbent tissue. They were then carefully broken parallel to the tube axis using a hammer and chisel, and the sections photographed under ultraviolet light. (It should be noted that under ultraviolet light the dye used for impregnation fluoresces. Thus the region of the material into which the dye has penetrated will show up, when photographed, as a white area). A typical result is shown in Fig. 20, p.107, the hot zone sample being on the left and the cold zone on the right.

---

* ZYGLO PENETRANT ZI - 1b, supplied by Solus-Schall, Stanmore, Middlesex.

It can be seen that no detectable penetration has occurred from either wall of the cold zone specimen, nor from the outer wall of the hot specimen: penetration from the inner wall is quite marked. It should further be noted that penetration has occurred to quite a substantial effect into the interior of the tube from the cut ends in both hot and cold zone specimens, the penetration in the cold section being a maximum at the wall centre and reducing to zero just inside the inner and outer walls. This extensive penetration could not have been solely due to surface grain removal during cutting.

E. ELECTRON PROBE ANALYSIS

Such an analysis was carried out on both hot and cold zone samples in order to detect semiquantitatively the presence and distribution of 'impurities'. The general levels of Mg, Mn, Cr, K and Na were below the level of detection of the instrument. The iron level was 250 ppm and the silicon 3000 ppm in both hot and cold zones. The calcium content was given as approximately 250 ppm in the hot zone and 580 ppm in the cold region. Calcium and silicon were found to be quite often present together, and usually associated with pores.

F. CHEMICAL ANALYSIS

Wet analyses were performed on alumina samples at the British Ceramic Research Association, Stoke-on-Trent. The hot zone samples were taken from the area adjacent to that from which the previous hot zone sample had been obtained, this first sample having been used up in the tests described earlier. The sample taken was thus not at the peak temperature of the previous sample

and was estimated to be at a mean temperature of about 1260°C. The following analyses were obtained:-

	Cold Zone Analysis (wt.%)	Hot Zone Analysis (wt.%)
SiO_2	.09	.04
CaO	.07	.05
MgO	.01	< .01
K_2O	< .01	< .01
Na_2O	< .01	< .01

Further, from analysis of the emission spectrum data, obtained at the Analytical Services Laboratory, Imperial College, it could be seen that the sodium level in the hot zone specimen was approximately half that in the cold zone. The estimated sodium level was approximately 40 ppm in the hot zone (equivalent to 55 ppm Na_2O) and 70 ppm in the cold zone (equivalent to 95 ppm Na_2O).

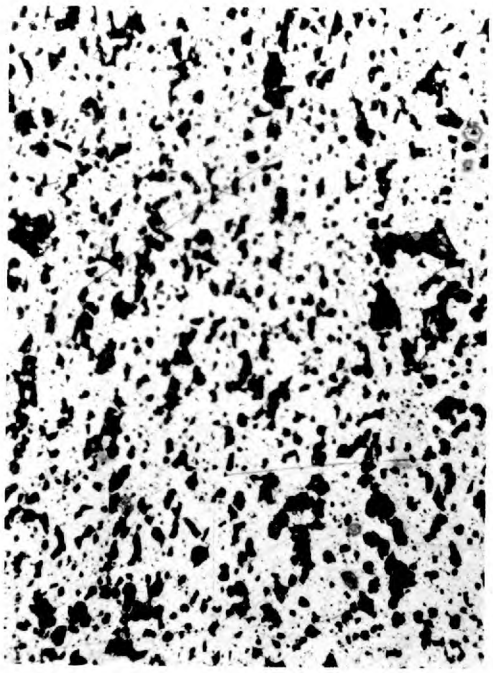

19a Cold zone section using Fryer and Roberts polishing technique

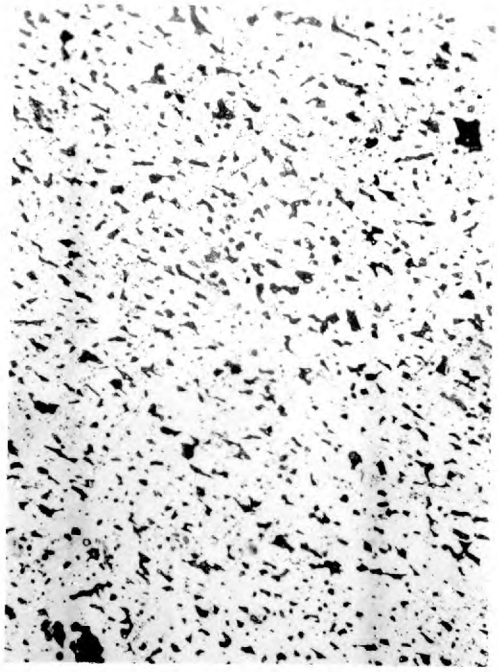

19b Similar section to that in Fig. 19a using author's technique

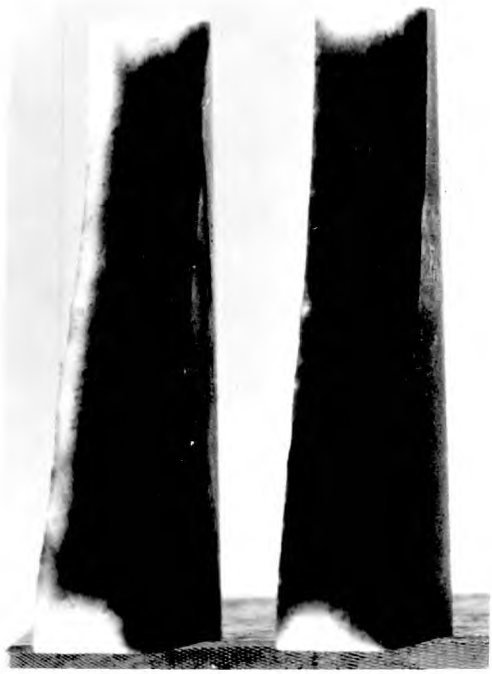

20a Dye impregnation of hot and cold zone wall sections parallel to tube axis (hot section on left)

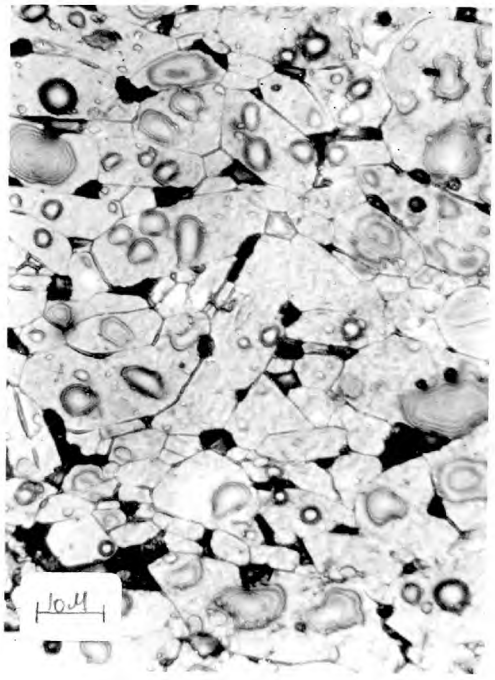

21 Thermally etched section showing glassy surface pools.

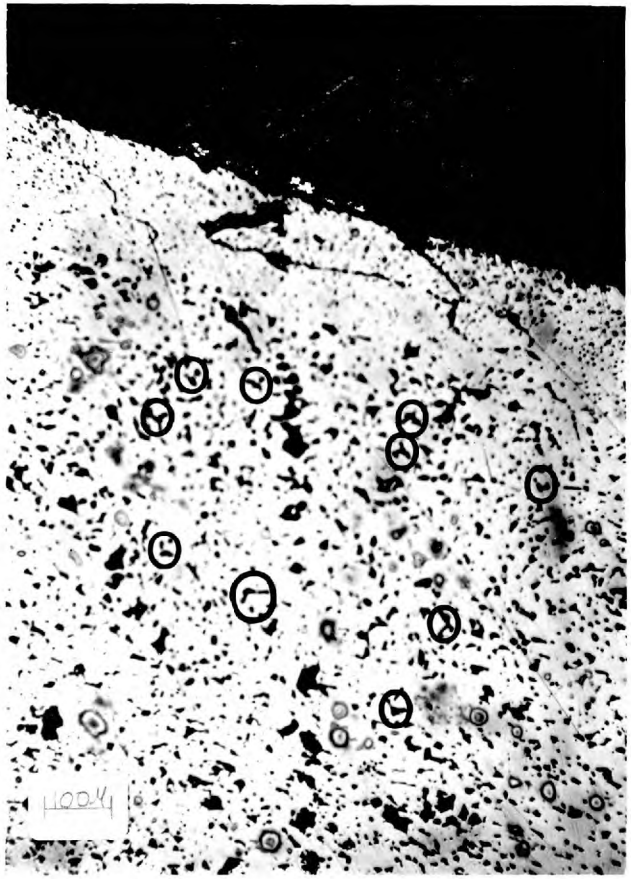

22a Polished inner wall section of hot zone showing porosity connecting surface interior (normal to tube axis)

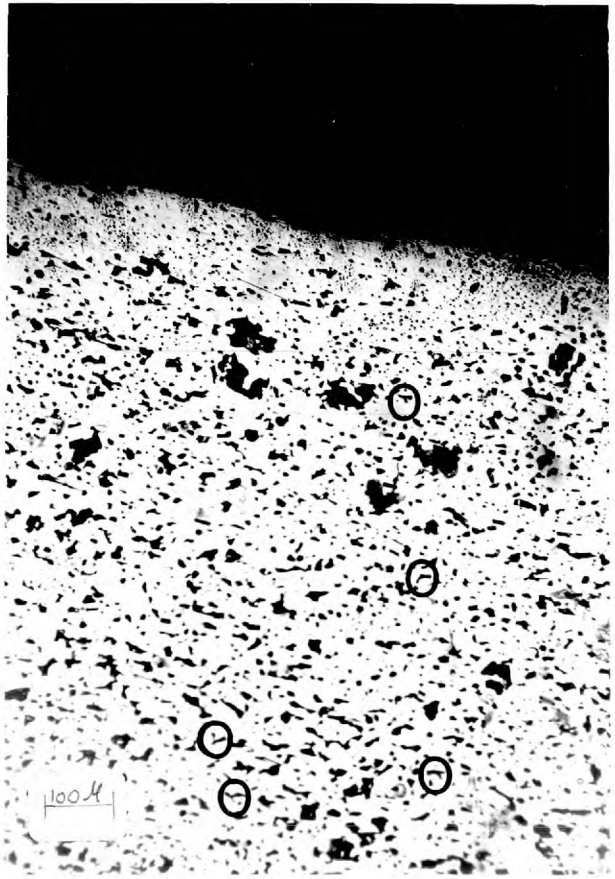

22b Polished inner wall section of cold zone (normal to tube axis)

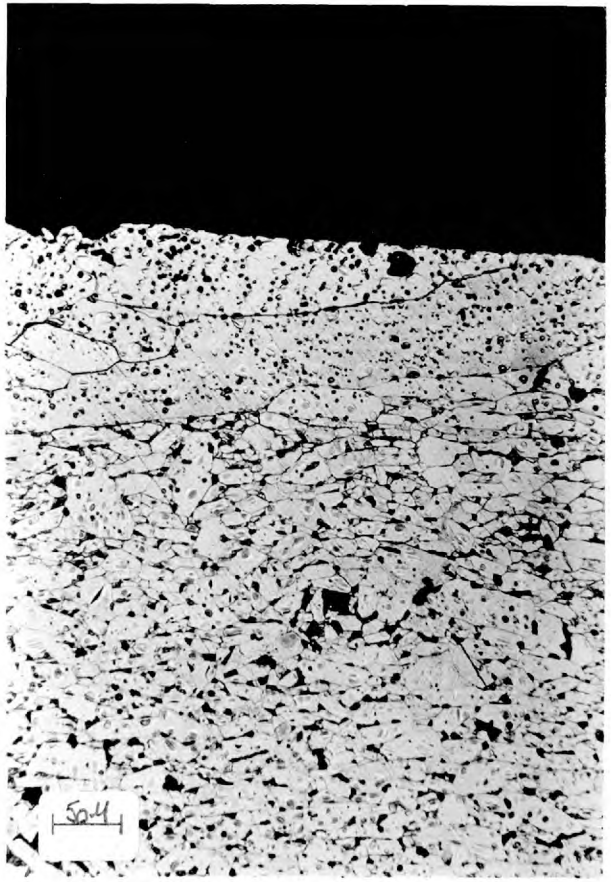

23a Thermally etched inner wall section of hot zone showing grain growth relative to similar cold section
(section normal to tube axis)

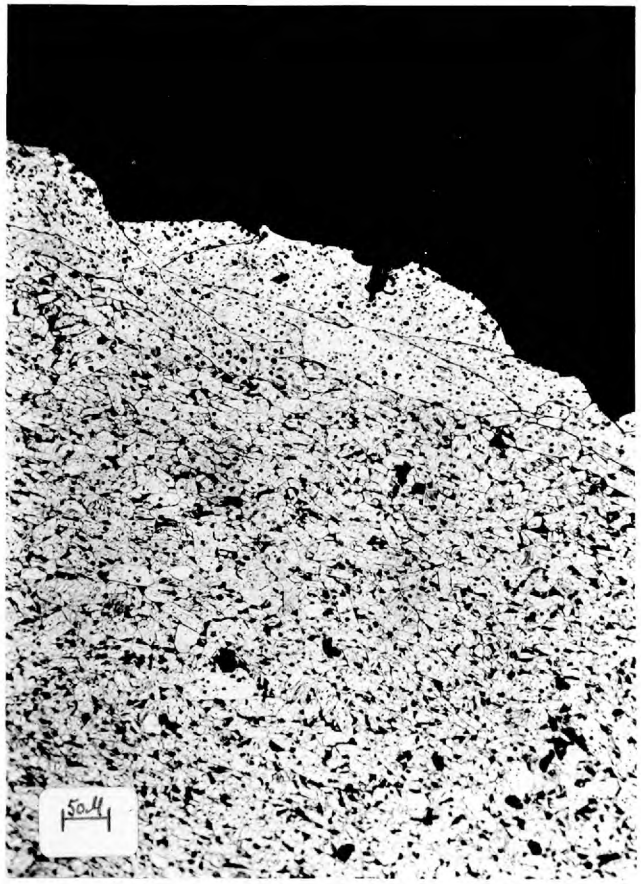

23b Thermally etched inner wall section of cold zone

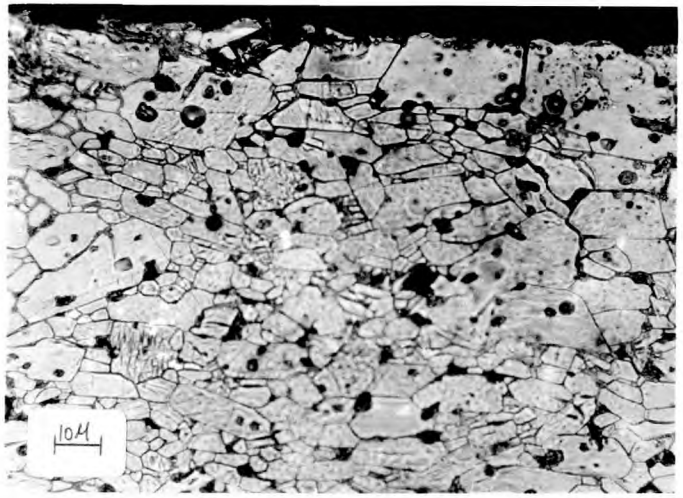

24a Thermally etched section of hot zone outer wall.
(normal to tube axis)

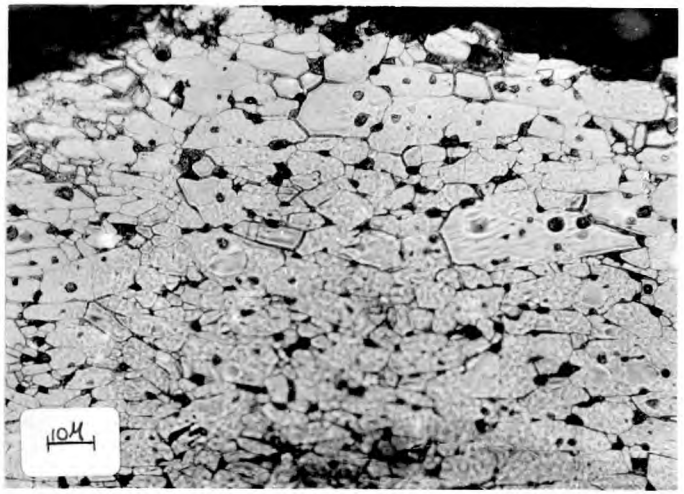

24b Thermally etched section of cold zone outer wall
(normal to tube axis)

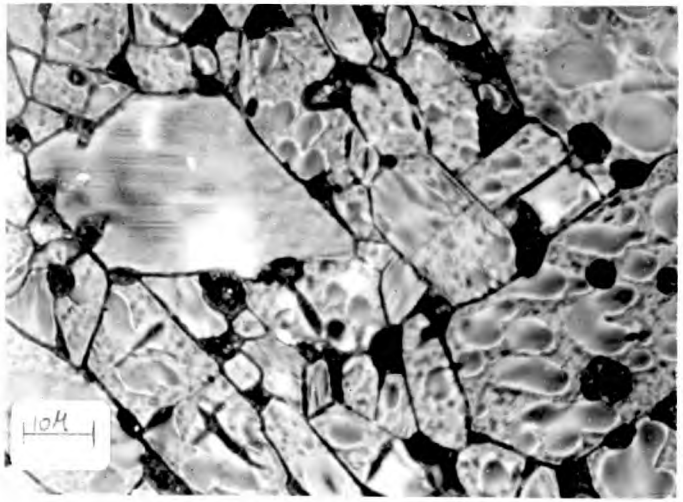

25a Thermally etched section of hot zone wall interior (normal to tube axis)

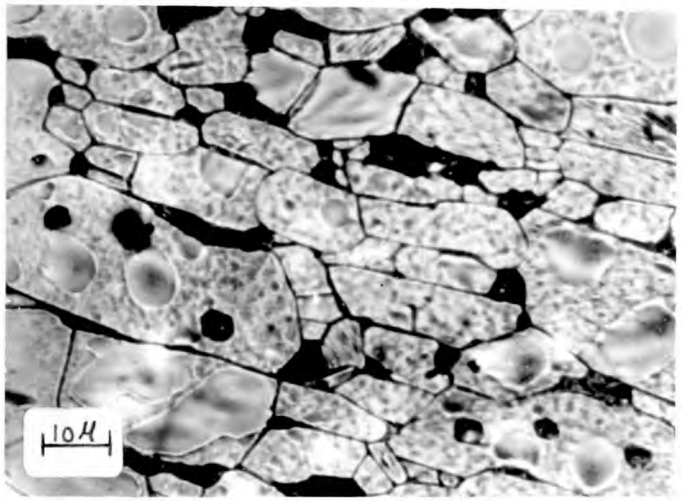

25b Thermally etched section of cold zone wall interior (normal to tube axis)

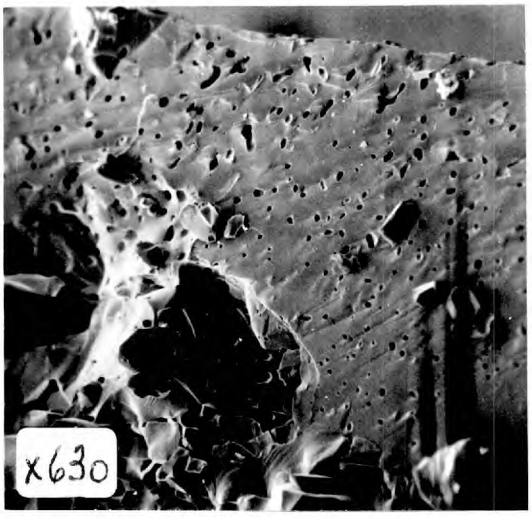

26a Scanning electron micrograph of the inner edge of a fractured surface in the hot zone
(normal to tube axis)

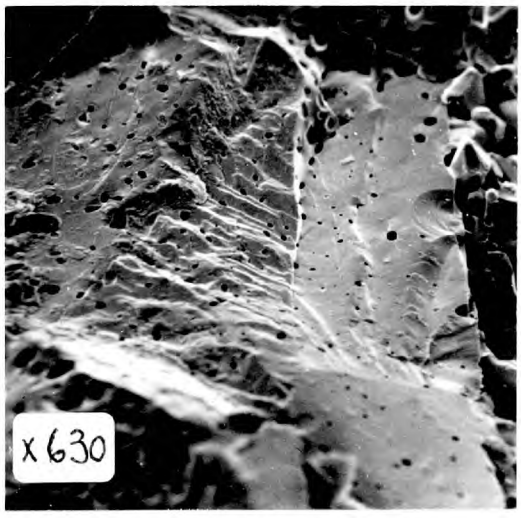

26b Scanning electron micrograph of the inner edge of a fractured surface in the cold zone
(normal to tube axis)

27a Scanning electron micrograph of hot zone tube interior
(normal to tube axis)

27b Scanning electron micrograph of cold zone tube interior
(normal to tube axis)

IV. DISCUSSION

No experimental work has been done on deterioration of tubes at the temperatures used in this investigation. All investigations to data have been conducted on tubes held at 1500°C upwards. Further, no work has been done on tubes in which the gaseous conditions on the wall interior were highly reducing. Work by ROBERTS[65-68] et al, and DHAVALE[70], has been under conditions of vacuum on both sides of the tube, vacuum on the inside of the tube and various gases on the outside, and finally with oxygen on both sides.

The main discussion will be confined to the particular tube tested. Later, reasons will be suggested for other tube failures.

Prior to systematic investigation, a small blob of ink was deposited on the inner surface of pieces of tube from the hot and cold zones. The ink was observed to permeate and branch quite quickly into the subsurface regions of the hot zone piece, whereas this did not occur with the cold zone specimen. This crude test thus initially suggested connected porosity or highly disordered grain boundaries in the inner surface regions of the hot zone section. A similar test was applied to the outer surfaces of both specimens, with no observed penetration. Dye penetration tests (Fig. 20) confirmed these observations and showed further that in the interior regions of both hot and cold specimens, the material was porous. This latter showed that connected porosity was inherent in the inner regions of the tubes as found by ROBERTS[67] in tubes from the same manufacturer.

From the results of the examination of microstructures

Figs. 22-26) it could be seen that the possible contributory causes of the observed increase in porosity of the hot zone specimen were -

(i) occasional fissures in the inner wall connecting the inner surface to the interior;

(ii) an increase in the number of channels at 3 grain edges in the area adjacent to the inner skin grains;

(iii) an increase in the size of the intragranular pores in the skin grains, providing a connection to the pore system in the tube interior.

It can be suggested that the cause of the appearance of these features was material volatilisation. From the chemical and emission spectrum data, it can be seen that .08% (or greater than one-quarter of the expected total impurity content) of the impurities in the tube have volatilised from the hot zone region (see also § III, F). The probe analyses for Si are uniformly high and are much greater than the Si content normally obtaining in this material; they are thus neglected.

If these volatiles are considered to come mainly from the inner surface skin of the tube (approximately 100μ thick), the difference between hot and cold zone inner skin densities can be shown to be about 1.9 gm/cc. (It should be noted that no skin densities were taken due to lack of time). Taking the theoretical density of alumina as 3.99 gm/cc, this would suggest an increase in porosity of greater than 50% in the hot zone skin grains

relative to the cold zone, and by observation of the microstructures this is seen to be unreasonable. Thus it is suggested that once connected porosity is formed in the inner surface skin, volatilisation of impurities occurs from the interior.

Thermodynamically, the deterioration of these alumina tubes due to volatilisation of impurity under reducing conditions is quite favourable. It has been demonstrated that the tube material contains a glassy phase (Fig. 21 and § III A). For the soda-silica system it has been shown that for mixtures quenched from above the transition temperature (a maximum of 530°C) the the activity of Silica is approximately 1, when the weight of Silica is $> 50\%$[72]. Thus at 1320°C, one would consider the a_{SiO_2} near unity over a greater composition range. Considering the reaction $2SiO_2 = 2SiO + O_2$, we have $K_{1350°C} = 2 \times 10^{-25}$. If we assume that $a_{SiO_2} = 1$, and $pO_2 = 10^{-18}$ats. (approximately that used within the furnace tube), then $pSiO = 2 \times 10^{-4}$ ats. Similar magnitudes for pSiO are expected if we consider $MgO-SiO_2$ and $CaO-SiO_2$ systems. Thus with the continual sweeping out of the furnace gases, it can be seen that conditions are favourable for continuous impurity volatilisation.

As far as the distribution of the impurities is concerned, it has been shown by JORGENSEN & WESTBROOK[71] that the impurities tend to reside mainly in the grain boundary regions. Diffusion of these materials will tend to occur down a concentration gradient from the outer wall of the tube to the inner surface along the grain boundaries, as the impurities are volatilised from the inner surface. Diffusion will occur either via the glassy

phase or as cation and oxygen ions, along the grain boundaries. Diffusion of vacancies will be in the reverse direction leading to gaps at 2 grain edges and 3 grain corners. Impurities associated with intragranular pores will also tend to volatilise at the inner surface. However, intragranular volatilisation is is expected to be a minor contribution to the increase in porosity, since at this comparatively low temperature, diffusion of vacancies through the lattice will tend to be much slower than along the grain boundaries.

It should be noted here that in dye penetration experiments performed on tubes with internal and external skins which had become permeable after heating at 1700°C for 50 hours under internal vacuum, DHAVALE found that the dye did not penetrate the outer surface skin. Further, examination of the microstructure did not reveal channels at this outer surface. However, X-radiography of the tubes impregnated with tin chloride showed that there were occasional single channels connecting the outer wall with the interior, as well as the threadlike channels at the inner surface. In no cases was trans- or intergranular cracking observed.

It should be noted that although no equipment was to hand to carry out such X-radiography tests on specimens of the author's material, it is quite possible that deterioration in the tube had occurred, not only at the inner surface (as observed), but also at the outer surface.. This tentative suggestion is based on comparison of total impurity loss from the author's materials (§ III F) and that of DHAVALE. The total loss obtained from the tube used

in the present investigation is greater than that obtained from a typical analysis of DHAVALE's.

Summarising, it can thus be said that under the conditions of usage of the author's alumina tube, the available techniques suggested connected porosity in the interior and inner surface skin of the hot zone, the probable cause being material loss by volatilisation. Further, tentative suggestions regarding connected porosity in the outer skin are made, by comparison with DHAVALE.

Although experiments prior to final failure of the tube were successful, in that oxidation of the iron crucible was at a minimum, local surface oxidation had occurred in an area near the top of the crucible where it was in contact with the tube. This thus suggested that even prior to ultimate cracking of the tube, substantial quantities of oxygen were diffusing through the tube wall and being partially gettered by the iron crucible before the low oxygen potential furnace atmosphere could dilute it and flush it out. Part of the oxide formed would tend to react with the alumina as subsequently observed in the region round the crack in the failed tube. No calculations regarding the oxygen coming into the tube per unit time were made due to lack of available data. However, an idea of the relative magnitudes involved regarding the leak rates can be obtained by comparison of the figures for leak rates in undeteriorated tubes (.05 μ/minute) and a typical leak rate in a deteriorated tube (5 μ/minute) both at 1700°C in DHAVALE's investigation. This shows an increase of 100 times in the leakrate - in many deteriorated tubes the leak was even greater.

The final failure of the tube by cracking is complicated, due to the differing effects of variation in grain size and porosity upon creep, fracture, and strength, In general an increase in grain size and porosity decreases the impact strength, compression strength and modulus of rupture, but increases the resistance to creep and fracture.

Under the operating conditions, the sources of stress on the hot zone of the tube are compression due to the weight of the tube above the hot zone plus the weight of the top brasshead (total approximately 20 lbs.), impact stresses of the crucible on introduction into the furnace (approximately 0.2 inch lbs.), and the internal stresses within the material due to anisotropic expansion. (It is considered that stresses due to thermal shock are negligible considering the slow rate of introduction of the crucible into the hot zone.

It is considered probable that deterioration of the tube and crack propagation went hand in hand. Both intergranular and intragranular porosity and very large grain size, on the inner skin, would make the inner surface of the hot zone weaker. Even after this inner skin had been breached, the overall furnace atmosphere was still capable of being controlled since oxygen permeation is still very small, the rate controlling step being oxygen ion grain boundary diffusion through the unbreached outer skin. It is suggested that crack propagation by a fracture mode would tend to be less important in the interior regions of the tube than in the inner surface skin, since the interior grains are much smaller and the glassy phase present would tend to give a slight amount of plastic flow, and thus stress relief. Here, creep under compressive stresses would tend to be dominant.

When the crack reached the outer surface area, crack propagation would be relatively simpler than in the interior, due to the lower porosity, and cracking both by fracture and creep would tend to occur.

Other types of failure of tubes occurred when using evacuation of the hot furnace as a criterion of furnace gas tightness. After obtaining a vacuum of 35 μ in the furnace after initial heating of the tubes, failures occurred under the following conditions:-

(i) After a total of 17 days under the reducing conditions employed in the furnace, a vacuum of only 300 μ was obtainable.

(ii) The furnace was allowed to stand at temperature for two days in air prior to run insertion. Prior to insertion of the crucible into the hot zone, the furnace was retested and a vacuum of better than 1000 μ was unobtainable. Subsequently, the furnace was cooled to room temperature where the best vacuum obtained was 75 μ.

It is suggested that in (i) deterioration of the tube throughout the wall occurred due to volatilisation of impurities mainly under reducing conditions.

In (ii), the deterioration is difficult to explain.

V. CONCLUSION

The initial failure of the tube material was partially due to the reducing conditions employed. These promoted volatilisation of impurity materials, and the porosity produced, combined with the substantial grain growth of the inner skin grains, served to make the inner surface of the tube in the hot zone comparatively weak. Modes of crack propagation are postulated to be by fracture within the inner surface grains, and creep and mainly fracture in the tube interior and outer surface grains respectively.

APPENDIX.1

Fig.5 PLOT OF CO/CO_2 vs. N_{WO}/N_{WC} AT 1473°K

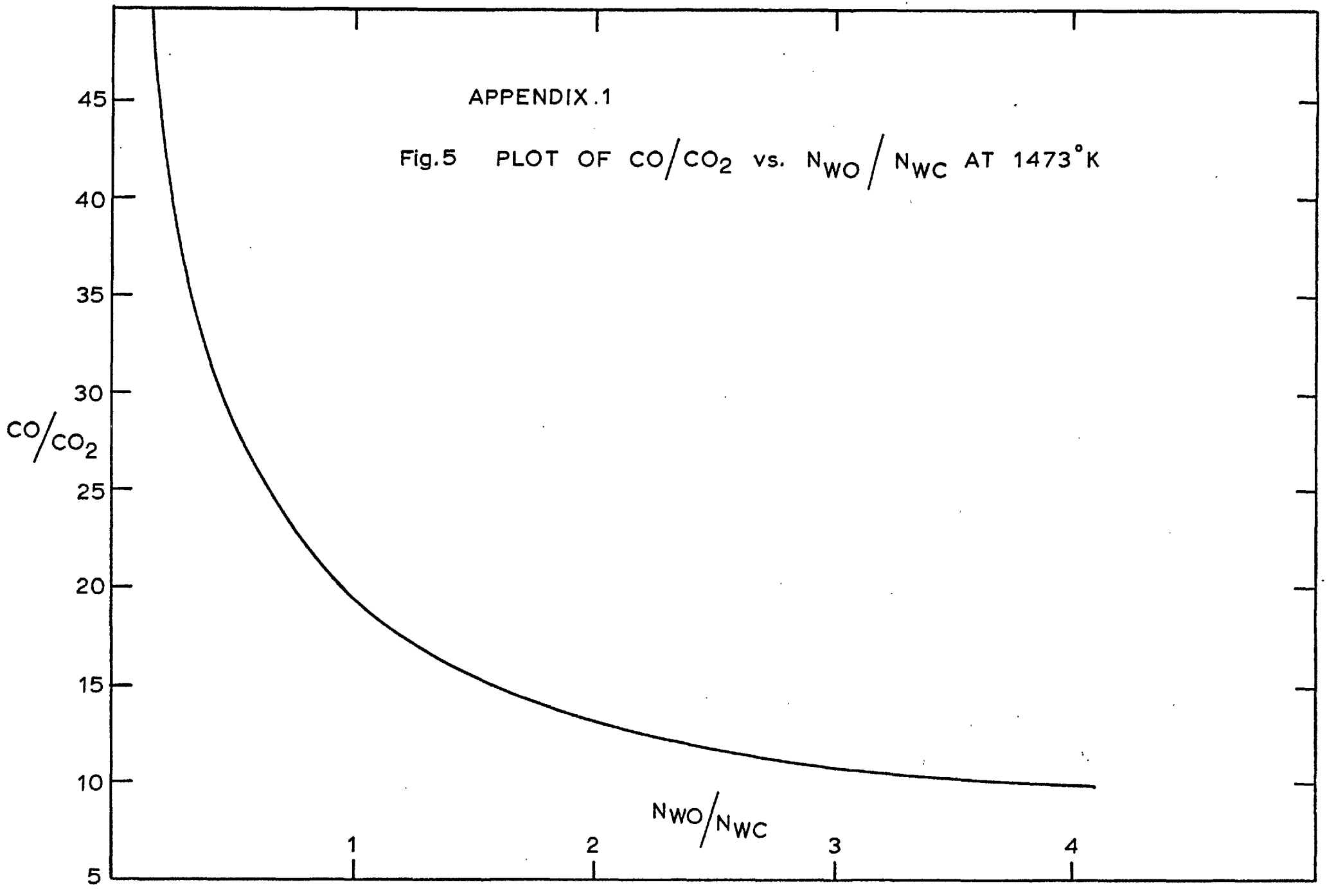

APPENDIX II

DATA ON CO/CO_2 EQUILIBRATION WITH TiC

CO/CO_2	$\frac{N_{TiO}}{N_{TiC}}$	N_{TiO}	N_{TiC}	a_{Ti}	a_C	pO_2(ats.)
1	5.27×10^{5}	1.	1.9×10^{-6}	3.31×10^{-8}	1.79×10^{-4}	2.09×10^{-10}
10	2890	.9996	3.45×10^{-4}	3.30×10^{-7}	3.26×10^{-3}	2.09×10^{-12}
50	107.6	.99	.009	1.63×10^{-6}	1.76×10^{-2}	8.35×10^{-14}
100	26.6	.964	.036	3.17×10^{-6}	3.55×10^{-2}	2.09×10^{-14}
110	21.95	.956	.044	3.49×10^{-6}	3.89×10^{-2}	1.71×10^{-14}
120	18.45	.946	.054	3.76×10^{-6}	4.53×10^{-2}	1.44×10^{-14}
130	15.69	.94	.06	4.05×10^{-6}	4.64×10^{-2}	1.23×10^{-14}
140	13.52	.931	.069	4.31×10^{-6}	4.99×10^{-2}	1.07×10^{-14}
150	11.78	.922	.078	4.55×10^{-6}	5.35×10^{-2}	9.29×10^{-15}
180	8.16	.891	.109	5.31×10^{-6}	6.42×10^{-2}	6.45×10^{-15}
200	6.63	.869	.131	5.74×10^{-6}	7.14×10^{-2}	5.22×10^{-15}
1,000	.2637	.208	.792	6.88×10^{-6}	.359	2.09×10^{-16}
10,000	.0026	.003	.997	9.94×10^{-6}	3.135	2.09×10^{-18}

Appendix 3

Fig. 14 PLOT OF LOG pO_2 vs. T °K Ca

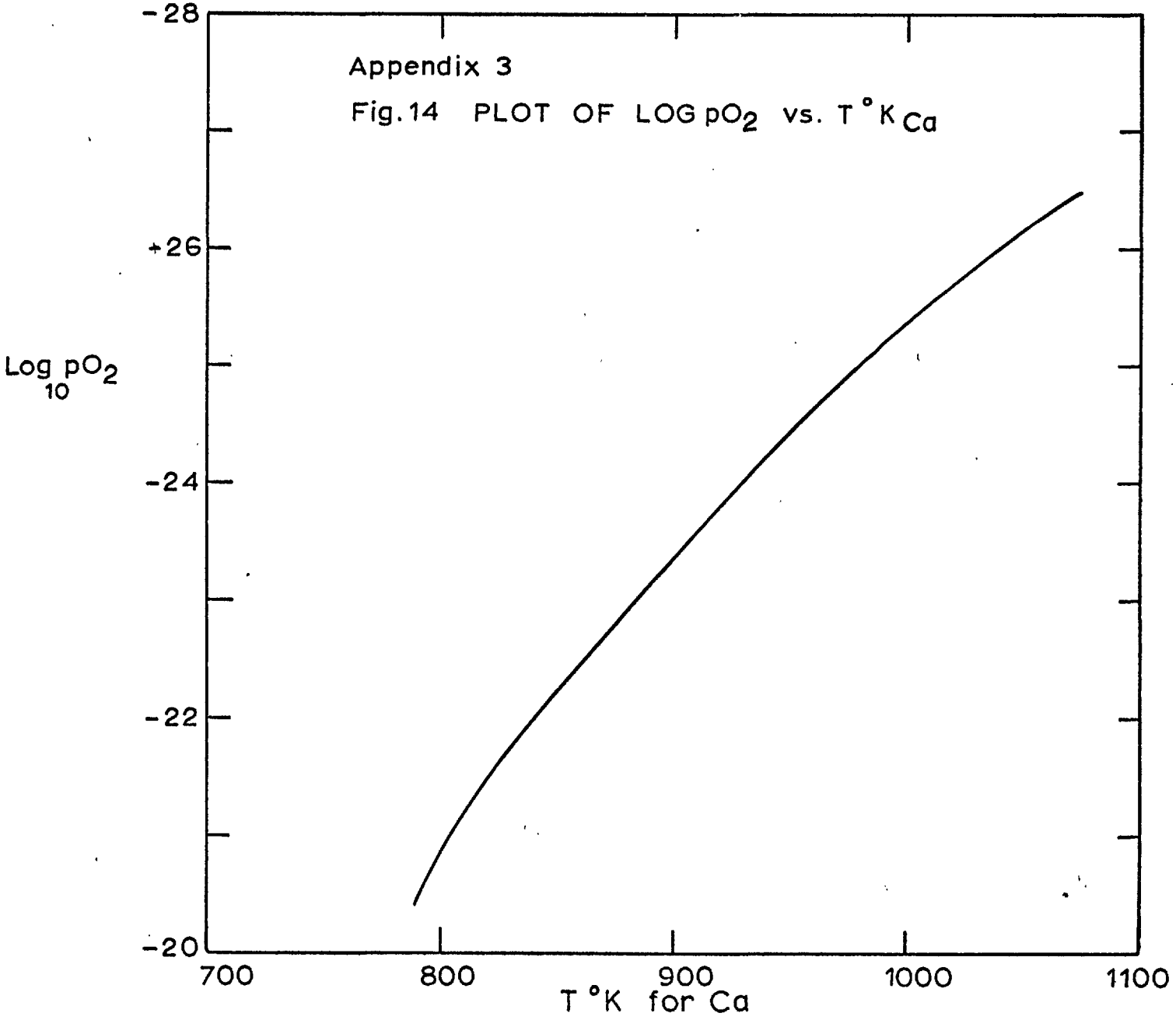

APPENDIX IV

Table showing the highest and lowest carbon activities on the boundaries to be investigated at 1573°K, and the carbon activities required to produce CaC_2 at unit activity corresponding to the calcium activities required to produce the pO_2's shown.

Temperature	a_C	pO_2	System	a_{Ca}	a_C
1300°C	1.32×10^{-3}	5.76×10^{-20}	Ti_2O_3-Ti(C,O)	8.14×10^{-5}	> 1
1300°C	2.81×10^{-6}	4.36×10^{-27}	Ti-Ti(C,O)	2.89×10^{-3}	.369

ACKNOWLEDGMENTS

Firstly, I am most grateful for the financial support given to this work by the United Kingdom Atomic Energy Authority, Harwell.

To my supervisor, Dr B.C.H. Steele, go my sincerest thanks for his constant advice and encouragement throughout the work, and for checking the manuscript.

The help and advice of the Chemical Metallurgy Laboratory staff, and members of the Nuffield Research Group - especially Laboratory G.29 - are gratefully acknowledged.

Many thanks are given to all the staff of the Metallurgy Department Workshop for their technical advice and their fabrication of the iron crucibles used.

I am most grateful also to the staff of (1) the Analytical Sciences Division, U.K.A.E.A., Harwell, (especially Mr E.A. Terry); (2) the Analytical Services Laboratory, Imperial College; and (3) the British Ceramic Research Association Laboratories, Stoke-on-Trent, for carrying out chemical and electron probe analyses.

To Dr E.W. Roberts of the Ceramics Department, University of Leeds, go many thanks for the supply of the dye used in the detection of connected porosity in alumina, and for his advice on microscopy of ceramics.

Thanks are also due to the photography sections of both Metallurgy and Civil Engineering Departments for their co-operation in the production of photographs for Chapter 4 of this Thesis.

Lastly, I thank my parents for their constant support and encouragement throughout the project. Special thanks are due to my mother for her meticulous typing and arrangement of the final manuscript.

M. A. WILLIAMS.

REFERENCES

1. H.J. GOLDSCHMIDT and J.A. BRAND
   J. Less-Common Metals, 5, 181-194. 1963.

2. A.G. METCALFE. Metal Treatment, 13, 127. 1946.

3. M. GLEISER and J. CHIPMAN
   Trans. A.I.M.E., 224, 1278. Dec. 1962.

4. W.L. WORRELL
   Trans. A.I.M.E., 233, 1173. June, 1965.

5. G.W. ORTON
   Trans. A.I.M.E., 230, 600. April, 1964.

6. G.W. ORTON
   Ph.D. Thesis, Ohio State Univ. 1961.

7. O.H. KRIKORIAN
   Ph.D. Thesis, Univ. of California, 1955.

8. SCHENCK, WESSELCOCK and KURZEN
   Z. Anorg. Allgem. Chem. Vol. 203, 159. 1932.

9. G.R. St. PIERRE et al.
   Trans. A.I.M.E., 224, 264. April, 1962.

10. W. WORRELL
    U.C.R.L. 11609. Rev. 1965.

11. W. WORRELL
    University of Pennsylvania, Philadelphia, 1967.

12. G.R. St. PIERRE
    Trans. A.I.M.E., 236, 1363-67. 1966.

13. I.A. VASIL'EVA et al.
    Zh. Fiz. Khim. Vol. 31, 682. 1957.

14. I.A. VASIL'EVA et al.
    Dokl. Akad. Nauk. S.S.S.R. (Engl. Trans.) 143, 1105-07, 1960.

15. I.A. VASIL'EVA et al.
    J. Phys. Chem. 36, 180-183. 1962.

16. D.F. FRANK et al.
    Trans. A.I.M.E., 239, 1905. Dec. 1967.

17. I.A. VASIL'EVA et al.
    Dokl. Akad. Nauk. S.S.S.R. 134, 1350-52. 1960.

18. J. BOUSQUET et al.
    Compt. Rend. 258, 934-936. 1964.

19. A.F. GERASIMOV et al.
    Fiz. Metal Metalloved 11, No. 4, 596-699. 1961.

REFERENCES

(Continued)

20. E.K. STORMS
'Refractory Carbides' - Academic Press, New York & London, 1967.

21. LUX & IGNATOWICZ
Chem. Berichte. 101, 811-814, 1968.

22. KUBASCHEWSKI, EVANS & ALCOCK
'Metallurgical Thermochemistry', 4th Edn. Pergamon Press, 1967.

23. N.A. JAVED
Ph.D. Thesis, Univ. London, 1968.

24. S. LUO
J. Less-Common Metals. 15(3), 299-302, 1968.

25. S. ARONSON & J. SADOFSKY
J. Inorg. & Nuclear Chem.27, 1769-1778, 1965.

26. H. KLUG & L. ALEXANDER
X-ray Diffraction Procedures. Wiley.

27. B. STEELE & C.B. ALCOCK
Trans. A.I.M.E., 233, 1359-1367, 1963.

28. E. DEMPSEY. Phil. Mag. Vol. 8, No. 86, p.225, 1963.

29. R. LYE & E.M. LOGOTHETIS
Phys. Rev. Vol. 147, No. 2, 1966.

30. P. COSTA & R.R. CONTÉ.
Nucl. Met. Symp. Met. Soc. A.I.M.E. Vol.10, p.3. N.Y. 1964.

31. COFFMAN et al. WADD-TR-60-646 (1963).

32. PARTHÉ et al. AFOSR-1721 (1961).

33. L. DARKEN & R.B. SMITH
J. Amer. Chem. Soc. Vol.68, p.1172, 1946.

34. R.P. SMITH.
Trans. Met. Soc. A.I.M.E., Vol. 230, pp. 476-480, 1964.

35. I. CADOFF & J. NIELSEN. J. Metals 5. 248. 1953.

36. E. RUDY, D. HARMON & C. BRUKL. AFML-TR-65-2 Part 1, Vol.2.

37. J. NORTON & R.K. LEWIS NASA-CR-58046. 1964.

REFERENCES

(Continued)

38. L. STONE & A. MARGOLIN. J. Metals. N.Y. 5. 1498. 1953.

39. P. GRIEVSON. Proc. Brit. Ceram. Soc. No.8. p.137. June 1967.

40. E.K. STORMS. To be published.

41. N. GORBUNOV et al.
Izv. Akad. Nauk. S.S.S.R. Otd. Khim. Nauk. p.2093. 1961.

42. H. RASSAERTS, BENESOVSKY & NOWOTNY.
Planseeber. Pulvermet. 14. 23. 1966.

43. P. COSTA & R. CONTÉ. In "International Symposium on Compounds of Interest in Nuclear Reactor Technology."
(J.J. Waber, P. Chictti and W.N. Miner, Eds. p.3.
Met. Soc. A.I.M.E.).

44. H. BITTNER & E. GORETSKI. Monatsh. Chem. 93. 1000. 1962.

45. J.T. NORTON & R.K. LEWIS. NASA-CR-321. (1963).

46. I. CADOFF, J.P. NIELSEN & E. MILLER. Plansee Proc.
2nd Seminar, Reutte Tyrol (1955) p.50. Pergamon Press, Oxford.

47. E.K. STORMS, W.G. WITTEMAN & M. KRUPKA (1966) To be published.

47a. P. EHRLICH. Z. Anorg. Allgem. Chem. 259.1. 1949.

48. O. KUBASCHEWSKI & W.A. DENCH. J. Inst. Metals 82. 87. 1953.

49. O. KUBASCHEWSKI. Rev. Hautes. Tempér et Refract. t3, No.3 1966.

50. A.D. MAH et al BM-RI-5316. 1957.

51. WICKS & BLOCK. Bulletin 605. Bureau of Mines.

52. E. VOLF et al. Russian Journal of Inorganic Chemistry
(English Translation) 2. 16. 1957.

53. G.L. HUMPHREY. J. Amer. Chem. Soc. 73. 2261. 1951.

54. P. GILLES & R. WAHLBECK. J. Chem. Phys. 46. 2465. 1967.

55. JANAF. Thermochemical Tables.

56. BRANTLEY & BECKMANN. J. Amer. Chem. Soc. 52. 3956. 1930.

57. V.S. KUTSEV & B.F. ORMONT.
Russian Journal of Applied Chemistry. 29. 597-601. 1955.

58. I. KOSOLAPOVA et al.
Izvest. Akad. Nauk. S.S.S.R. Neorgan. Mater. Vol.2. No. 8.
pp. 1516-1520. August, 1966.

REFERENCES

(Continued)

59. P. DUWEZ & F. ODELL. J. Electrochem. Soc. 97. 299. 1950.

60. K. KOMAREK, A. VEINBACHS & M. SILVER.
I.A.E.A. Symposium on Nuclear Materials. Vienna. May, 1962.

61. I. AHMAD. Ph.D. Thesis. University of London, 1963.

62. H.M. LEE & L.R. BARRETT.
Proc. Brit. Ceram. Soc. No. 7. Feb. 1967.

63. S. SARIAN et al.
J. App. Phys. 39(7), 3305, 1968.

64. E. RYSCHKEWITSCH. Ber. Deut. Keram Ges. 16. 111. 1935.

65. D. HAYES, D.W. BUDWORTH & J.P. ROBERTS.
Trans. Brit. Ceram. Soc. 60. 494. 1961.

66. D. HAYES, D.W. BUDWORTH & J.P. ROBERTS.
Trans. Brit. Ceram. Soc. 62. 507. 1963.

67. G. FRYER, D.W. BUDWORTH & J.P. ROBERTS.
Trans. Brit. Ceram. Soc. 62. 525. 1963.

68. D. HAYES, E.W. ROBERTS & J.P. ROBERTS.
Science of Ceramics. Vol.2, p.331. 1965. Ed. G.H. Stewart.
Wiley.

69. R.L. FULLMAN.
Trans. A.I.M.E. 197. 447. 1267. 1953.

70. A.K. DHAVALE. Ph.D. Thesis. Leeds University, 1970.

71. P. JORGENSEN & J. WESTBROOK.
G.E.C. Research Laboratory Report No. 63-RL-3525M. 1963.

72. VON CRISTOPH HUMMEL & HANS ERNST SCHWIETE.
Glastechnische Berichte. 32. 10. p.413-420. Oct. 1959.